ON AND OFF PATHWAY ERGS, VEPS AND PSYCHOPHYSICS IN ASSOCIATION WITH AXIAL LENGTH

A thesis presented to the graduate faculty of New England College of Optometry in partial fulfillment of the requirements for the degree of Master of Science

Raviv Katz

April 2026

ON AND OFF PATHWAY ERGS, VEPS AND PSYCHOPHYSICS IN ASSOCIATION WITH AXIAL LENGTH

Raviv Katz

This manuscript has been read and accepted by the Thesis Committee in satisfaction of the thesis requirement for the degree of Master of Science

5/12/2026

Date

DocuSigned by:
78A8AD972399447...

Thanasis Panorgias, MS, PhD
Graduate Faculty Advisor

DocuSigned by:
Chris Taylor
8C96C99C286D4CA...

Christopher Patrick Taylor, PhD
Graduate Faculty Advisor

DocuSigned by:
Fuensanta Vera-Diaz
1502BB240B7D484...

Fuensanta A. Vera-Diaz, OD, PhD, FAAO, FARVO
Thesis Committee Member

DocuSigned by:
Peter Bex
3E92398B601647F...

Peter J. Bex, PhD
Thesis Committee Member

5/12/2026

Date

DocuSigned by:
78A8AD972399447...

Thanasis Panorgias, MS, PhD
Director of Graduate Studies

ON AND OFF PATHWAY ERGS, VEPS AND PSYCHOPHYSICS IN ASSOCIATION WITH AXIAL LENGTH

Raviv Katz

New England College of Optometry, 2026

Abstract

Purpose: Myopia is characterized by progressive axial elongation of the eye and has been associated with functional changes across the visual system. To our knowledge, this is one of the first simultaneous multimodal assessments of ON and OFF visual pathway function from retina to cortex to perception as a function of axial length (AXL) in human myopia.

Methods: 36 participants aged 18 to 32 were recruited from the New England College of Optometry, of whom all completed at least one psychophysical or electrophysiological component of the study (AXL: 22.50 - 27.51 mm). Photopic flash and flicker electroretinography (ERG) and visually evoked potentials (VEP) were recorded using rapid-on and rapid-off sawtooth stimuli to selectively activate the ON and OFF pathways. Psychophysical contrast sensitivity was measured using Difference-of-Gaussian stimuli of ON or OFF contrast polarity at lower (LSF, 1.19 cpd) and relatively higher low spatial frequency condition (HSF, 2.37 cpd) by a two-alternative forced-choice paradigm. Continuous relationships with AXL were assessed using Spearman rank correlations. Exploratory median split comparisons between shorter and longer AXL groups were Holm-corrected within outcome families.

Results: ON and OFF flash ERG and VEP components showed no significant correlations with AXL. Flicker electrophysiology showed selected ON-pathway associations not observed

in the flash paradigms. ON VEP amplitude at 1f1 correlated negatively with AXL ($r = -0.39$, $p = 0.026$), while ON ERG amplitude at 2f1 showed a trend-level negative correlation with AXL ($r = -0.32$, $p = 0.070$). OFF flicker ERG and VEP amplitudes were not significantly associated with AXL. Psychophysical contrast sensitivity showed a spatial-frequency-dependent pattern: ON LogCS at the higher of the two low spatial frequency conditions decreased significantly with increasing AXL ($r = -0.44$, $p = 0.010$), while OFF LogCS showed a weaker trend in the same direction ($r = -0.29$, $p = 0.094$). Relative sensitivity across spatial frequency also increased with AXL for the ON pathway ($r = 0.45$, $p = 0.008$) and when averaged across pathways ($r = 0.39$, $p = 0.024$). ON/OFF ratio and OFF/ON index measures were not significantly associated with AXL.

Conclusions: This study indicates that AXL-related ON/OFF pathway differences are condition-dependent rather than global. Flash ERG and VEP responses were largely preserved, whereas flicker electrophysiology revealed selected ON-pathway associations not evident in the flash paradigms. Psychophysical contrast sensitivity showed a spatial-frequency-dependent reduction in longer eyes, strongest for ON contrast sensitivity at the higher of the two low spatial frequency conditions, with a weaker OFF trend in the same direction. ON/OFF ratio indices were not significantly associated with AXL, suggesting preserved relative pathway balance within the axial length range studied. This multimodal pattern provides a baseline for future longitudinal studies examining whether ON/OFF-biased functional changes precede, accompany, or follow increases in axial length.

Acknowledgements

I would like to express my sincere gratitude to my thesis advisors, Dr. Peter Bex, Dr. Fuensanta Vera-Diaz, Dr. Chris Taylor, and Dr. Thanasis Panorgias, for their guidance, encouragement, and mentorship throughout this project. I am particularly grateful to Dr. Panorgias and Dr. Taylor, whose patience, scientific insight, and willingness to share their time shaped every part of this work and whose mentorship I will carry with me well beyond this thesis. I am also deeply thankful to my fellow lab mates, Rachel Harmon, Simon Wong, and Srini Srirangam, for the long hours we shared in the lab, for their willingness to troubleshoot and problem solve alongside me, and for the camaraderie and friendship that helped me through every stage of this work. Above all, I am especially grateful to my parents, Hedva and Alan, whose love, sacrifices, and unwavering belief in me made this journey possible, and to my siblings, Ohad and Orel, for their constant encouragement and support along the way. I am also deeply thankful to my girlfriend, Bri, for her patience, understanding, and support during the long hours, challenges, and revisions that went into this thesis. Finally, I am grateful to my friends for their encouragement, kindness, and for helping me keep perspective throughout the process. This thesis would not have been possible without all of you.

Table Of Contents

List of Figures and Tables

1 - Introduction

1.1 - ON and OFF Visual Pathways: Parallel Processing in the Visual System

The human visual system is organized into parallel ON and OFF pathways that selectively encode luminance increments ("lights") and decrements ("darks") in the visual scenes, respectively (Werblin and Dowling 1969; Schiller et al. 1986; Masland 2012). This separation begins at the first retinal synapse where photoreceptor signals are transmitted through distinct ON and OFF bipolar cell circuits (Werblin and Dowling 1969). OFF bipolar cells preserve the sign of the photoreceptor signal, while ON bipolar cells invert it through a metabotropic signaling cascade (Slaughter and Miller 1981; Nomura et al. 1994; Morgans et al. 2009; Koike et al. 2010). As a result, increments and decrements are separated early in retinal processing through ON and OFF bipolar cell circuits, and this organization remains at least partially segregated through the retina, lateral geniculate nucleus and primary visual cortex (Schiller et al. 1986; J. Z. Jin et al. 2008). Although this parallel organization allows increments and decrements to be processed separately, the ON and OFF pathways are not simply matched channels carrying opposite signs of the same signal.

Although ON and OFF pathways process opposite contrast polarities, they are not simply mirror-image channels. OFF pathway responses are generally faster than ON pathway responses, consistent with faster sign-preserving transmission through OFF bipolar circuits compared with the slower sign-inverting metabotropic cascade of ON bipolar circuits

(Chichilnisky and Kalmar 2002; J. Jin et al. 2011; Komban et al. 2014). OFF-center ganglion cells also tend to have smaller receptive field centers than ON-center ganglion cells, which may bias the OFF pathway toward finer spatial sampling and sensitivity to small features (Dacey and Petersen 1992; Wässle 2004). Functionally, OFF responses tend to dominate at higher contrast, whereas ON responses may contribute more strongly at lower contrast levels (Rahimi-Nasrabadi et al. 2023). These anatomical and physiological asymmetries provide the basis for testing whether axial elongation affects ON and OFF pathway function differently.

1.2 - ON and OFF Pathways in Emmetropization and Myopia

Myopia has emerged as one of the most pressing public health challenges in vision science, with large-scale projections indicating that approximately 4.8 billion people worldwide will be myopic by 2050, and roughly 9.8%, or 938 million people, will meet criteria for high myopia (Holden et al. 2016). While low myopia is usually fully correctable with spectacles or contact lenses, high myopia is strongly associated with an increased risk of myopic maculopathy, retinal detachment, open-angle glaucoma, and cataract, pathologies that can lead to severe, often irreversible vision loss during working-age adulthood (Williams and Hammond 2019; Bullimore et al. 2025). For this reason, AXL is not simply an optical measurement; it is a structural marker of myopia severity and long-term ocular risk.

A fundamental question underlying this area of research is whether ON and OFF pathway dysfunction represents a cause of axial elongation, a consequence of it, or whether the relationship is more dynamic. Emmetropization is a visually guided homeostatic process through which the developing eye uses retinal defocus signals to regulate axial growth

toward a matched focal length (Schaeffel and Swiatczak 2024). When this regulatory process is disrupted by sustained hyperopic defocus or abnormal retinal input, axial elongation can exceed the emmetropization set point and can result in myopia (Wallman and Winawer 2004). A key unresolved question is therefore whether altered ON/OFF pathway function contributes to abnormal eye-growth signaling, emerges because of axial elongation, or reflects a more dynamic interaction between retinal function and ocular structure. Although eye-growth regulation is retina-mediated, the relative contributions of foveal, parafoveal, and peripheral signals remain unresolved. This uncertainty supports the need to study pathway-specific retinal processing rather than assuming that emmetropization depends on a single retinal locus (Chakraborty, Schaeffel, and Wildsoet, 2025).

The ON and OFF pathways are biologically plausible candidates for involvement in emmetropization because they encode opposite contrast polarities and differ in their temporal, spatial, and contrast-response properties (Schiller, 1992; Jin et al., 2011; Komban et al., 2014; Rahimi-Nasrabadi et al., 2023). These differences mean that the visual input available to the growing eye is not represented by a single uniform luminance channel. Instead, increments and decrements are processed through partially distinct retinal circuits that may provide different information about blur, contrast, and spatial structure (Dacey and Petersen, 1992; Chichilnisky and Kalmar, 2002; Wässle, 2004; Burkhardt, 2011). Because emmetropization depends on retinal detection of visual signals related to image quality and defocus, a change in the balance or gain of ON and OFF signaling could plausibly alter the retinal signal that guides ocular growth (Wallman and Winawer, 2004; Schaeffel and Swiatczak, 2024).

Animal models provide some of the strongest evidence that ON/OFF signaling can influence refractive development. In chicks, pharmacologic suppression of ON or OFF retinal responses disrupts compensation to imposed defocus, suggesting that intact polarity-specific signaling is needed for normal eye-growth responses to positive and negative lenses (Crewther and Crewther, 2003). Mouse models with impaired ON-bipolar transmission also show abnormal refractive development, reduced retinal dopamine, and increased susceptibility to form-deprivation myopia (Pardue et al., 2008; Chakraborty et al., 2015). Dopamine provides a possible neurochemical bridge between light-driven ON/OFF activity and eye-growth regulation. Retinal dopamine is modulated by light-driven retinal input, is reduced in experimental models of myopia, and can influence axial elongation through pharmacologic or genetic manipulation (Puopolo et al. 2005; Feldkaemper and Schaeffel 2013; Bergen et al. 2016; Munteanu et al. 2018; Thomson et al. 2020a, 2020b; Tian et al. 2021). Because dopamine receptors are expressed across bipolar-cell circuits, dopamine may influence eye growth by modulating post-receptoral gain, contrast processing, and retinal adaptation rather than acting as an isolated chemical signal (Farshi et al. 2016; Mazade et al. 2019; Roy and Field 2019).

Human evidence also supports a relationship between ON/OFF pathway function and axial myopia, although the direction and location of the effect remain unresolved. Complete congenital stationary night blindness, a disorder involving ON-bipolar pathway dysfunction, is commonly associated with high myopia, suggesting that impaired ON pathway signaling can be linked to abnormal refractive development in humans (Zeitz et al., 2023a). In individuals without inherited retinal disease, electrophysiological and psychophysical studies

suggest that axial elongation can be associated with altered visual function even when high-contrast acuity is corrected. Multifocal ERG studies have reported reduced response amplitudes and delayed timing in myopic eyes, although these effects vary by retinal eccentricity, age, stimulus conditions, and whether refractive error or AXL is used as the primary predictor (Chen et al., 2006; Ho et al., 2012; Gupta et al., 2021). This variability suggests that myopia-related functional changes are unlikely to reflect a uniform global reduction in retinal function.

More recent pathway-selective work suggests that ON pathway function may be especially vulnerable in some forms of human myopia. Poudel et al. (2024) reported that increasing AXL was associated with reduced ON pathway response amplitude, prolonged response latency, and reduced ON contrast sensitivity, while OFF pathway measures were relatively preserved. Psychophysical work using Difference-of-Gaussians stimuli also found that the OFF/ON sensitivity ratio increased with AXL, suggesting that axial elongation may be associated with altered perceptual balance between contrast polarities (Hogue and Taylor, 2022). However, because psychophysical measurements reflect the combined output of retinal, cortical, optical, and decision-level processing, perceptual ON/OFF differences alone cannot determine where the underlying alteration originates.

Together, these findings support a biologically plausible relationship between ON/OFF pathway signaling and AXL, but they do not establish whether ON/OFF differences in human myopia arise at the retina, cortex, perception, or across multiple levels of visual processing. The literature also suggests that these effects may be paradigm-specific rather than global, varying with stimulus polarity, contrast, spatial frequency, temporal demand, and

retinal eccentricity. This uncertainty motivates a multimodal approach that can assess ON and OFF pathway function across the visual hierarchy within the same individuals. The following section therefore reviews the electrophysiological and psychophysical methods used to measure ON/OFF pathway function at the retinal, cortical, and perceptual levels.

1.3 - Electrophysiological and Psychophysical Assessment of ON and OFF Pathway Function

Determining whether AXL is associated with ON/OFF pathway functional differences requires measurements at multiple levels of the visual system. Psychophysical contrast sensitivity can reveal whether perception differs for luminance increments and decrements, but it cannot determine whether those differences arise from retinal, cortical, optical, or decision-level factors. Electrophysiological measures provide complementary information because electroretinography (ERG) assesses retinal activity, whereas visually evoked potentials (VEPs) assess post-retinal and cortical responses to visual stimulation. Combining ERG, VEP, and psychophysics therefore allows ON/OFF pathway function to be evaluated across retina, cortex, and perception within the same individuals.

ERG provides an objective measure of retinal function by recording the summed electrical response of retinal neurons to light stimulation (Robson et al., 2022). This makes ERG directly relevant to ON/OFF pathway assessment because photopic ON and OFF responses can be emphasized using luminance increments and decrements, including rapid-on and rapid-off sawtooth stimuli. In transient flash paradigms, the light-adapted b-wave is largely driven by depolarizing ON bipolar cell activity, whereas the d-wave at light offset

reflects activity from OFF bipolar pathways (Stockton and Slaughter, 1989; Hirasawa et al., 2021). Flicker ERG adds a temporal-processing dimension by measuring how reliably retinal circuits follow repeated stimulation in the frequency domain. In myopia, prior ERG studies have reported reduced amplitudes and, in some cases, delayed timing with increasing refractive error or AXL, but findings vary across full-field, focal, and multifocal paradigms (Yamamoto et al., 1997; Luu et al., 2006; Gupta et al., 2021; Ribeiro et al., 2025). What remains less clear is whether these retinal changes are pathway-specific and whether ON and OFF responses are affected differently when tested with polarity-selective stimuli.

VEPs complement ERGs by measuring electrical activity recorded over the occipital cortex in response to visual stimulation. Because VEPs reflect activity along the visual pathway from the retina through primary visual cortex, they provide a way to test whether ON/OFF differences observed at the retinal or perceptual level are also detectable at a cortical level (Robson et al., 2018; Šuštar Habjan et al., 2025). ON and OFF pathway responses remain functionally asymmetric in cortex, with luminance increments and decrements producing differences in response timing and magnitude (Jin et al., 2008; Norcia et al., 2020). In myopia, the VEP literature is much smaller than the ERG literature, but available studies suggest that myopia can be associated with reduced amplitude or delayed cortical responses, even when refractive error is corrected (Agrawal et al., 2022; Ribeiro et al., 2025). However, cortical ON/OFF pathway function in relation to AXL has not been well characterized, leaving unresolved whether any AXL-related pathway differences are present beyond the retina.

Psychophysical contrast sensitivity provides the perceptual endpoint of ON/OFF pathway processing. By measuring detection thresholds for positive- and negative-contrast stimuli, psychophysics can test whether luminance increments and decrements are perceived differently as AXL increases. This is relevant because myopes can show reduced contrast sensitivity even when high-contrast acuity is corrected, suggesting that myopia-related visual changes are not explained by optical defocus alone (Ehsaei et al., 2011). Recent pathway-selective studies have reported ON-biased vulnerability in myopia, including reduced ON contrast sensitivity and delayed ON responses with increasing AXL (Poudel et al., 2024). Psychophysical work using Difference-of-Gaussians stimuli also found that OFF/ON sensitivity balance changed with AXL, suggesting that axial elongation may be associated with altered contrast-polarity processing at the perceptual level (Hogue and Taylor, 2022). The limitation is that psychophysics alone cannot determine whether these perceptual effects arise from retinal function, cortical processing, optical factors, or compensatory gain changes across the visual hierarchy.

The present study was designed to address this localization problem. Specifically, it tested whether AXL is associated with differential ON versus OFF pathway function; whether any associations are detectable at the retinal, cortical, perceptual, or multiple levels; and whether relative ON/OFF balance changes with AXL. Based on prior evidence suggesting ON pathway vulnerability in myopia, stronger AXL-related associations were hypothesized for ON pathway measures, particularly under temporally demanding flicker and contrast sensitivity conditions. By combining pathway-selective ERG, VEP, and psychophysical testing in the same cohort, this thesis evaluates whether AXL-related

ON/OFF differences are localized to one level of the visual system or appear across the visual hierarchy.

2. - Rationale and Specific Aims

The literature supports a role for bipolar-cell-mediated ON/OFF signaling in emmetropization, but whether ON/OFF pathway differences are a cause, consequence, or correlate of human axial myopia remains unresolved (Schaeffel and Swiatczak, 2024). Prior animal and human studies suggest that ON and OFF pathways may be differentially involved in refractive development and myopia, with recent human work reporting ON-biased reductions in retinal pathway function and contrast sensitivity as axial length increases (Poudel et al., 2024). Psychophysical studies also suggest that relative sensitivity to ON- and OFF-polarity stimuli may vary with axial length (Hogue and Taylor, 2022). However, these studies have generally examined retinal, cortical, or perceptual responses separately, leaving uncertain where along the visual hierarchy AXL-related ON/OFF differences arise.

The rationale for the present study is that a multimodal design can help localize pathway-specific effects of axial length. ERG provides an objective measure of retinal ON/OFF pathway activity, VEP provides an objective measure of cortical responses to ON/OFF stimulation, and psychophysical contrast sensitivity provides a perceptual measure of ON/OFF pathway output. By measuring all three levels in the same cohort, this study tested whether longer axial length is associated with selective ON- or OFF pathway differences, whether these effects are consistent across retina, cortex, and perception, and whether ON/OFF pathway balance is preserved or altered with axial elongation.

Specific Aim 1: To investigate the relationship between AXL and ON/OFF pathway function at the retinal level using flash and flicker ERG recordings with pathway-selective sawtooth stimuli. We hypothesize that increasing AXL will be associated with reduced ON

pathway amplitudes, consistent with animal model predictions of preferential ON pathway vulnerability

Specific Aim 2: To investigate the relationship between AXL and ON/OFF pathway processing at the cortical level using flash and flicker VEP recordings. We hypothesize that cortical signatures of pathway differences will be parallel retinal-level changes, with possible additional effects on signal coherence reflecting degraded cortico-retinal processing

Specific Aim 3: To investigate the relationship between AXL and psychophysical contrast sensitivity for ON and OFF pathway-selective stimuli at higher and lower radial spatial frequency in the low spatial frequency range. We hypothesize that the OFF/ON sensitivity ratio will change systematically with AXL, with possible spatial frequency dependent effects reflecting the interaction of neural factors.

Together, these aims test whether axial length is associated with ON/OFF pathway differences at the retinal, cortical, and perceptual levels, and whether any observed effects represent a pathway-specific imbalance.

3. - Methods

3.1 - Subject recruitment

Thirty-six participants aged 18 to 32 years were recruited from the New England College of Optometry community by institutional email outreach as part of a larger cross-sectional study investigating the relationship between AXL and retinal structure and function. Of the 36 participants enrolled, all completed at least one psychophysical or electrophysiological component of the study.

Participants were eligible if they were 18 to 32 years of age, had best-corrected visual acuity of 0.00 logMAR, equivalent to 20/20 Snellen acuity, or better in each eye, and had spherical equivalent refractive error between +5.00 D and −6.00 D with cylindrical refractive error no greater than 2.50 DC. Refractive group assignment was based on the final spherical equivalent refractive error determined during the baseline clinical assessment, as described in Section 3.2. Participants were classified as emmetropic if spherical equivalent refractive error was between +0.75 D and −0.25 D with cylindrical power within 0.75 DC, myopic if spherical equivalent refractive error was between −0.50 D and −6.00 D with cylindrical power within 2.50 DC, or hyperopic if spherical equivalent refractive error was between +1.00 D and +5.00 D with cylindrical power within 2.50 DC.

Participants were excluded if they had a history of ocular surgery, ocular disease that could affect retinal health or visual function, strabismus or near binocular vision anomalies, orthokeratology or rigid gas-permeable contact lens wear within the previous 14 days, use of ocular or systemic medications that could affect vision, allergy to study eye drops, pregnancy

or nursing, or a history of seizures or epilepsy. All participants provided written informed consent before participation. The study was approved by the Institutional Review Board of the New England College of Optometry and adhered to the tenets of the Declaration of Helsinki.

3.2 - Screening and Baseline Clinical Assessment

At the initial visit, all participants completed a screening and baseline clinical assessment to confirm eligibility and characterize refractive status, ocular biometry, and ocular health. The screening included a comprehensive ocular and medical history, with attention to prior ocular surgery, ocular disease, contact lens wear, medication use, allergy to eye drops, pregnancy or nursing status, and history of seizures or epilepsy. Clinical testing included lensometry of the participant's habitual distance correction, habitual distance and near visual acuity, distance and near cover testing, near point of convergence, confrontation visual fields, pupil assessment, extraocular muscle testing, intraocular pressure measurement by rebound tonometry, monocular estimated method retinoscopy, distance retinoscopy, slit lamp anterior segment evaluation, ocular biometry with the Lenstar LS 900, optical coherence tomography, and objective refraction using static retinoscopy and a WAM open-field autorefractor.

The WAM open-field autorefraction result was used as the primary objective estimate of refractive error for group assignment and statistical analysis when the participant achieved visual acuity of +0.10 logMAR or better through that correction. If visual acuity through the WAM-derived objective refraction was not sufficient to achieve +0.10 logMAR or better,

distance subjective refraction with binocular balance was performed, and the subjective refraction was used as the final refractive value. This final refractive value was used for refractive group assignment, power vector calculations, and subsequent statistical analyses. Appropriate refractive correction, determined during this baseline testing, was also used for subsequent psychophysical and electrophysiological testing as indicated.

Spherical equivalent refractive error (M) was calculated as the spherical power plus one-half of the cylindrical power in diopters, where $M = S + C/2$. Astigmatic components were calculated using power vector notation as described by Thibos et al. (1997), where S is sphere, C is cylinder, and β is the cylinder axis in degrees: $J0 = (-C/2) \cos[2(\beta - 90)]$ and $J45 = (-C/2) \sin[2(\beta - 90)]$.

3.3 - Visit Structure Relevant to the ON/OFF Bipolar Substudy

The present thesis used a subset of procedures from the larger Retinal Layers Study, a four-visit cross-sectional protocol examining relationships between AXL and retinal structure and function. Study visits were scheduled approximately 7 ± 3 days apart and, when possible, at comparable times of day within ±2 hours. The subset relevant to ON/OFF bipolar pathway function included Visit 1, Visit 3, and Visit 4.

During Visit 1, participants completed eligibility screening, baseline clinical measurements, ocular biometry, and one psychophysical ON/OFF contrast sensitivity session. The polarity tested during Visit 1 was randomized so that participants completed either the ON or OFF condition first. Within that session, participants were tested at two viewing distances, with the order of near and far testing randomized according to the study

randomization schedule. AXL was measured before and after the psychophysical testing session.

During Visit 3, participants completed the electrophysiological portion of the ON/OFF substudy. Photopic ON and OFF flash and flicker ERGand VEP recordings were obtained using pathway-selective sawtooth stimuli. These recordings were used to assess ON/OFF pathway function at the retinal and cortical levels.

During Visit 4, participants returned to complete the complementary psychophysical polarity condition that was not tested during Visit 1. The same near and far viewing-distance structure was used, and AXL was again measured before and after psychophysical testing. Visit 2 was part of the larger Retinal Layers Study but did not include procedures analyzed in the present ON/OFF bipolar pathway thesis.

3.4 - Electroretinography and Visually Evoked Potentials

Electrophysiological recordings were performed during Visit 3 to assess ON and OFF pathway function at retinal and cortical levels. ERG recordings were used to measure retinal responses, and VEP recordings were used to measure cortical responses to the same visual stimuli. Recordings were obtained under photopic conditions using rapid-on and rapid-off sawtooth luminance stimuli designed to preferentially emphasize ON- or OFF pathway responses. Both transient flash responses and steady-state flicker responses were recorded. The flash stimuli were analyzed in the time domain, whereas the 10 Hz flicker stimuli were analyzed in the frequency domain at the fundamental frequency and second harmonic.

3.4.1 Sawtooth Stimuli for Electrophysiological Testing

ON and OFF pathway activity were isolated using rapid-ON and rapid-OFF sawtooth luminance profiles presented under photopic adaptation. (Barboni et al. 2013; Sustar et al. 2018; Kremers et al. 2014). This methodology employs asymmetric luminance ramps that preferentially stimulate either ON or OFF bipolar cell population, providing an alternative to long-duration flash protocols for evaluating pathway-specific retinal responses (Barboni et al. 2013; Sustar et al. 2018).

Two stimulus formats were used. First, 10 Hz flicker sawtooth stimuli were used to assess steady-state ON and OFF pathway responses. For ON flicker, each 100 ms cycle begins with an abrupt luminance increase to peak luminance followed by a linear decrease back to background luminance. For OFF flicker, each 100 ms cycle began with a linear increase to peak luminance followed by an abrupt luminance decrease to background luminance. Ten cycles were presented per 1000 ms sweep, allowing frequency-domain analysis at 10 Hz and 20 Hz, corresponding to the fundamental frequency and second harmonic, respectively (Figure 3.1).

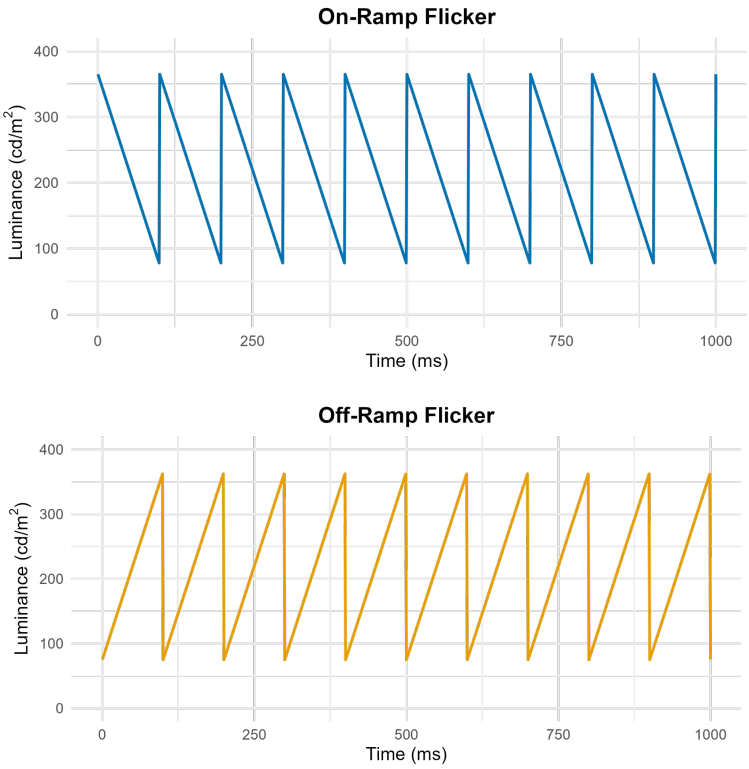

Figure 3.1 Luminance profile of ON and OFF 10 Hz flicker sawtooth stimuli.
Left: ON - Ramp flicker; each 100 ms cycle begins with an instantaneous luminance increase to peak (365 cd/m^2), followed by a linear ramp down to background luminance (65 cd/m^2). Right: OFF-Ramp flicker; each 100 ms cycle begins with an instantaneous luminance decrease to minimum (65 cd/m^2) followed by a linear ramp up to peak luminance (365 cd/m^2). Ten cycles were presented over 1000 ms, enabling Fast Fourier Transform analysis at the fundamental frequency (10 Hz) and second harmonic (20 Hz).

Second, single-flash sawtooth stimuli were used to assess transient ON and OFF pathway responses. For ON flash stimulation, luminance increased abruptly from background to peak luminance and then decreased linearly over 100 ms back to background. For OFF flash stimulation, luminance increased linearly over 100 ms from background to peak luminance and then decreased abruptly back to background. The abrupt luminance transition was used

to emphasize the pathway of interest: the rapid luminance increment emphasized the ON response, and the rapid luminance decrement emphasized the OFF response (Figure 3.2).

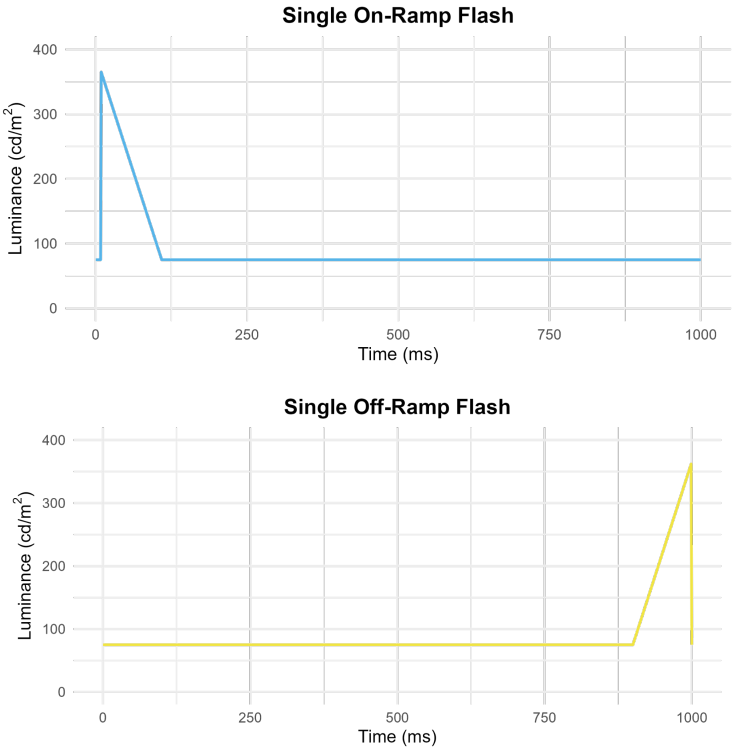

Figure 3.2 Luminance profiles of ON and OFF flash sawtooth stimuli Top: ON-flash stimulus with a rapid luminance increment followed by a 100 ms ramp back to background; bottom: OFF-flash stimulus with a rapid luminance decrement followed by a 100 ms ramp back to background, preferentially activating ON and OFF bipolar pathways, respectively.

3.4.2 ERG Protocol

Full-field ERGs were recorded monocularly from the right eye of each participant using a ColorDome Desktop Ganzfeld controlled by the Espion software platform (Diagnosys LLC, Lowell, MA, USA). All procedures adhered to the updated standards of the

International Society for Clinical Electrophysiology of Vision (ISCEV) for full-field ERGs (Robson et al. 2022) and to the extended protocol for the photopic negative response in full-field ERGs (Sustar et al. 2018). Participants' right pupils were dilated with a single drop of 0.5% tropicamide to reduce accommodative fluctuation and standardize retinal illumination (Sustar et al. 2018). A Dawson-Trick-Litzkow (DTL) fiber electrode, placed on the lower eyelid, served as the active electrode; a reference gold-cup electrode was placed at the temporal canthus, and a ground gold-cup electrode was positioned on the forehead, following appropriate skin preparation with a mild exfoliating paste. Electrode impedances were verified at <5 kΩ prior to recording. Signals were amplified and band-pass filtered (1-300 Hz), then averaged over 40-50 sweeps for flash ERGs, or 10 sweeps for flicker stimulation, depending on noise levels and participant cooperation. Signals over 500 uV were removed and the sweep was recorded again. During the recordings, participants were instructed to fixate on a red fixation target at the center of the Ganzfeld.

For each participant, ON and OFF flash and flicker ERG responses were obtained using a fixed protocol order. The protocol order was not randomized because ERG and VEP recordings were acquired simultaneously within a preprogrammed Espion protocol, and using a fixed sequence maintained consistent calibration, acquisition settings, and electrode conditions across participants. Brief rest periods were provided between stimulus conditions to reduce fatigue. Representative ON and OFF flash and flicker ERG waveforms are shown in Figure 3.3.

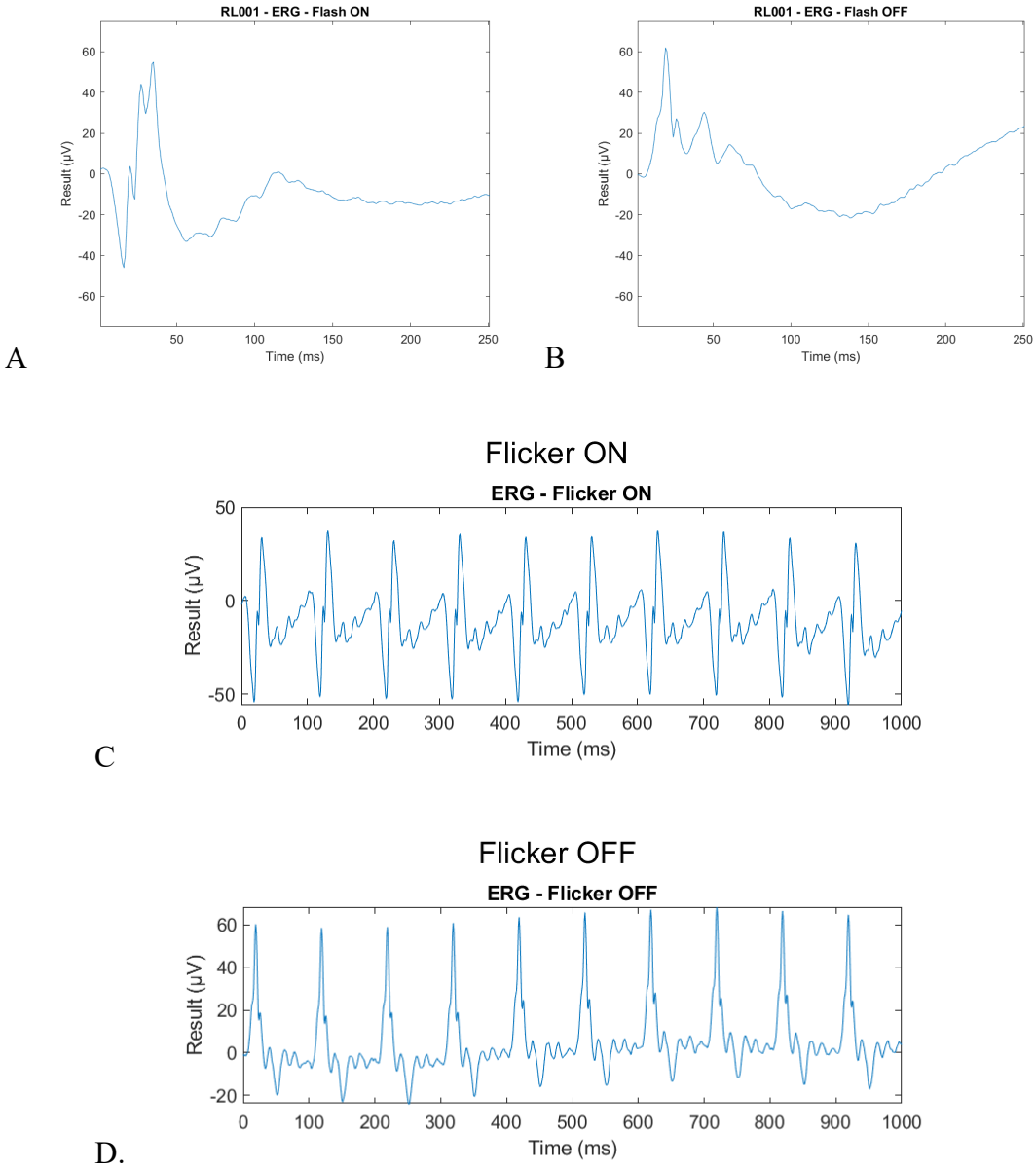

Figure 3.3 Representative ERG waveforms for ON and OFF pathway stimulation. (A–B) Single-stimulus ERG waveforms for ON- and OFF-ramp flash stimulation; (C–D) steady-state ERG waveforms for 10 Hz ON- and OFF-flicker stimulation, plotted as electrical response amplitude (uV) over time (ms).

Component Identification of Flash ERGs

Flash ERG waveforms were analyzed according to the ISCEV extended protocol for the photopic ON-OFF ERG (Sustar et al. 2018) and the extended protocol for the photopic negative response (Frishman et al. 2018). Although these protocols specify long-duration (150-200 ms) light steps for pathway isolation, the sawtooth methodology achieves equivalent pathway selectivity through asymmetric temporal modulation while offering advantages of faster acquisition and reduced transient artifacts (Pangeni and Kremers 2013; Barboni et al. 2013). An example of ON and OFF ERG recordings is shown in Figure 3.4.

For ON-Flash ERG recordings, the following components were identified

- a-wave - The initial negative deflection, measured from baseline to the first negative trough, reflecting photoreceptor hyperpolarization.
- b-wave - The subsequent positive deflection, measured from the a-wave trough to the positive peak, primarily reflecting ON bipolar cell depolarization.
- Photopic negative response (PhNR): The slow negative wave following the b-wave, measured from the baseline to the negative trough, reflecting retinal ganglion cell activity.

For OFF-Flash ERG recordings, the following components were identified

- d-wave - the initial positive deflection, measured from baseline to the first positive peak, reflecting OFF bipolar cell depolarization

- Photopic negative response (PhNR): The negative wave following the d-wave measured from baseline to the negative trough.

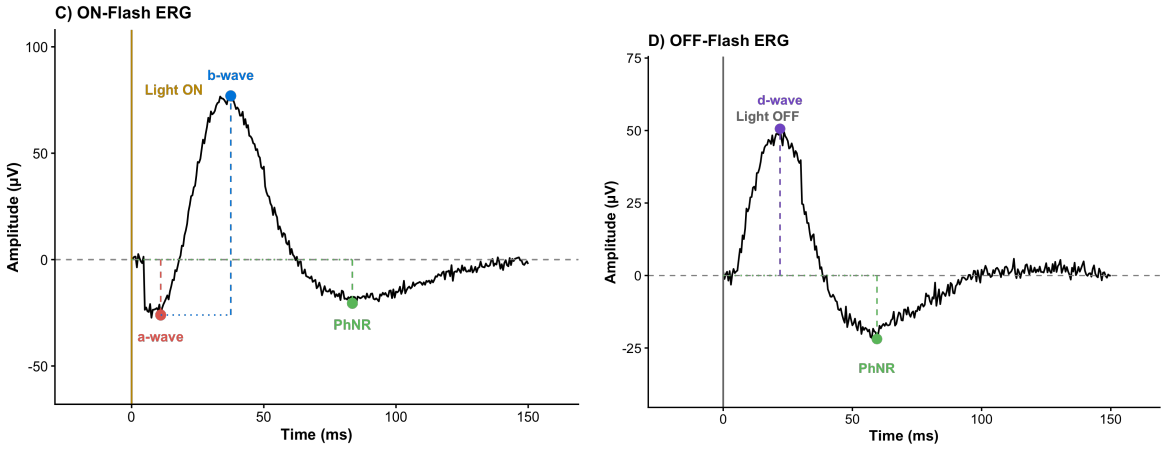

Figure 3.4 Representative ON-Flash and OFF-Flash ERG waveforms. Representative ON and OFF Flash ERG waveforms. On-flash ERG with a-wave, b-wave and PhNR components labeled. OFF-flash ERG with d-wave PhNR components labeled.

3.4.3 VEP Protocol

VEPs were recorded simultaneously with ERGs under photopic conditions using the Espion system's multi-channel capability. All procedures adhered to the ISCEV standard for clinical VEP (Šuštar Habjan et al. 2025) and the guideline for standard electrode position nomenclature (American Clinical Neurophysiology Society 2006). This simultaneous recording approach ensured the retinal and cortical responses to identical stimuli could be directly compared without inter-session variability. Scalp electrodes were positioned according to the 10-20 system, which defines electrode locations as proportional distance

along the head surface relative to anatomical landmarks (Figure 3.5). Prior to electrode placement, the nasion-to-inion distance along the midline was measured using a flexible tape measure.

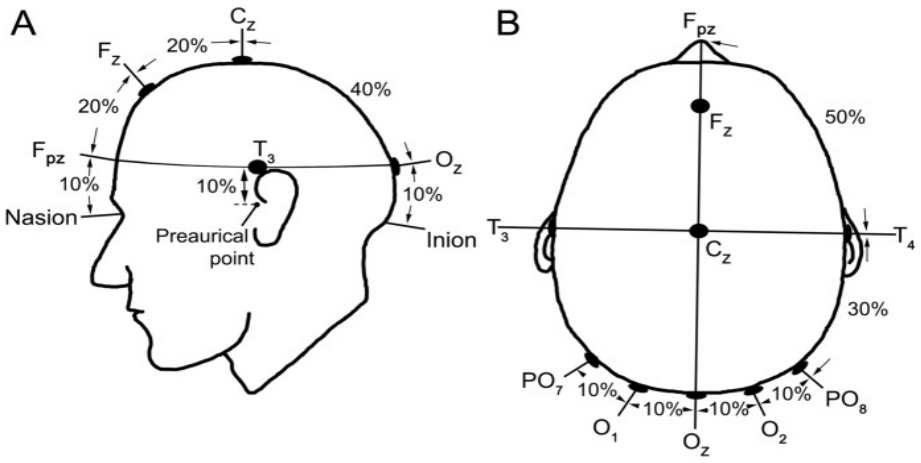

Figure 3.5 VEP Electrode Placement According to the International 10-20 system. Sagittal view schematic showing electrode positions along the midline: Fz(reference) at 30% of the nasion-inion distance from the nasion, Fpz (ground) at 10% above the nasion, and Oz (active) at 10% above the inion over the primary visual cortex. Image taken from ISCEV 2025 (Šuštar Habjan et al. 2025).

The following electrode orientation was employed:

- Active Electrode (Oz): Positioned at 10% of the nasion-inion distance above the inion, over the primary visual cortex. This occipital placement optimally captures pattern and flash VEP responses generated in striate and extrastriate cortex.

- Reference electrode (Fz): Positioned at 30% of the nasion-inion distance above the nasion, on the midline frontal scalp. This anterior placement provides a relatively inactive reference for occipital potentials.

- Ground Electrode (Fpz): Positioned at 10% of the nasion-inion distance above the nasion serving as the common ground for the both ERGs and VEPs.

All VEP electrodes were gold-cup electrodes (Grass Technologies, 10 mm diameter) filled with Ten20 conductive paste (Weaver and Company). Skin preparation at each site involved gentle abrasion with NuPrep exfoliating gel using a cotton-tipped applicator until mild erythema was observed, followed by cleaning with an alcohol pred pad and air drying. This preparation typically achieved electrode impedance below 5kΩ. Electrodes were secured in place with medical specialty headstraps. Signals were amplified and band-pass filtered (1–100 Hz), then averaged over 40 sweeps per condition, depending on noise levels and participant cooperation. Representative waveforms for Flash and Flicker VEPs are shown in Figure 3.6

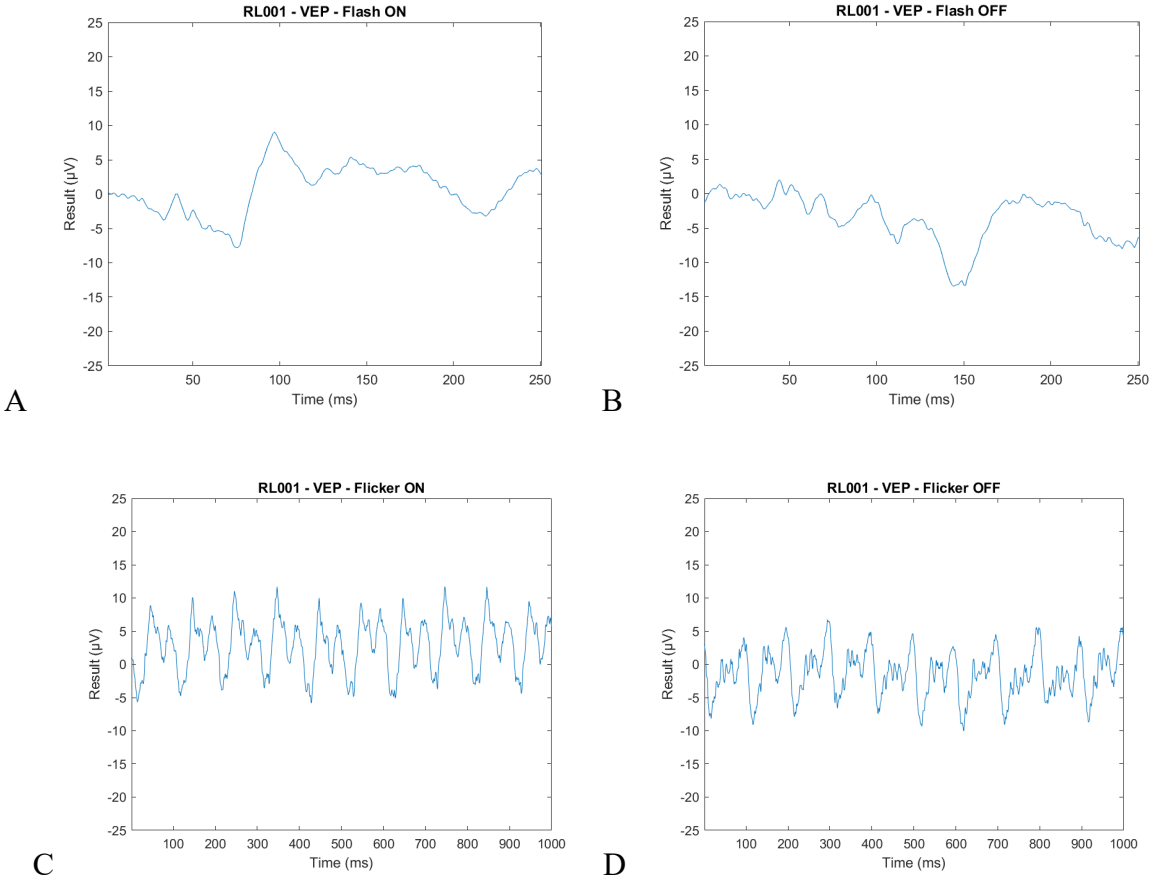

Figure 3.6 Representative VEP waveforms isolating ON and OFF pathway responses. Four-panel waveform plot displaying VEP amplitude (uV) over time (ms) for a representative subject under four stimulus conditions: (A) ON-flash, (B) OFF-flash, (C) 10 Hz rapid-on sawtooth ON-flicker, and (D) 10 Hz rapid-off sawtooth OFF-flicker.

An automatic artifact rejection threshold of ±500 uV applied to the ERG channel excluded sweeps contaminated by eye movements, blinks, or muscle activity. This approach ensured that the same sweeps contributed to both the retinal and cortical averages, maintaining correspondence between ERG and VEP recordings and allowing direct comparison of retinal-level and cortical-level responses to identical stimuli.

Component Identification of flash VEPs

Flash VEP waveforms were analyzed according to the updated ISCEV standard for clinical VEP shown in Figure 3.7 (Šuštar Habjan et al. 2025). Components were identified using numerical nomenclature (N1, P1, N2, P2, N3, P3), where "N" denotes negative deflections and "P" denotes positive deflections in sequence of occurrence. Because the present analysis focused on the most reliable and consistently identifiable flash VEP components, component identification was limited to the P1, N2, and P2 peaks.

P1 was identified as the first reproducible positive deflection following stimulus onset. N2 was identified as the major negative deflection following P1, and P2 was identified as the major positive deflection following N2. Peak time was measured from stimulus onset to the corresponding component peak. The N2-P2 peak-to-peak amplitude was calculated as the voltage difference between the N2 trough and the P2 peak.

The P1, N2 and P2 components were selected as primary outcome measures because they represent the most consistent and largest amplitude deflections in adult flash VEP recordings (Šuštar Habjan et al. 2025). Earliest components (N1,P1) are often small or absent in Ganzfeld flash stimulation, while later components (N3,P3) show greater inter-subject variability.

For steady state (flicker) VEP recordings, time-domain waveforms were transformed to the frequency domain using Fast Fourier Transform analysis. Amplitude and phase were extracted at the fundamental frequency and second harmonic, identical to the approach used for flicker ERGs.

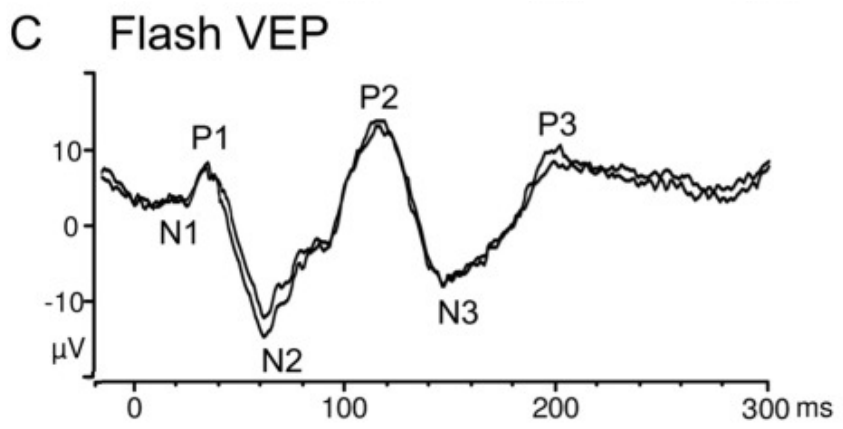

Figure 3.7 Standard Flash VEP waveform. Waveform plot of a standard flash VEP showing amplitude (uV) over time (ms), featuring numerically sequenced labels for characteristic negative and positive components (adapted from Šuštar Habjan et al., 2025).

3.4.4 Electrophysiological Data Processing

All electrophysiological signals were processed using custom analysis developed in MATLAB (MathWorks, Natick, MA).

Flash ERG and VEP Analysis

Flash ERG and VEP responses were analyzed in the time domain following principles established by the ISCEV extended protocol for the photopic ON-OFF ERG (Sustar et al. 2018), and the extended protocol for the photopic negative response (Frishman et al. 2018). Component amplitudes and implicit times were extracted using semi-automated peak detection in Matlab, with all waveforms subsequently verified through visual inspection and manual adjustment when necessary.

To assess ON/OFF pathway balance at the retinal level, several amplitude ratios were calculated for participants with valid recordings in both pathways. b/d amplitude ratio, the b-wave to d-wave amplitude ratio was calculated for each participant with valid recordings for both components. This ratio provides a functional index of relative ON versus OFF bipolar cell activity, where values greater than 1.0 indicate ON pathway dominance. Similarly, implicit time ratios were calculated relative to temporal processing between pathways. In addition VEP amplitude ratio (ON P2-N2 amplitude/ OFF P2-N2 amplitude): cortical-level index of ON/OFF pathway balance.

Flicker ERG and VEP analysis

Flicker ERG and VEP responses were analyzed in the frequency domain using MATLAB's Fast Fourier Transform (FFT) function fft(). This function computes the FFT of the sampled waveform, allowing the steady-state response to be described in the frequency domain. In the present study, each averaged flicker waveform was sampled at 1000 Hz and contained 1000 time points, producing a frequency resolution of 1 Hz. This allowed response amplitude and phase to be extracted directly at the stimulus frequency and its harmonics, shown in Figure 3.8 for OFF ERG waveform and amplitude extracted FFT.

The flicker stimulus was presented at 10 Hz. Therefore, the main response frequency of interest was 10 Hz, also called the fundamental frequency or 1f1 and the second harmonic at 20 Hz or 2f1. The two response frequencies were analyzed, the fundamental at 10 Hz, referred to as 1f1, which corresponds to the stimulus presentation rate, and the second

harmonic at 20 Hz, referred to as 2f1. The second harmonic was included because the focal flicker ERG studies have shown that the second-harmonic can reflect postreceptor, middle-to-inner retinal activity, whereas the fundamental response is strongly associated with outer retinal activity (Falsini et al. 1994). For VEP recordings, harmonic responses are also commonly analyzed in flicker paradigms because periodic visual stimuli can generate cortical responses at the stimulus frequency and at multiple of that frequency, providing additional information about nonlinear visual processing (Norcia et al. 2015)

For each participant, amplitude and phase were exported at each frequency. Amplitude represented response strength and was measured in microvolts. Phase represented the timing of the response within the flicker cycle and was measured in radians. Because phase values repeat every cycle, phase was also converted into a phase-derived delay in milliseconds. This delay was calculated separately for each frequency and represents where the response occurred within that frequency cycle, rather than a traditional peak latency. This per frequency latency was computed independently at 1f1 and at 2f1 for ON ERG, OFF ERG, ON VEP, and OFF VEP responses, and was the latency metric carried forward into all subsequent statistical analyses.

$$latency = \frac{\Phi}{2\pi \times f} x\ 1000$$

where Φ is the unwrapped phase in radians and f is frequency in Hz. This approach provides a single metric summarizing response latency that accounts for the delay from signal to response for the retina and cortex

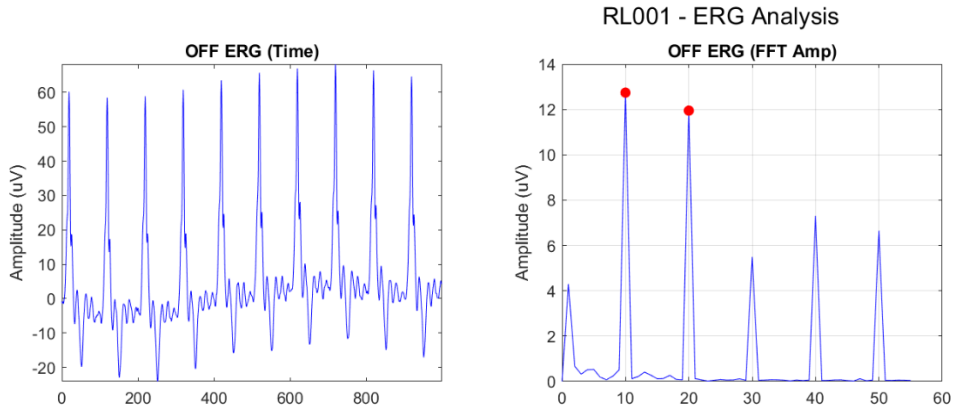

Figure 3.8 Representative FFT of OFF ERG Time-Domain Signal
The FFT applied to the time-domain signal (left panels), extracting the amplitude of the fundamental frequency (1f1) and its second harmonic (2f1).

To assess response reliability, signal to noise ratio (SNR) was computed at each harmonic by dividing the amplitude at the stimulus frequency (10 Hz) by the amplitude at the immediately adjacent non-stimulus frequency bin below the harmonic (9Hz for the 10 Hz fundamental). This metric is established practice for steady-state responses analysis (Cooper and Norcia 2015). Participants with SNR below 2 at either the fundamental or second harmonic were excluded from subsequent analyses for that specific channel, as responses below this threshold cannot be reliably distinguished from background noise.

3.5 - Psychophysical Measurements

Psychophysical testing was conducted to assess contrast sensitivity for ON and OFF pathway-selective stimuli at two spatial frequencies. This behavioral paradigm complemented the electrophysiological recordings by providing a perceptual measure of pathway function that integrates processing across the entire visual system.

3.5.1 Apparatus and Display Calibration

Stimuli were generated and displayed using an HP workstation running Linux, interfaced with a VPixx Technologies DataPixx display system (VPixx Technologies, Montreal, Canada). The 12-bit display operated at a 100 Hz refresh rate, providing precise temporal control of stimulus presentation. Custom software written in MATLAB (MathWorks, Natick, MA), utilizing the Psychophysics Toolbox extension (Brainard 1997) controlled stimulus generation and response collection. The display was gamma-corrected to ensure linear luminance output across the full contrast range. Mean display luminance was maintained at 65 cd/m, matching the background luminance conditions employed during electrophysiological testing to facilitate comparison between retinal/cortical responses and perceptual performance. Participants viewed the display binocularly with their habitual refractive correction, with head position stabilized using a chin and forehead rest

3.5.2 Difference-Of-Gaussians Stimuli

Pathway-selective stimuli consisted of circularly symmetric difference of gaussians (DoG) patterns, which approximate the center-surround receptive field organization of retinal ganglion cells (Figure 3.9). The DoG luminance profile was defined by equation:

$$DoG\ (x)\ =\ 2.56\, e^{-2.56x^2/2a^2} - e^{-x^2/2a^2}$$

where α represents the standard deviation of the center of the Gaussian. This formulation produces a balanced stimulus with zero mean luminance, ensuring that ON and OFF stimuli differ only in contrast polarity. For ON stimuli, the center was brighter than the surround (positive contrast); for OFF stimuli, the center was darker than the surround (negative contrast)

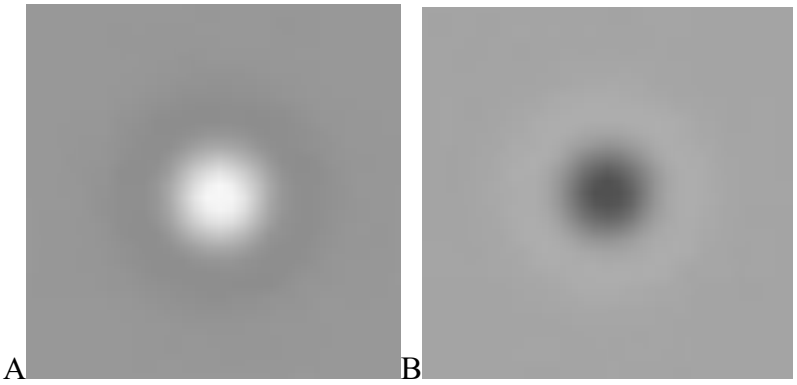

Figure 3.9 Difference-of-Gaussians (DoG) stimuli
(A) ON stimulus with positive contrast polarity: the center region is brighter than the surrounding annulus, preferentially activating the ON pathway. (B) OFF stimulus with negative contrast polarity: the center region is darker than the surrounding annulus preferentially activating the OFF pathway.

Participants were tested at two viewing distances to assess contrast sensitivity under high- and low-spatial-frequency conditions that preferentially stimulate the ON and OFF visual pathways. The ON and OFF pathways differ systematically in receptive field center size and spatial frequency tuning, with OFF pathway retinal ganglion cells possessing smaller receptive field centers and greater sensitivity to high spatial frequencies, while ON pathway cells have larger centers tuned to lower spatial frequencies (Ravi et al. 2018). The same physical DoG stimulus was therefore presented at two distances to exploit this asymmetry. At 114 cm, the DoG center subtended 0.18° of visual angle at half height and the surround was 0.27°, targeting the lower spatial frequency preferences of the ON pathway. At 228 cm, the same stimulus subtended 0.09° of visual angle at half height and the surround was 0.135°, effectively doubling the spatial frequency content and shifting stimulus parameters toward the OFF pathway's tuning range. The radial spatial-frequency content of the DoG stimulus was estimated from the angular size of the center and surround Gaussians using the following formula

$$\sigma = \frac{HWHH}{\sqrt{2ln2}}$$

where σ is the Gaussian standard deviation in degrees of visual angle. The peak spatial frequency of the DoG was then estimated using the following equation

$$fpeak = \sqrt{\frac{ln(\sigma s^2 / \sigma c^2)}{2\pi^2(\sigma s^2 - \sigma c^2}}$$

where σc is the standard deviation of the center Gaussian, σs is the standard deviation of the surrounding Gaussian, and fpeak is expressed in cycles per degree (cpd).

At the 114 cm viewing distance, the center and surround HWHH values were 0.18° and 0.27°, respectively. These values corresponded to σc = 0.153° and σs = 0.229°, producing an approximate peak spatial frequency of 1.19 cpd. At the 228 cm viewing distance, the same physical stimulus subtended half the angular size, with center and surround HWHH values of 0.09° and 0.135°, respectively. These values corresponded to σc = 0.076° and σs = 0.115°, producing an approximate peak spatial frequency of 2.37 cpd. Thus, the 114 cm condition corresponded to a lower-spatial-frequency DoG stimulus of approximately 1.19 cpd, whereas the 228 cm condition corresponded to a higher-spatial-frequency DoG stimulus of approximately 2.37 cpd. For clarity, the 114 cm viewing condition is referred to hereafter as the lower spatial frequency condition (LSF) and the 228 cm viewing condition is referred to hereafter as the higher spatial frequency condition (HSF). Therefore, doubling the viewing distance approximately doubled the peak spatial frequency of the stimulus. This approach enabled psychophysical assessment of ON and OFF pathway contrast sensitivity across two spatial frequency conditions using the same identical physical stimuli.

Centrally presented DoG stimuli were used because the psychophysical component of this thesis was designed as a planned replication and extension of prior work from our laboratory using the same ON/OFF DoG detection paradigm. Hogue and Taylor (2022) reported that the OFF/ON sensitivity ratio for DoG targets increased with axial length, suggesting that axial elongation may be associated with altered perceptual balance between contrast polarities. The present study retained a comparable central DoG detection task to test whether this relationship would replicate in an independent cohort and to determine whether

psychophysical ON/OFF effects aligned with retinal and cortical responses measured using ERG and VEP. This design does not assume that the fovea is the only retinal region involved in emmetropization. Rather, the relative contributions of foveal, parafoveal, and peripheral retinal signals to eye-growth regulation remain unresolved. Recent point-counterpoint discussion has emphasized both local peripheral retinal mechanisms and the continued biological plausibility of central retinal contributions to human refractive development (Schaeffel et al. 2025).

3.5.3 Experimental Paradigm

Contrast detection thresholds were measured using a two-alternative forced-choice (2AFC) temporal paradigm wherein two 100 ms stimuli were presented 300 milliseconds apart. One interval contained the DoG target stimulus, while the other contained only the uniform background (foil). The target appeared with equal probability in either the first or second interval.

Each observation interval was accompanied by a distinct auditory tone to clearly demarcate the observation periods. To minimize spatial uncertainty regarding the target location, two horizontal reference lines were displayed to the left and right of the stimulus region throughout each interval. Participants indicated whether the target appeared in the first or second interval by pressing the corresponding button on a response controller (left button for first interval; right button for second interval). Immediate auditory feedback was provided following each response, which was a high-pitched tone indicating a correct response, and a low-pitched tone indicated an incorrect response.

The 2AFC paradigm was selected for its robustness against response bias, as the criterion-free nature of the forced-choice design ensures that threshold estimates reflect sensory sensitivity rather than decision criteria (García-Pérez and Alcalá-Quintana 2011). This methodological approach is widely employed in psychophysical research for precisely this advantage. This makes the method well suited for estimating contrast detection thresholds for ON- and OFF-polarity DoG stimuli.

3.5.4 Contrast Levels and Threshold Estimation

Stimulus contrast was varied according to the method of constant stimuli. For the LSF, seven contrast levels spanning 0.01 to 0.10 root mean square (RMS) contrast were employed. For the HSF, seven contrast levels ranged from 0.05 to 0.20 RMS to accommodate the expected elevation in thresholds at HSF. The higher contrast range in HSF condition was selected because the smaller angular size of the stimulus was expected to produce a higher detection threshold. These contrast ranges were determined through pilot testing to ensure adequate sampling of the psychometric function across the transition from chance to ceiling performance.

Psychometric functions were fitted to the response data using a generalized linear model (GLM) with a binomial error distribution and contrast threshold was defined as the stimulus contrast yielding 75% correct performance, on the fitted psychometric function (Figure 3.10). Threshold values were subsequently converted to log sensitivity for statistical analysis.

$$LogCS = log10(\frac{1}{threshold})$$

Higher LogCS values therefore indicate better contrast sensitivity, whereas lower LogCS values indicate poorer contrast sensitivity.

3.5.5 Testing Protocol and Session Structure

Before experimental trials, each participant completed ten practice trials at maximal contrast to ensure task comprehension. Successful completion, defined as at least nine correct responses, was verified by the experimenter before proceeding. Participants who did not meet this criterion repeated the practice block. If performance remained below threshold after two attempts, double the standard maximum contrast was used for practice before testing commenced.

Testing was conducted across two sessions on separate days. In one session, participants completed all ON stimulus conditions (near and far viewing distances); on the other day, they completed all OFF stimulus conditions. The order of stimulus conditions across days and the order of viewing distances within each day were counterbalanced across participants using a randomized schedule. This design ensured that every four consecutive participants began with a different combination of conditions, controlling for potential order effect.

Each testing session comprised four blocks of 175 trials, yielding 700 trials per stimulus polarity and viewing distance combination. The task was self-paced, and

participants were permitted breaks between blocks as needed; sessions typically lasted 45-60 minutes.

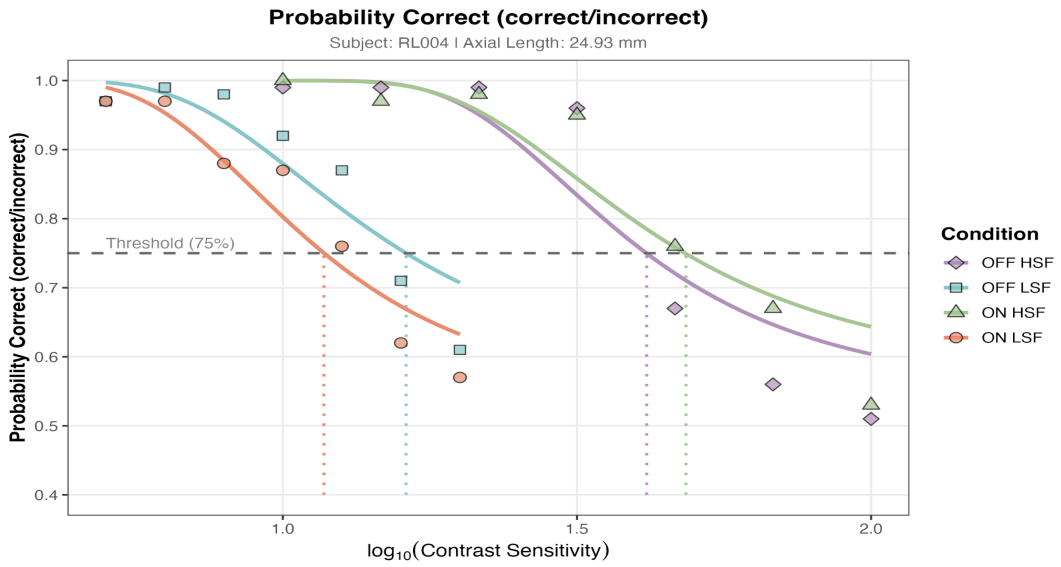

Figure 3.10 Representative psychometric functions for ON and OFF DoG contrast detection at higher and lower spatial frequency.
Psychometric function plots of proportion of correct responses against stimulus contrast (RMS units) for one representative subject completing the two-alternative forced-choice (2AFC) task, featuring fitted curves and a horizontal dashed line indicating the 75% correct criterion.

3.5.6 Psychophysical Indices

All derived indices were computed on long-transformed contrast sensitivity values to ensure that pathway comparisons were made on a perceptually linear scale. Two complementary indices were computed to assess the relative balance between ON and OFF pathways at each spatial frequency. The OFF/ON Index was calculated as (OFF-ON)/(OFF+ON), where OFF represents OFF pathway log contrast sensitivity and ON

represents ON pathway log contrast sensitivity. Positive values indicate relatively greater OFF sensitivity compared with ON sensitivity, negative values indicate relatively greater ON sensitivity compared with OFF sensitivity, and values near zero indicate relatively balanced ON and OFF sensitivity. This index was used to test whether axial length was associated with a shift in perceptual balance between contrast polarities, rather than a proportional reduction in both pathways. To assess whether contrast sensitivity differed across spatial scales within each pathway, relative spatial-frequency sensitivity ratios were also calculated. The ON Relative Sensitivity was computed as LSF ON/ HSF ON, and the OFF Relative Sensitivity as LSF OFF/ HSF OFF. Values greater than 1.0 indicate low spatial frequency sensitivity exceeds high spatial frequency for that pathway. An Average Relative Sensitivity was additionally computed as the average of near sensitivity across both pathways divided by the average of far sensitivity across both pathways, providing a single distance-dependent index collapsed across pathway identity.

3.6 - Data Processing and Analysis

All data processing and statistical analysis were performed using standardized methods to ensure reproducibility and consistency across participants. Electrophysiological signals were processed in MATLAB 2023b (Mathworks, Natick, MA), while psychophysical data and statistical analyses were conducted in R version 4.5.2 (R Foundation for Statistical Computing, Vienna, Austria).

Before inferential testing, continuous variables were assessed for normality using the Shapiro-Wilk test, with visual inspection of histograms and Q-Q plots used to supplement

formal testing. Because several outcome variables were not normally distributed and because the primary question concerned whether each measure changed monotonically with AXL, Spearman rank correlation coefficients were used as the primary correlation analysis. Correlations were performed between axial length and each ON- and OFF pathway outcome measure, including flash ERG, flash VEP, flicker ERG, flicker VEP, psychophysical contrast sensitivity, and derived ON/OFF ratio or index measures. Statistical significance for the planned correlation analyses was set at $\alpha = 0.05$ using two-tailed tests.

The correlation analyses were treated as the primary planned analyses and were reported using unadjusted p-values. This approach was chosen because the study was designed a priori to test biologically motivated relationships between axial length and pathway-specific function across distinct levels of the visual hierarchy. Flash ERG, flash VEP, flicker ERG, flicker VEP, and psychophysical contrast sensitivity were considered separate planned outcome domains because they reflect different neural generators, stimulus paradigms, and levels of visual processing. Therefore, the correlation analyses were interpreted using effect direction, effect magnitude, exact p-values, and consistency across related measures rather than as a single exploratory search across interchangeable endpoints.

Median-split analyses were performed as secondary exploratory follow-up comparisons for variables that demonstrated significant or trend-level associations with axial length in the primary correlation analysis, defined as $p \leq 0.10$. Participants were divided into shorter- and longer-axial-length groups using the sample median axial length for the relevant analysis cohort. Because this cutoff was determined from the observed sample rather than from an independently established biological threshold, median-split analyses were used only

to aid visualization and describe group-level differences. These analyses were not interpreted as evidence of a true threshold effect. Group differences between shorter- and longer-axial-length participants were evaluated using Wilcoxon rank-sum tests.

Because the median-split analyses were exploratory follow-up tests, their p-values were adjusted for multiple comparisons using the Holm step-down procedure (Holm 1979). All median-split tests were treated as one pooled exploratory family. For a family of m median-split tests, the raw p-values were ordered from smallest to largest:

$$p(1) \leq p(2) \leq \ldots \leq p(m)$$

For the p-value at ordered rank i, the Holm adjusted value was calculated as:

$$p(i)' = (m - i + 1)p(i)$$

Adjusted p-values were constrained to be nondecreasing across the ordered sequence and capped at 1.0. This procedure controls the familywise error rate while being less conservative than a standard Bonferroni correction. Only Holm-adjusted p-values were used for statistical interpretation of the exploratory median-split analyses.

It is also worth noting that the range of refractive error and AXL in this sample was narrower than in many earlier studies, and the relationship between the two was weaker than usually reported. Participants were split into Short and Long AXL groups based on the sample median. In the overall cohort, the short group consisted of 5 emmetropes, 1 hyperope and 12 myopes (22.50 - 25.00 mm; RE -4.38 D – +1.15 D), while the long group consisted entirely of 18 myopes (25.07 - 27.51 mm; RE -6.88 D – 0.00 D) with median split of 25.04

mm. A similar distribution was observed within the ERG/VEP cohort, where the short group included 5 emmetropes, 1 hyperope and 11 myopes (22.50-25.00 ; RE -4.38 D – +1.15 D), and the long group included 16 myopes (25.07-27.51 mm; RE -6.88 D – 0.00 D) with median split of 25.00mm. In the psychophysics cohort, the short group comprised 5 emmetropes and 12 myopes (22.50-25.07 mm; RE -6.00 D – +0.50 D) and the long group 17 myopes (AXL: 25.30 – 27.51 mm; RE -6.88 D – 0.00 D) with median split of 25.19 mm. Group differences were evaluated using the Wilcoxon rank-sum test, a non-parametric alternative to the independent samples t-test that does not assume normal distributions.

3.7 - Equipment Calibration and Reliability

All devices underwent calibration before data collection. The ColorDome system was verified for uniform luminance and flash accuracy with a self-calibrating routine. The DataPixx display was characterized and gamma-corrected to ensure that contrast increments were linear and that the bit-depth of the display resolved fine contrast steps, such that one percent contrast was distinguishable from one point one percent contrast (Brainard 1997). Testing took place in a quiet, dim environment to reduce ambient interference. These measures were intended to maintain high-quality, reproducible data.

4 - Results

4.1 Baseline Characteristics

The overall study cohort comprised 36 subjects (mean age: 25.0 ± 2.2 years; 21 female). Baseline ocular biometry for full cohort revealed a mean spherical equivalent refraction of -3.11 ± 2.30 D (-6.88 to +1.15 D) and a mean AXL of 24.97 ± 1.17 mm (22.50 to 27.51 mm). All 36 participants contributed at least one analyzable electrophysiology or psychophysical ON/OFF pathway measure. Within this cohort, 34 subjects completed the psychophysics and 33 completed the ERG and VEP protocol. AXL was significantly associated with spherical equivalence of refractive error, shown in Figure 4.1. Cohort baseline demographics and ocular characteristics are summarized in Table 4.1.

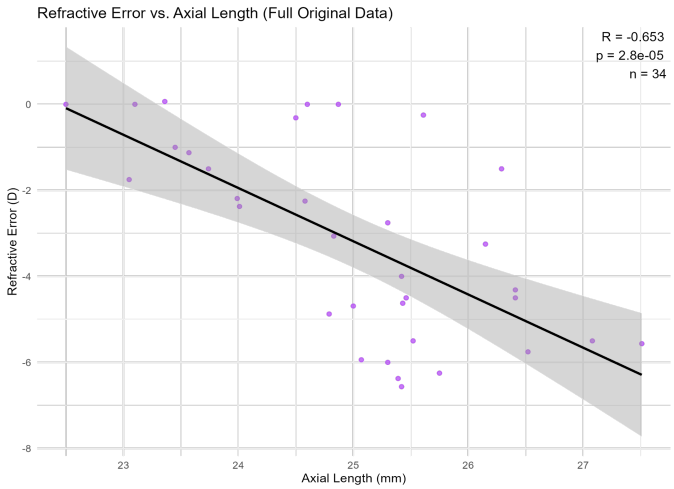

Figure 4.1 Baseline Refractive Error vs. Axial Length.
Scatter plot displaying individual participant data between spherical equivalent refractive error (D) and axial length.

Table 4.1 Baseline Demographics and Ocular Characteristics. Summary of participant demographics and ocular characteristics.

Variable	Mean	Median	SD	CV %	Min	Max
Age (yrs)	25.00	25.00	2.22	8.89	22.00	32.00
Axial Length (mm)	24.97	25.04	1.17	4.67	22.50	27.51
IOP (mmHg)	15.11	16.00	2.39	15.80	10.00	20.00
CCT (um)	542.11	541.00	26.85	4.95	487.00	597.00
ACD (mm)	3.54	3.62	0.35	10.00	2.83	4.18
LT (mm)	3.61	3.59	0.17	4.78	3.18	4.04
K1 (D)	42.95	42.97	1.60	3.72	39.47	45.82
K2 (D)	43.99	44.35	1.62	3.68	40.78	47.11
M (D)	-3.04	-3.00	2.49	-81.72	-6.75	2.00
J0 (D)	0.20	0.00	0.33	167.17	-0.36	1.25
J45 (D)	0.00	0.00	0.15	10543.85	-0.50	0.37
Pupil Dim (mm)	5.61	6.00	0.85	15.13	4.00	7.00
Pupil Bright (mm)	3.31	3.00	0.72	21.67	2.00	5.00
MEM (D)	0.52	0.50	0.24	46.86	0.00	1.00

Abbreviations:
ACD: Anterior Chamber Depth; CCT: Central Corneal Thickness; CV: Coefficient of Variation; IOP: Intraocular Pressure
LT: Lens Thickness; MEM: Monocular Estimation Method (Retinoscopy); SD: Standard Deviation

4.2 Electroretinography and Visual Evoked Potentials

To address Aim 1, the relationship between AXL and ON/OFF pathway function at the retinal level was examined using flash and flicker ERG recordings with pathway-selective sawtooth stimuli. Spearman rank correlations served as the primary analytical approach, with median split analysis applied to variables demonstrating trend-level associations ($p<0.10$)

4.2.1 ON and OFF Flash ERG

Flash ERG responses were successfully recorded from 33 participants for ON pathway stimulation and 32 participants for OFF pathway stimulation. Figure 4.2 presents representative ON-flash and OFF-flash ERG waveforms with component markers indicating measurement locations used for amplitude and implicit time extraction. The ON-Flash

response exhibits the characteristic a-wave, b-wave, and photopic negative response (PHNR), while the OFF flash response shows the d-wave followed by the PHNR.

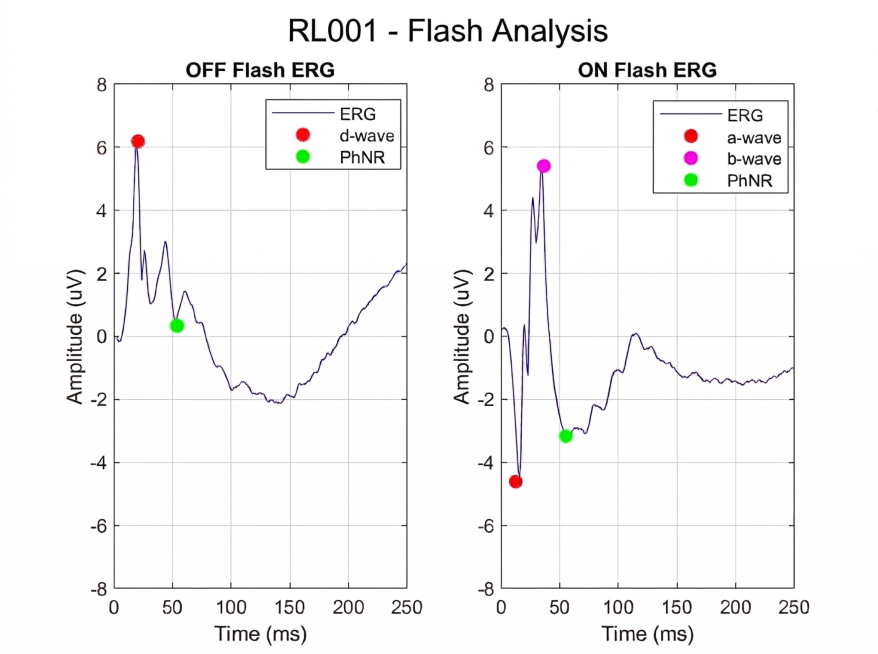

Figure 4.2 Representative ON and OFF Flash ERG Waveforms with Component identification. The OFF Flash on the left shows the d-wave (red dot) and the PhNR (green dot). The ON-Flash on the right shows the a-wave (red dot), b-wave (purple dot) and PhNR (green dot).

Descriptive statistics for all transient ERG amplitude and implicit time variables, along with b/d amplitude ratios, are summarized in Table 4.2. ON pathway components showed a mean a-wave amplitude of 28.54 ± 9.84 uV and mean b-wave amplitude of 52.99 ± 18.86 uV. OFF pathway d-wave amplitude averaged 28.48 ± 15.19 uV, and the mean b/d ratio of 2.33 indicates modest ON pathway dominance, consistent with normal photopic recordings.

Variability was higher for the PhNR components than for the a-wave, b-wave, and d-wave, as reflected in the larger coefficients of variation.

Table 4.2 Summary Statistics for ERG Variables. Summary of flash ERG wave component implicit times (ms), amplitudes (uV), and amplitude ratios including Mean, Median, Standard Deviation (SD), Minimum (Min), Maximum (Max), and Coefficient of Variation (CV %).

Variable	Mean	Median	SD	Min	Max	CV %
d-wave Implicit Time (ms)	20.19	20.00	0.90	19.00	22.00	4.44
d-wave Amplitude (uV)	28.48	25.29	15.19	7.30	67.05	53.33
OFF PhNR Implicit Time (ms)	44.94	34.00	14.54	29.00	65.00	32.37
OFF PhNR Amplitude (uV)	17.14	13.04	19.00	0.37	94.49	110.83
a-wave Implicit Time (ms)	16.48	16.00	0.76	16.00	19.00	4.58
a-wave Amplitude (uV)	28.54	27.54	9.84	12.48	55.66	34.49
b-wave Implicit Time (ms)	33.42	35.00	4.11	27.00	38.00	12.29
b-wave Amplitude (uV)	52.99	50.79	18.86	16.10	100.94	35.58
ON PhNR Implicit Time (ms)	66.03	70.00	9.16	52.00	80.00	13.87
ON PhNR Amplitude (uV)	38.37	35.25	13.10	16.46	62.90	34.13
b/a Amplitude Ratio	1.89	1.89	0.45	1.24	2.70	23.75
b/d Amplitude Ratio	2.33	1.72	1.82	0.91	10.70	78.04

Correlation with Axial Length

Spearman correlation analyses were conducted to examine relationships between AXL and flash ERG parameters for both the ON and OFF pathways.

ON Pathway Flash ERG:

No statistically significant correlations with AXL were observed for any ON pathway flash ERG parameters (Figure 4.3). For amplitude measures, a-wave amplitude ($r = 0.058$, $p = 0.749$) and b-wave amplitude ($r = -0.209$, $p = 0.243$) showed no significant associations with AXL. In the temporal domain, a-wave implicit time ($r = -0.093$, p-0.607) or b-wave implicit

time (r = -0.128, p = 0.477) were similarly non-significant. PhNR amplitude (r = 0.170, p = 0.345) and PhNR implicit time (r = 0.174, p = 0.332) showed no significant correlations with AXL.

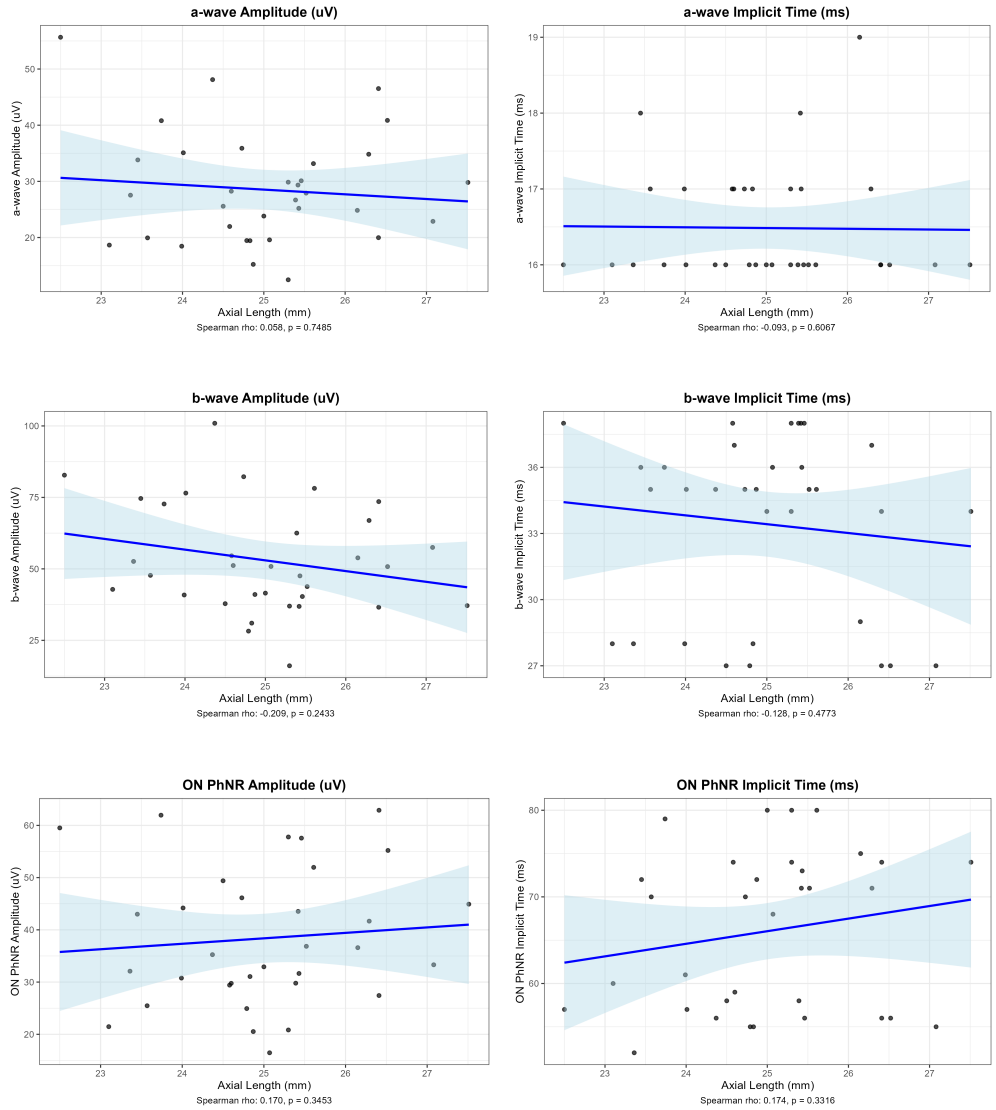

Figure 4.3 Correlation between Axial Length and ON Flash ERG Parameters. Scatter plots between AXL (mm) and ON Flash ERG amplitude (uV) and implicit time (ms) parameters of 33 subjects from the flash ERG experiments with linear regression lines of best fit and 95% confidence intervals (shaded regions).

OFF Pathway Flash ERG:

No statistically significant correlations with AXL were observed for OFF pathway flash ERG parameters (Figure 4.4). Neither Amplitude (r = 0.217, p = 0.212) nor implicit time (r = 0.217,p = 0.233) of d-wave demonstrated any significant association with AXL. OFF PhNR amplitude (r = -0.102, p = 0.586) and implicit time (r = -0.016, p = 0.932) showed no associations with AXL.

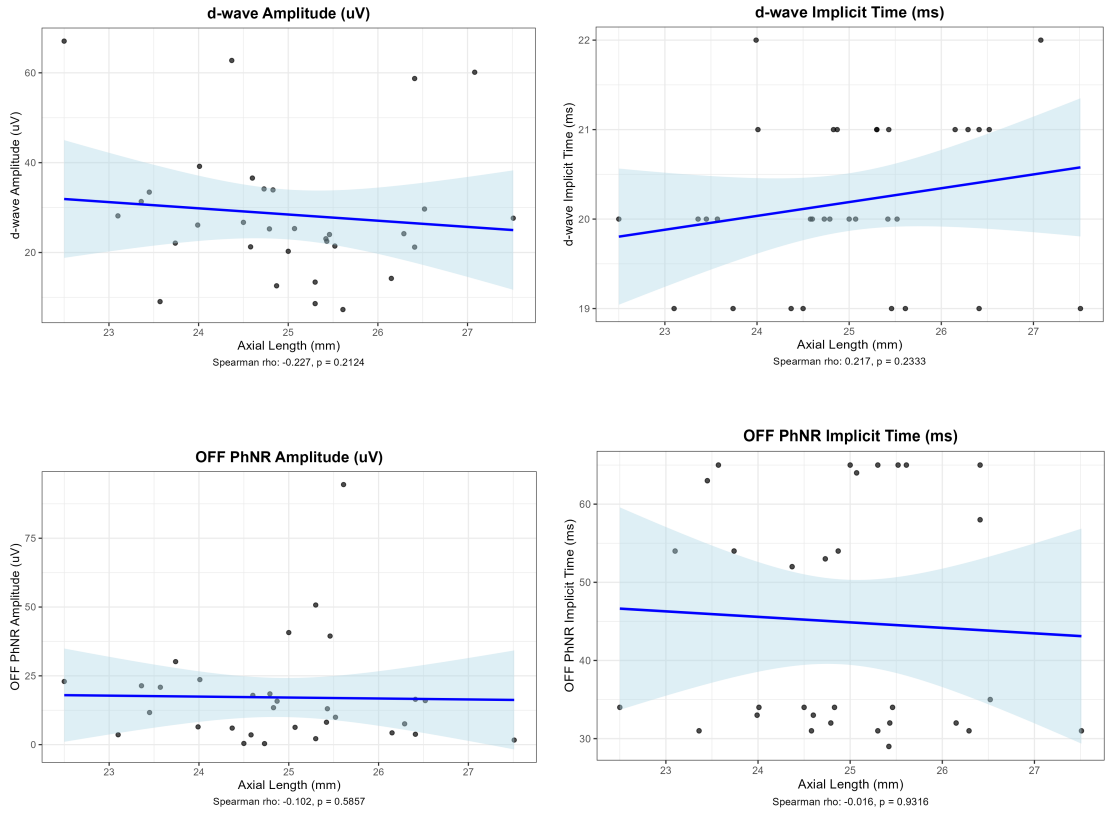

Figure 4.4 Correlation between Axial Length and OFF Flash ERG Parameters.
Scatter plots between AXL (mm) and OFF Flash ERG amplitude (uV) and implicit time (ms) parameters of 32 subjects from the flash ERG experiments with linear regression lines of best fit and 95% confidence intervals (shaded regions).

ON/OFF Pathway Balance: b/d amplitude ratio

The mean b-wave to d-wave amplitude ratio across all participants was 2.33. In Figure 4.5, Spearman correlation analysis revealed no significant associations between b/d ratio and AXL ($r = -0.011$, $p = 0.953$). The mean b-wave to a-wave amplitude ratio across all participants showed no correlation with AXL ($r = -0.243$, $p = 0.174$). No flash ERG parameters met the $p<0.10$ threshold for supplementary median split analysis.

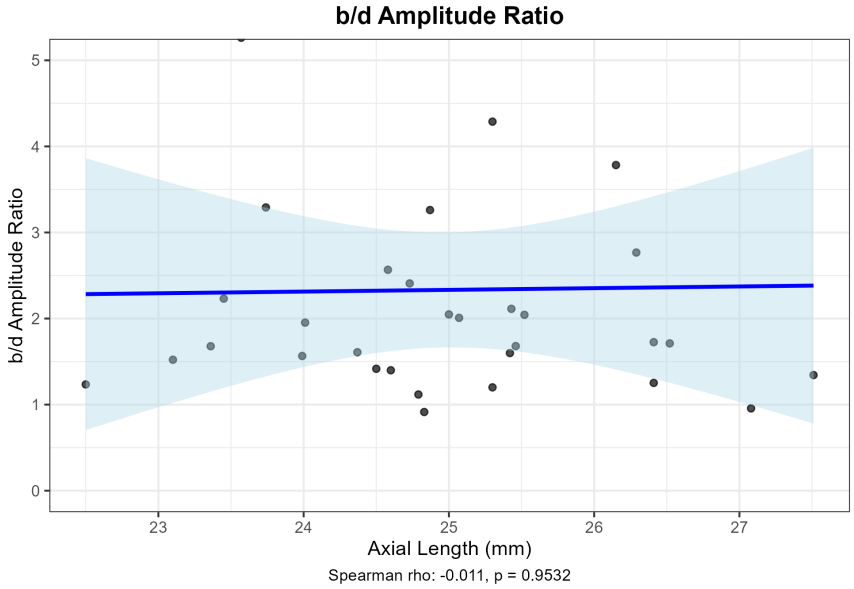

Figure 4.5 Correlation between axial length and b-wave to d-wave ratios in flash ERG. Scatter plot between AXL (mm) and the calculated b/d amplitude ratio of 32 subjects from the flash ERG experiments with a linear regression line of best fit and 95% confidence intervals (shaded region).

4.2.2 ON and OFF Flash VEPs

To further address Aim 2, the relationship between AXL and ON/OFF pathway processing at the cortical level was examined using flash VEP recordings. Flash VEP recordings were

successfully obtained from 33 participants. Representative ON-Flash and OFF-Flash VEP waveforms from a single participant are shown in Figure 4.6, with component markers identifying the N1, N2, N3, and P1, P2, P3 peaks used for amplitude and time to peak extraction. Both pathways exhibited the characteristic flash VEP morphology, with N2 and P2 emerging as the most prominent and consistent components.

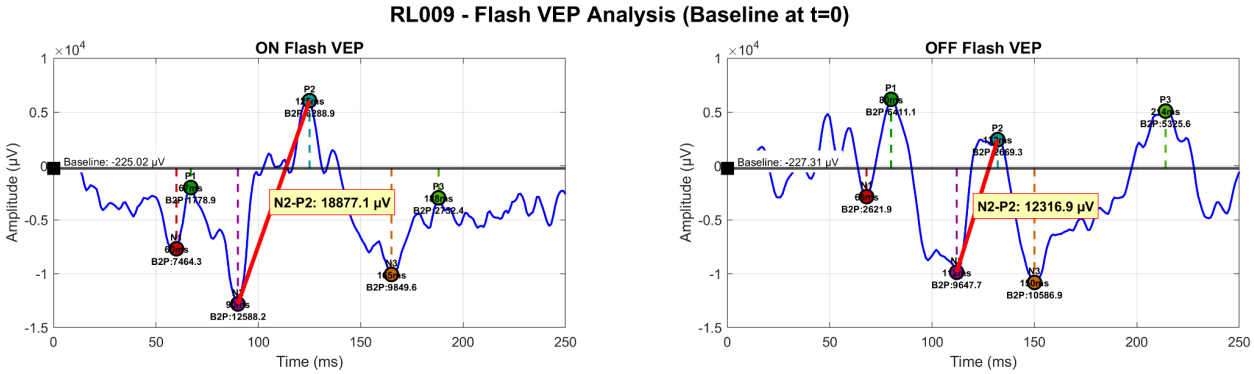

Figure 4.6 Representative Flash ON and OFF VEP waveforms. Line plots of amplitude (uV) versus time (ms) for representative ON Flash VEP and OFF Flash VEP waveforms from the flash VEP experiments with component peaks identified by circular markers and N2-P2 peak-to-peak amplitude differences highlighted.

Descriptive statistics for all flash VEP parameters, including N2 and P2 time to peaks, N2-P2 peak-to-peak amplitudes, and the dimensionless ON/OFF pathway ratios, are summarized in Table 4.4. Across the sample, ON pathway components showed mean N2 time to peak of 75.55 ± 10.91 ms and mean P2 time to peak of 115.48 ± 13.66 ms, with a mean N2-P2 peak-to-peak amplitude of 15.73 ± 6.60 uV. OFF pathway components were systematically delayed relative to the ON pathway, with mean N2 time to peak of 100.18 ± 12.17 ms and

mean P2 time to peak of 132.55 ± 17.27 ms, and showed a smaller mean N2-P2 peak-to-peak amplitude of 9.11 ± 4.79 uV. The mean VEP N2-P2 amplitude ratio (ON/OFF) was 2.57 ± 2.88, indicating ON pathway dominance at the cortical level. Variability was substantially higher for amplitude measures than for time to peaks, as reflected in the larger coefficients of variation.

Table 4. 3 Summary Statistics for VEP Variables. Summary of flash VEP component time to peak (ms), peak-to-peak amplitudes (uV), and pathway ratios including Mean, Median, Standard Deviation (SD), Minimum (Min), Maximum (Max), and Coefficient of Variation (CV %).

Variable	Mean	Median	SD	Min	Max	CV %
ON N2 Time (ms)	75.55	73.00	10.91	65.00	110.00	14.44
ON P2 Time (ms)	115.48	112.00	13.66	97.00	159.00	11.83
ON N2 P2 Peak-to-Peak	15.73	15.20	6.60	4.41	30.73	41.97
OFF N2 Time (ms)	100.18	102.00	12.17	68.00	120.00	12.15
OFF P2 Time (ms)	132.55	131.00	17.27	97.00	172.00	13.03
OFF N2 P2 Peak-to-Peak	9.11	7.99	4.79	1.78	19.38	52.62
VEP N2-P2 Amplitude Ratio	2.57	1.89	2.88	0.32	16.83	111.99
VEP N2 Time Ratio	0.77	0.73	0.17	0.54	1.28	22.33
VEP P2 Time Ratio	0.89	0.88	0.15	0.64	1.29	17.49

Correlation with Axial Length

Spearman correlation analyses examined relationships between AXL and flash VEP parameters.

On-Pathway Flash VEP

No significant correlation with AXL was observed for any ON pathway flash VEP parameters, shown in Figure 4.7. N2 peak time ($r = 0.165$, $p = 0.359$), P2 peak time ($r = -$

0.178, p = 0.322) and N2-P2 peak to peak amplitude (r = -0.232, p = 0.193) showed non-significant correlations with AXL.

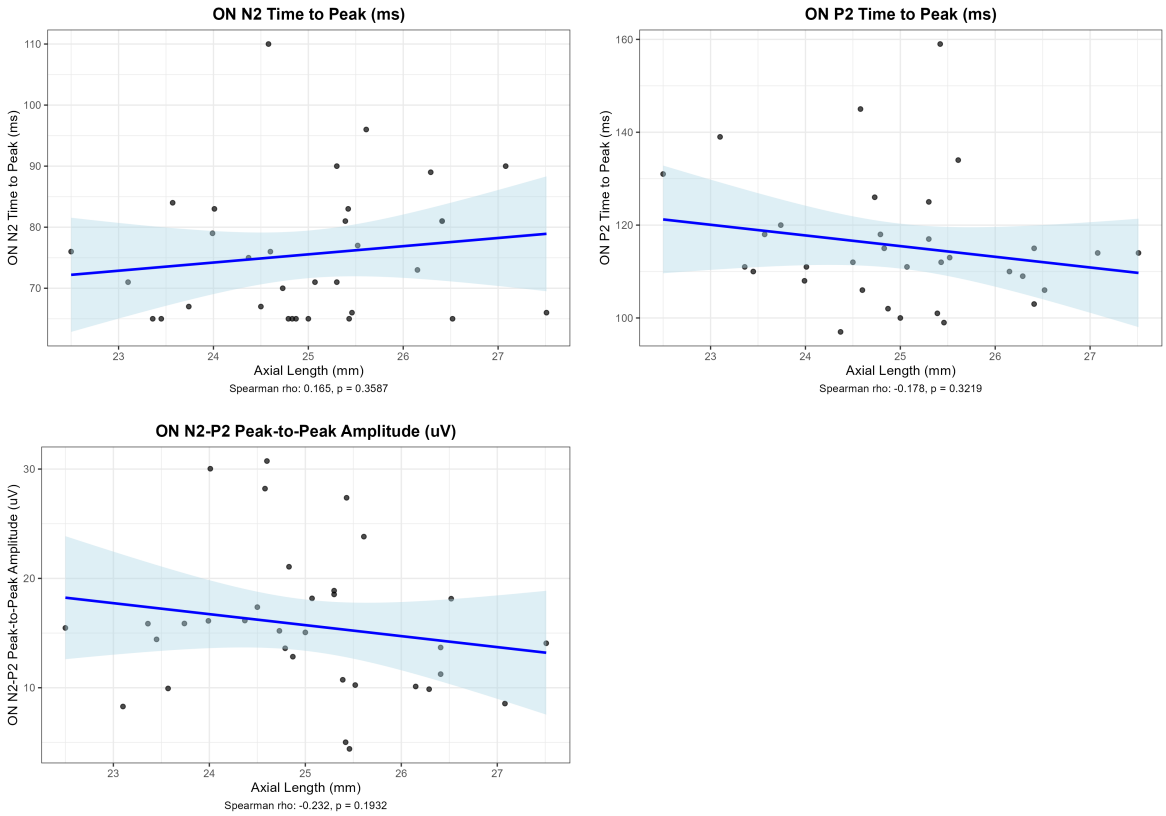

Figure 4.7 Relationship between Axial Length (AXL) and ON Pathway Flash VEP Parameters. Scatter plots between AXL (mm) and ON Pathway Flash VEP time to peak (ms) and peak-to-peak amplitude (uV) from the flash VEP experiments with linear regression lines of best fit and 95% confidence intervals (shaded regions).

OFF Pathway Flash VEP

No statistically significant correlations with AXL were observed for OFF pathway flash VEP parameters, though one parameter approaches significance (Figure 4.8). OFF N2 time to peak demonstrated a trend toward positive correlation with AXL (r = 0.316, p = 0.073). Neither P2

time to peak (r = 0.192, p = 0.284), nor did N2-P2 peak-to-peak amplitude (r = 0.057, p = 0.752) were significantly correlated with AXL.

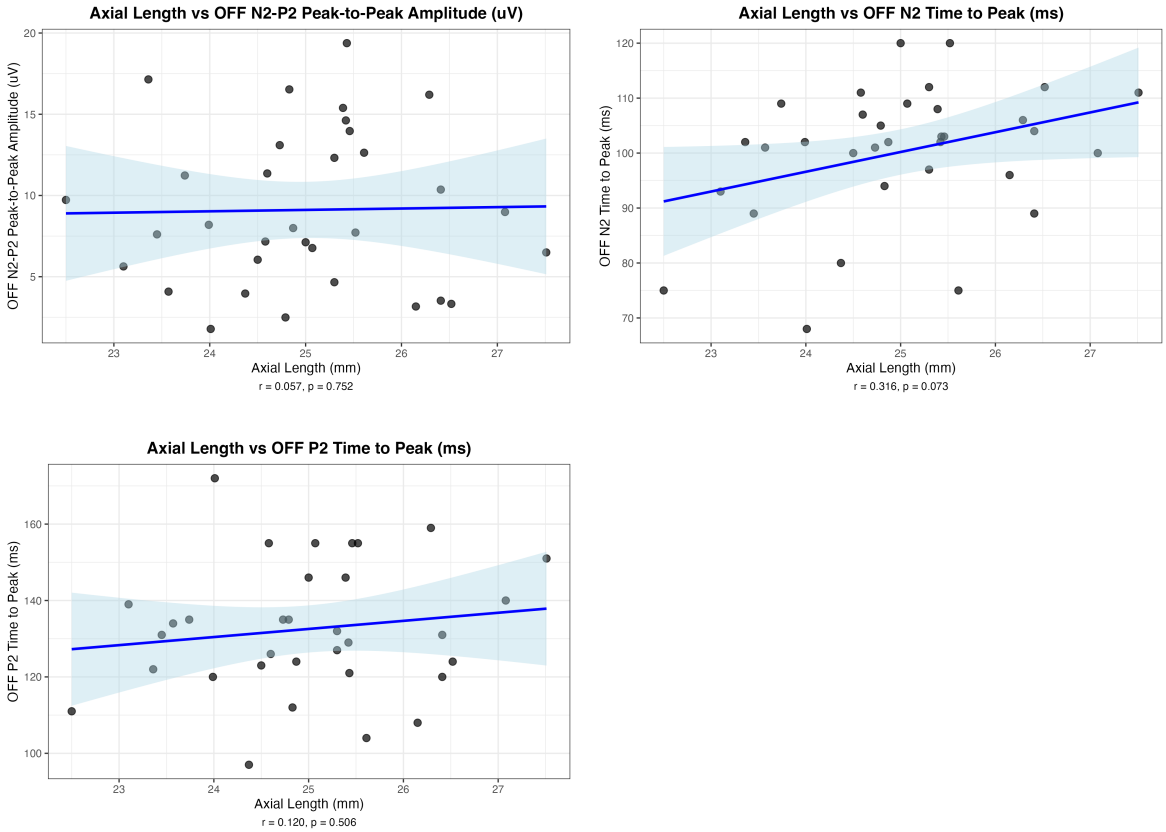

Figure 4.8 Relationship between axial length and OFF pathway Flash VEP Parameters. Scatter plots between AXL (mm) and OFF pathway Flash VEP time to peak (ms) and peak-to-peak amplitude (uV) from the flash VEP experiments with linear regression lines of best fit and 95% confidence intervals (shaded regions).

Median-Split Analysis:

Median-split analyses were included as exploratory follow-up comparisons to visualize group-level differences between shorter and longer AXL participants. Because AXL is a continuous variable, Spearman correlations were interpreted as the primary

analyses. Median-split comparisons were interpreted using Holm-adjusted p-values calculated across the pooled median-split family.

Because OFF N2 time to peak met the prespecified criterion for exploratory follow-up testing, a median split comparison was performed to visualize group-level differences. Longer AXL participants showed longer OFF N2 time to peak than shorter AXL participants (shorter AXL: 97.59 ± 13.34 ms, n = 17; longer AXL: 102.94 ± 10.52 ms, n = 16). This group-level pattern followed the same direction as the positive Spearman correlation, but the exploratory comparison was not statistically significant after correction for multiple comparisons (p = 0.159).

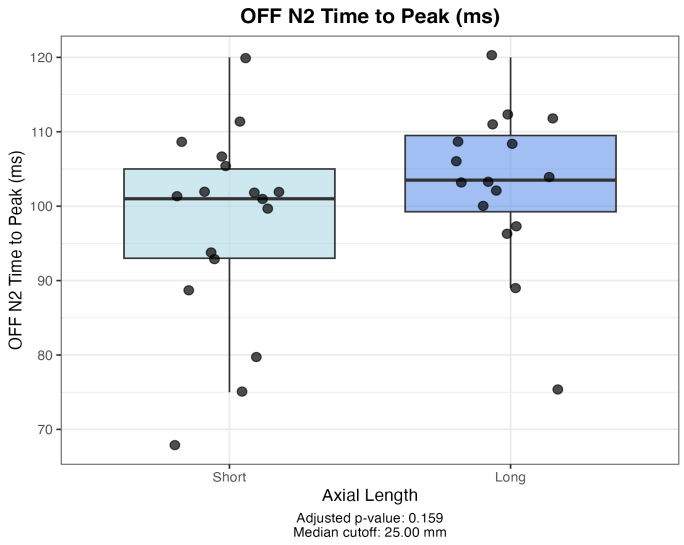

Figure 4.9 Median Split Analysis for OFF VEP N2 Time to Peak. Box plots of OFF N2 time to peak (ms) for shorter and longer AXL groups from the flash VEP experiments with overlaid individual participant data points and horizontal lines indicating the median.

ON/OFF pathway balance

ON/OFF ratios were calculated for N2-P2 amplitude, shown in Figure 4.10. None of the ON/OFF pathway balance demonstrated a significant correlation with AXL (r = -0.140, p = 0.438).

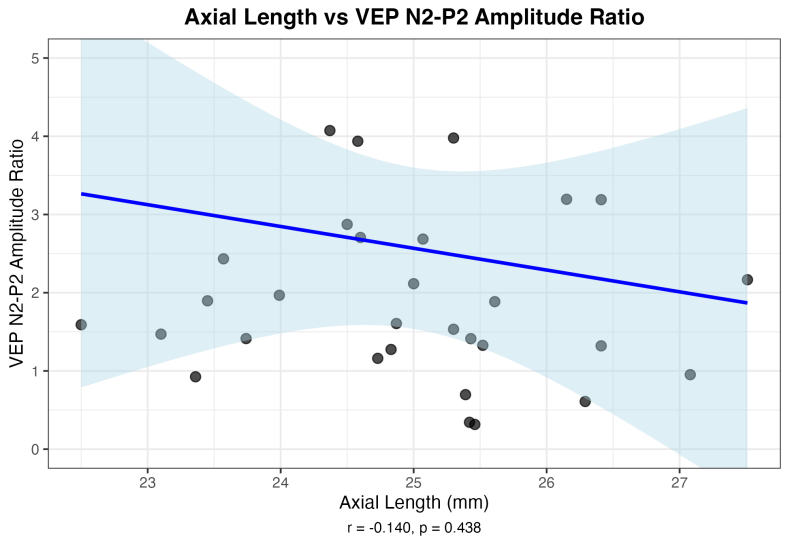

Figure 4.10 Correlation between Axial Length and VEP N2-P2 Amplitude Ratio. Scatter plot between AXL (mm) and the VEP N2-P2 amplitude ratio from the flash VEP experiments with a linear regression line of best fit and 95% confidence intervals (shaded region).

4.2.3 ON and OFF Flicker ERG

Steady-state flicker ERGs were successfully recorded from 33 participants. Following acquisition, each 1000 ms recording underwent Fast Fourier Transform (FFT) analysis to extract frequency-domain metrics, yielding amplitude and phase values at the 1f1 and 2f1. Representative time-domain waveforms and their corresponding frequency-domain spectra

from a single participant are shown in Figure 4.11. Both ON and OFF time-domain recordings exhibited clear stimulus-locked oscillations at the 10 Hz fundamental, and the FFT spectra, which shows energy concentrated at the 10 Hz fundamental (1f1) and the 20 Hz second harmonic (2f1) for both pathways.

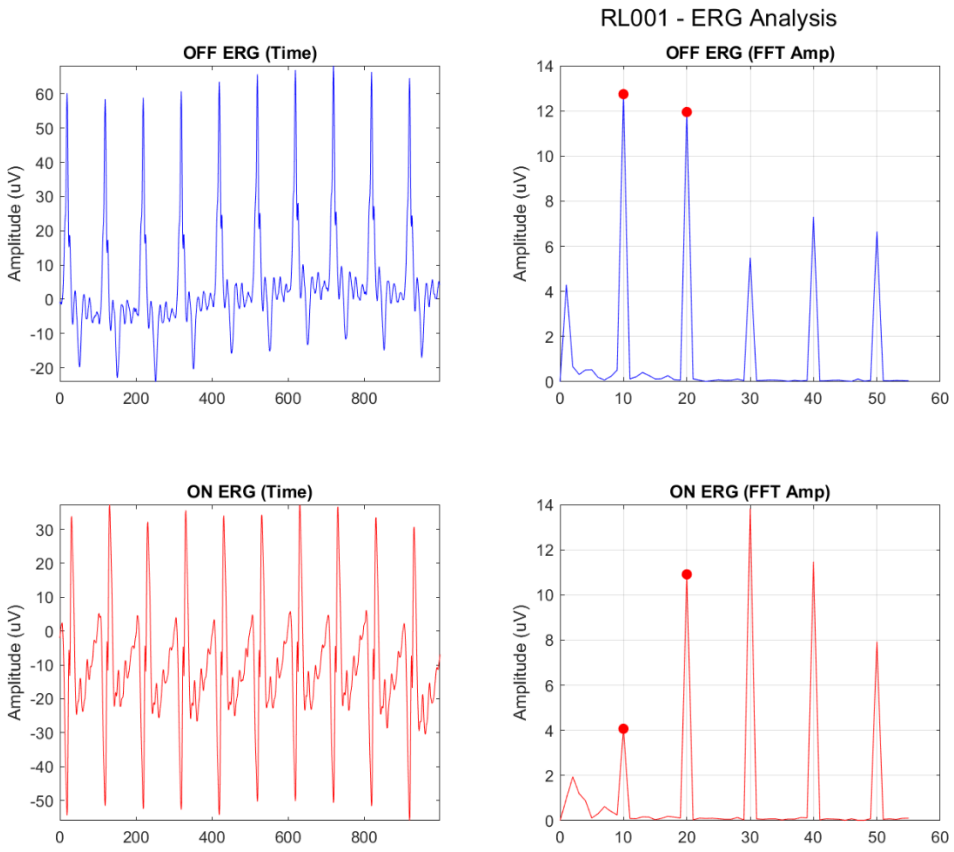

Figure 4.11 Time-Domain Waveforms and FFT Spectra of ON and OFF Pathway Flicker ERGs. (Left) Averaged time-domain retinal responses (electroretinograms) to 10 Hz flicker stimuli designed to isolate OFF (top) and ON (bottom) bipolar cell pathways. (Right) The corresponding frequency-domain amplitude spectra obtained by discrete Fast Fourier Transform (FFT) of the 1000 ms temporal signals.

Descriptive statistics for all flicker ERG amplitude and latency parameters at both the fundamental (1f1) and second harmonic (2f1) are summarized in Table 4.4. At the fundamental harmonic, the OFF pathway showed a larger mean amplitude (6.08 ± 2.76 uV) than the ON Pathway (4.94 ± 1.65 uV). At the second harmonic, mean amplitudes were comparable between pathways (ON 6.97 ± 1.90 uV, OFF 6.86 ± 2.55 uV). Latencies were positive across all conditions, consistent with the convention that higher values reflect greater temporal lag. Variability in latency was substantially higher at 1f1 (CV% 30 to 78) than at 2f1 (CV% 9 to 22), reflecting the greater stability of phase measurements at the higher harmonic.

Table 4.4 Descriptive Summary Statistics for Flicker ERG Variables. Summary of 1f1 and 2f1 Flicker ERG amplitudes (uV) and latencies (ms) including sample size (N), Mean, Median, Standard Deviation (SD), Coefficient of Variation (CV %), Minimum (Min), and Maximum (Max).

Variable	N	Mean	Median	SD	Min	Max	CV %
1f1 OFF ERG Latency (ms)	33	19.47	18.96	5.94	7.51	29.21	30.50
2f1 OFF ERG Latency (ms)	33	21.80	21.95	2.04	16.83	25.31	9.34
1f1 ON ERG Latency (ms)	32	21.65	14.53	23.96	2.58	99.31	110.70
2f1 ON ERG Latency (ms)	33	38.83	38.44	1.69	35.45	42.79	4.35
1f1 OFF ERG Amplitude (uV)	33	6.08	5.77	2.76	2.11	13.71	45.32
2f1 OFF ERG Amplitude (uV)	33	6.86	6.29	2.55	3.21	14.36	37.13
1f1 ON ERG Amplitude (uV)	32	4.94	4.87	1.65	2.08	8.82	33.32
2f1 ON ERG Amplitude (uV)	33	6.97	6.45	1.90	3.97	10.91	27.32
1f1 ERG ON/OFF Amplitude Ratio	32	0.95	0.95	0.41	0.27	1.80	43.32
2f1 ERG ON/OFF Amplitude Ratio	33	1.07	1.08	0.24	0.53	1.44	22.05

Amplitude Correlation with Axial Length

Spearman correlation analyses examined relationships between AXL and flicker ERG amplitude at both the fundamental (10Hz) and second harmonic (20Hz) frequencies for both ON and OFF pathways. Scatter plots showing each correlation are presented in Figure 4.12. At 2f1, the ON Pathway amplitude demonstrated a negative trend with increasing AXL that approached significance ($r = -0.319$, $p = 0.070$) but not significant at 1f1 ($r = -0.229$ $p = 0.207$). OFF Pathway ERG showed no relationship between amplitude and AXL at 1f1 ($r = 0.009$ $p = 0.962$) or 2f1 ($r = -0.255$ $p = 0.153$).

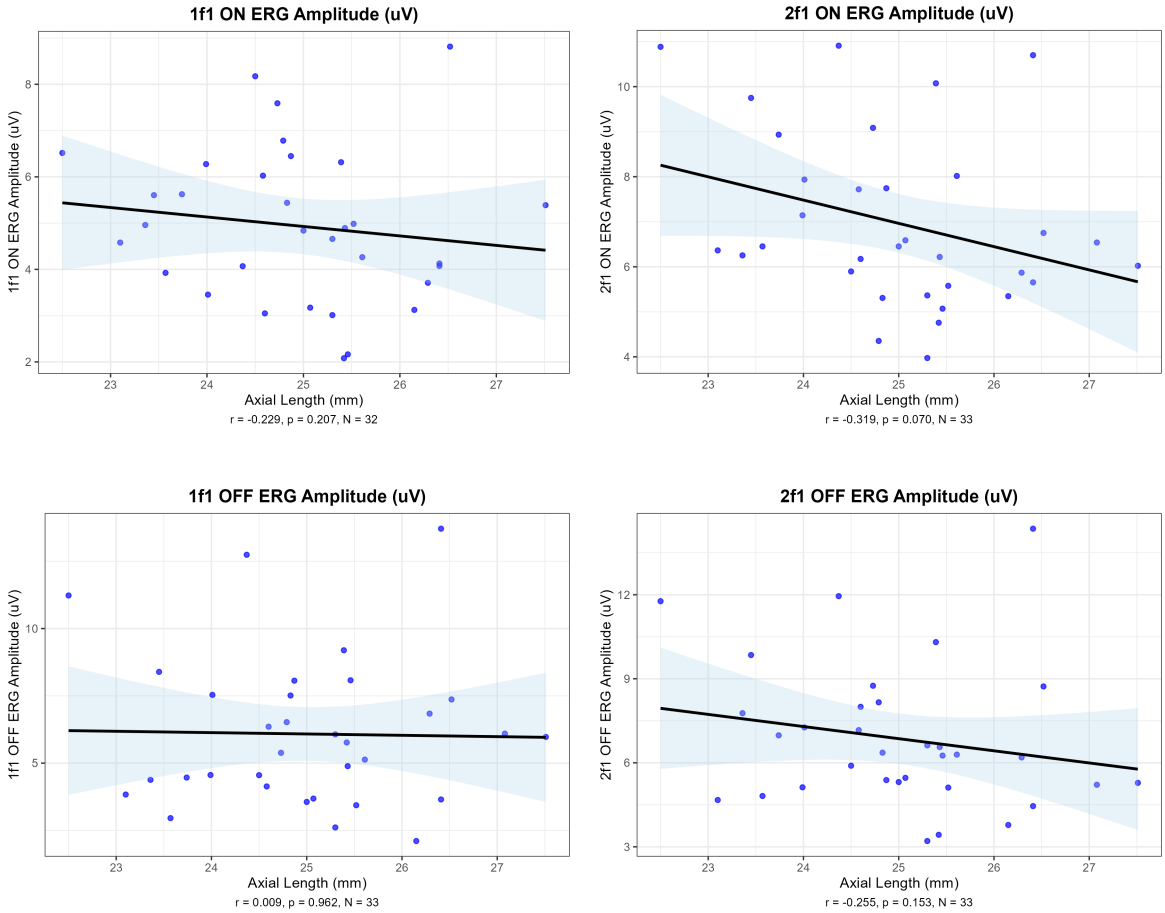

Figure 4.12 Correlation between Axial Length and Flicker ERG Amplitudes. Scatter plots between AXL (mm) and 1f1 and 2f1 ON and OFF Flicker ERG amplitudes (uV) from the flicker ERG experiments with linear regression lines of best fit and 95% confidence intervals (shaded regions).

Because 2f1 ON ERG amplitude met the prespecified criterion for exploratory follow-up testing, a median-split comparison was performed. Longer AXL participants showed lower 2f1 ON ERG amplitude than shorter AXL participants (shorter AXL: 7.49 ± 1.89 uV, n = 17; longer AXL: 6.41 ± 1.81 uV, n = 16). This group-level pattern followed the same direction as the negative Spearman correlation, but the exploratory comparison was not statistically

significant after correction for multiple comparisons (p = 0.137). The group comparison is shown in Figure 4.13.

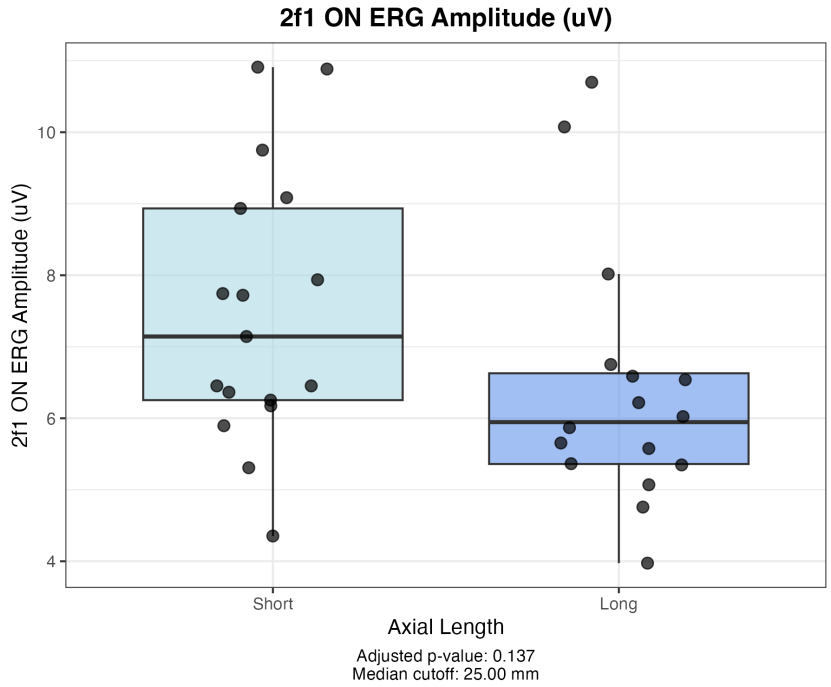

Figure 4.13 Median-Split Analysis for 2f1 ON Flicker ERG Amplitude. Box plots of 2f1 ON ERG amplitude (uV) for short and long AXL groups from the flicker ERG experiments with overlaid individual participant data points and horizontal lines indicating the median.

Latency Correlation with Axial Length

Spearman correlation analyses examined the relationships between AXL and Flicker ERG latency at the fundamental (1f1) and second-harmonic (2f1) response frequencies for both ON and OFF pathways, as shown in Figure 4.14. This analysis revealed a positive trend-level for ON ERG latency at 2f1 (r = 0.29, p = 0.100), suggesting that longer eyes may

exhibit longer delay in signal at this frequency. No significant correlations were observed for ON ERG at 1f1 (r = -0.236, p = 0.186). OFF pathway latency showed no relationship with AXL at either 1f1 (r = 0.005, p = 0.977) or 2f1 (r = -0.154, p = 0.391).

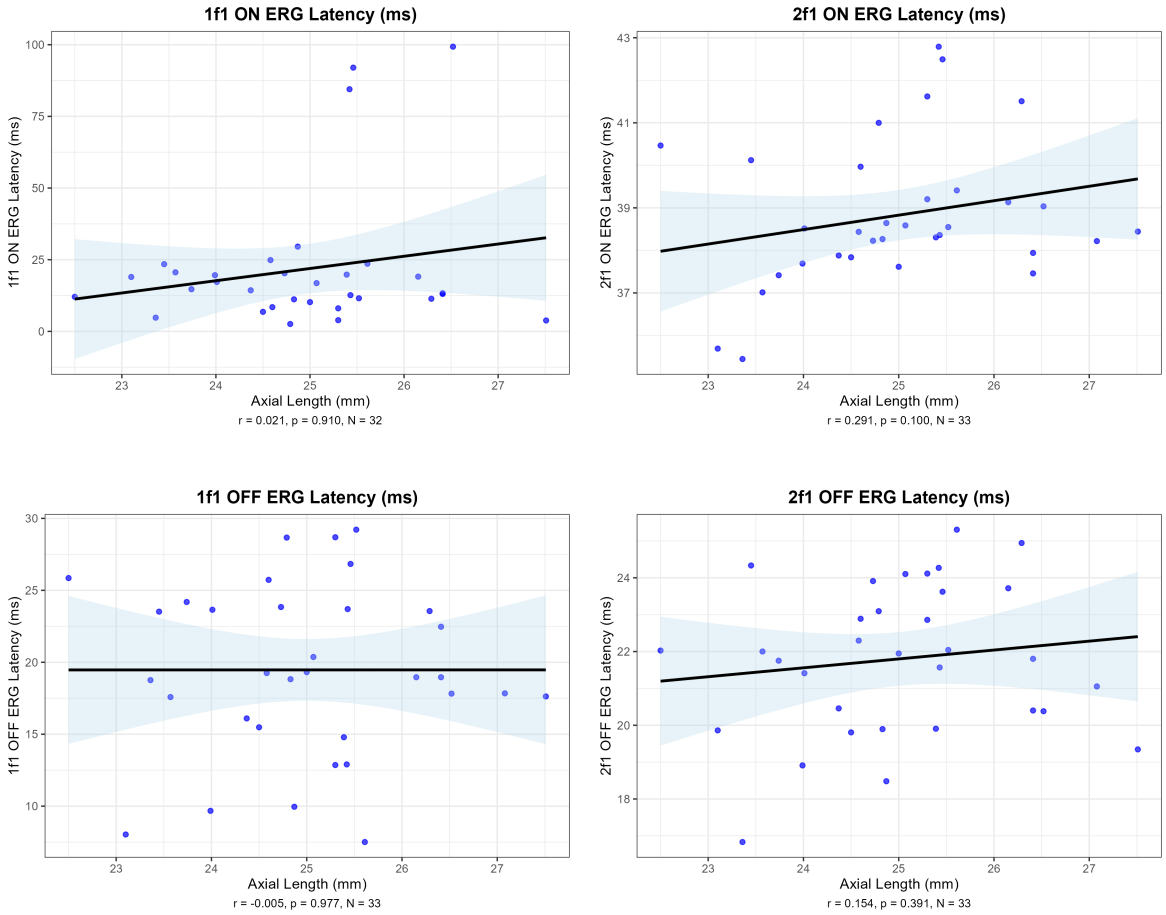

Figure 4.14 Correlation between Axial Length and Latency for Flicker ERG Scatter plots between AXL (mm) and 1f1 and 2f1 ON and OFF Flicker ERG latency (ms) from the flicker ERG experiments with linear regression lines of best fit and 95% confidence intervals (shaded regions).

Because ON ERG 2f1 latency showed a borderline association with AXL in the primary Spearman analysis (r = 0.29, p = 0.100), an exploratory median-split comparison was performed. Longer-AXL participants showed longer ON ERG 2f1 latency than shorter-AXL participants; however, this exploratory comparison did not remain statistically significant after Holm correction for multiple comparisons (p = 0.104).

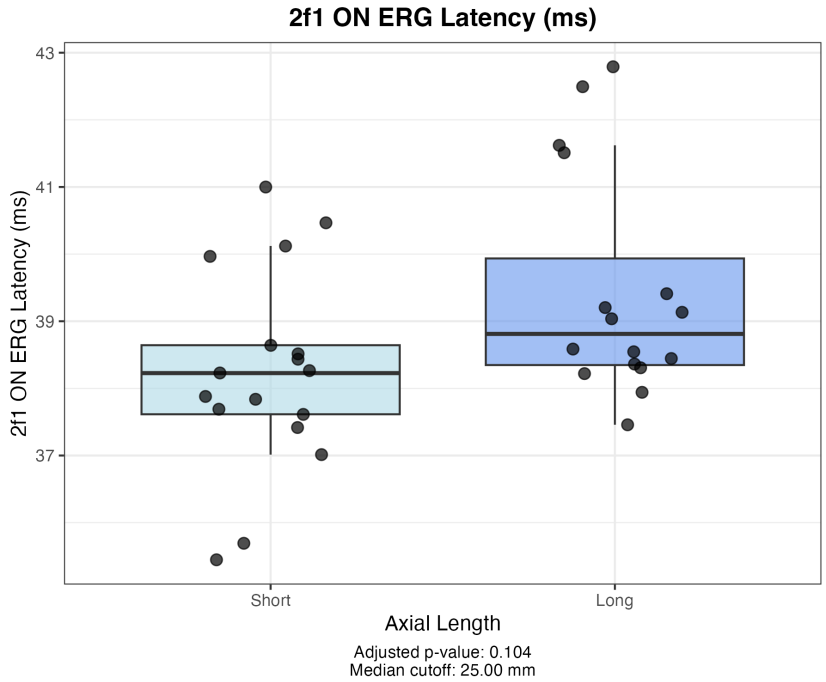

Figure 4.15 Median Split Analysis for 2f1 ON ERG Latency Box plot of 2f1 ON ERG latency (ms) for short and long AXL groups from the flicker ERG experiments with overlaid individual participant data points and horizontal lines indicating the median.

ON/OFF pathway balance

ON/OFF amplitude ratios were calculated at both the 1f1 and 2f1 frequencies for each participant with valid recordings in both pathways. The relationship between these amplitude ratios and AXL is shown in Figure 4.16. Neither the ON/OFF amplitude ratio at 1f1 (p =

0.558) nor the 2f1 (p = 0.916) demonstrated significant correlations with AXL. The mean ON/OFF ratio was 0.93 at 1f1 and 1.07 at 2f1, indicating similar temporal responses.

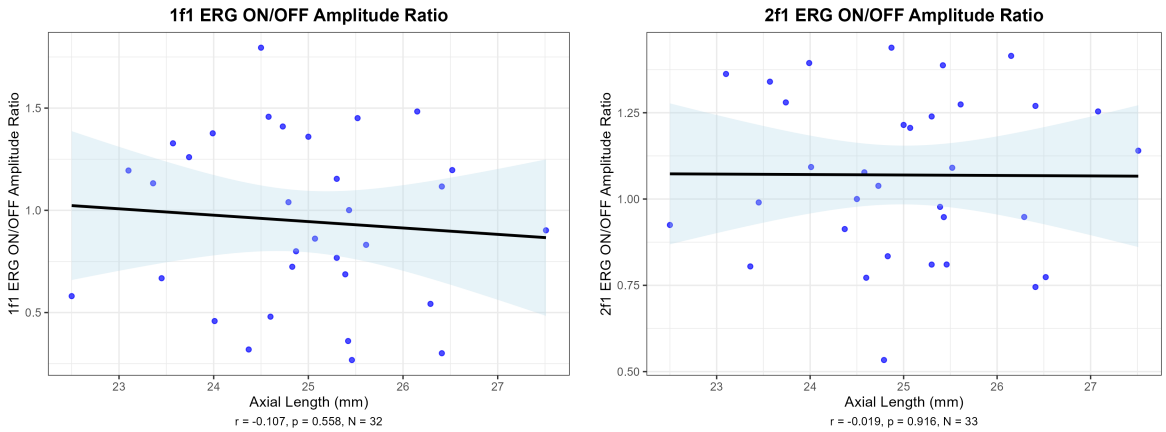

Figure 4.16 Correlation between Axial Length and ON/OFF Flicker ERG Amplitude Ratios. Scatter plots between AXL (mm) and 1f1 and 2f1 ON/OFF Flicker ERG amplitude ratios from the flicker ERG experiments with linear regression lines of best fit and 95% confidence intervals (shaded regions).

4.2.4 ON and OFF Flicker VEP

To further address Aim 2, flicker VEP responses were examined to characterize cortical processing of ON and OFF pathway signals as a function of AXL. Flicker VEP responses were successfully recorded from 33 participants using pathway-selective sawtooth stimuli at 10 Hz. Following acquisition, each 1000 ms recording underwent Fast Fourier Transform (FFT) analysis to extract frequency-domain metrics, yielding amplitude and phase values at the fundamental frequency (10 Hz) and second harmonic (20 Hz), example for subject RL001 shown in Figure 4.17.

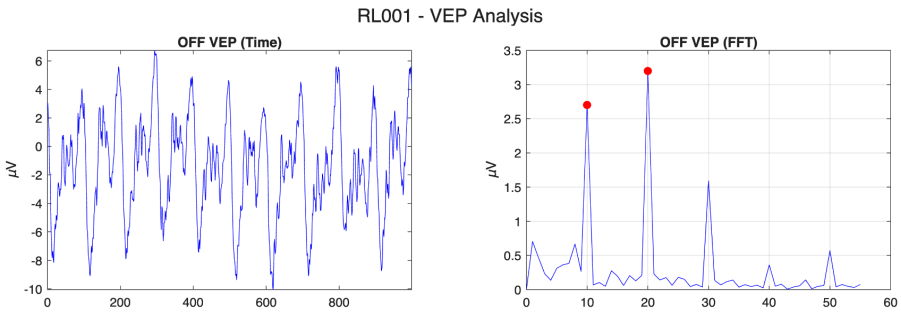

Figure 4.17 Time-Domain Waveforms and FFT Spectra of OFF Flicker VEPs.
Line plots of amplitude (uV) versus time (ms) and corresponding FFT frequency-domain amplitude (uV) spectra for representative OFF pathway 10 Hz flicker VEP responses from the flicker VEP experiments.

Descriptive statistics for all Flicker VEP Variables are presented in Table 4.5. At the 1f1 stimulation frequency, the mean ON VEP amplitude was 5.14 ± 3.00 uV, and the mean OFF VEP amplitude was 4.37 ± 2.74 uV. Both response distributions exhibited substantial inter-subject variability, yielding coefficients of variation (CV) exceeding 58% for both pathways. In response at 2f1, mean amplitudes were attenuated across both pathways, with the ON VEP averaging 2.68 ± 1.50 uV and the OFF VEP averaging 2.20 ± 1.50 uV. The reduced sample sizes at this higher frequency reflect the exclusion of recordings that failed to meet predefined signal-to-noise ratio (SNR) criteria. Furthermore, analysis of the 1f1 latency values revealed markedly greater variability in the OFF pathway (CV = 283.07%) than in the ON pathway (CV = 119.17%), suggesting pronounced inter-subject inconsistency in OFF pathway cortical timing at this temporal frequency. Conversely, at 2f1, the relative variability in latency was highly comparable between the two pathways.

Table 4.5 Descriptive Summary Statistics for Flicker VEP Variables
Summary of 1f1 and 2f1 Flicker VEP amplitudes (uV) and latency (ms) including sample size (N), Mean, Median, Standard Deviation (SD), Coefficient of Variation (CV %), Minimum (Min), and Maximum (Max).

Variable	N	Mean	Median	SD	Min	Max	CV %
1f1 OFF VEP Latency (ms)	33	41.48	37.36	33.11	0.75	99.54	79.81
2f1 OFF VEP Latency (ms)	28	25.59	25.38	16.25	0.52	49.12	63.51
1f1 ON VEP Latency (ms)	33	32.21	24.10	24.73	5.22	97.53	76.78
2f1 ON VEP Latency (ms)	31	17.75	15.10	15.01	0.17	49.81	84.59
1f1 OFF VEP Amplitude (uV)	33	4.37	3.59	2.74	0.58	10.23	62.65
2f1 OFF VEP Amplitude (uV)	28	2.20	1.82	1.50	0.65	6.98	68.28
1f1 ON VEP Amplitude (uV)	33	5.14	4.31	3.00	0.63	14.62	58.36
2f1 ON VEP Amplitude (uV)	31	2.68	2.53	1.50	0.36	7.32	55.88
1f1 VEP ON/OFF Amplitude Ratio	33	1.54	1.21	0.97	0.06	4.47	62.66
2f1 VEP ON/OFF Amplitude Ratio	27	1.41	1.25	0.87	0.30	3.83	61.66

Amplitude Correlation with Axial Length

Spearman correlation analyses and a median-split analysis examined the relationship between AXL and flicker VEP amplitudes, as shown in Figure 4.18. ON Pathway VEP amplitude at 1f1 demonstrated a statistically significant negative correlation with AXL ($r = -0.39$, $p = 0.026$). On-pathway amplitude at 2f1 showed no significant correlation ($r = -0.17$, $p = 0.364$). OFF pathway VEP amplitude showed no significant correlation with AXL at either 1f1 ($r = -0.12$, $p = 0.503$) or 2f1 ($r = -0.23$, $p = 0.248$).

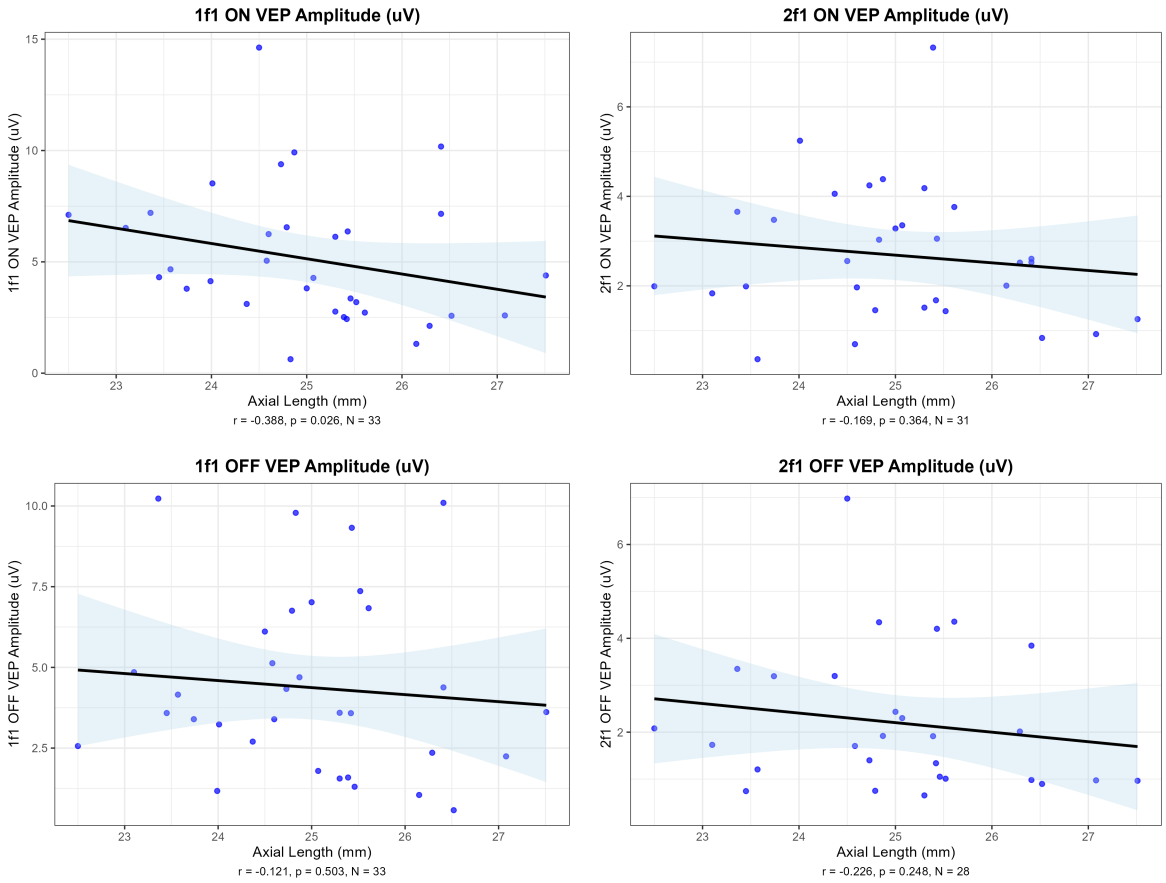

Figure 4.18 Correlation between Axial Length and Flicker VEP Amplitudes.
Scatter plots between AXL (mm) and 1f1 and 2f1 ON and OFF Flicker VEP amplitudes (uV) from the flicker VEP experiments with linear regression lines of best fit and 95% confidence intervals (shaded regions).

Because 1f1 ON VEP amplitude showed a significant negative association with AXL in the primary Spearman analysis (r = -0.388, p = 0.026), an exploratory median-split comparison was performed, shown in Figure 4.19. Longer AXL participants showed lower 1f1 ON VEP amplitude than shorter AXL participants (shorter AXL: 6.21 ± 3.22 uV, n = 17; longer AXL: 4.01 ± 2.34 uV, n = 16). This group-level pattern followed the same direction as the negative

Spearman correlation, but the exploratory comparison did not remain statistically significant after correction for multiple comparisons (p = 0.082).

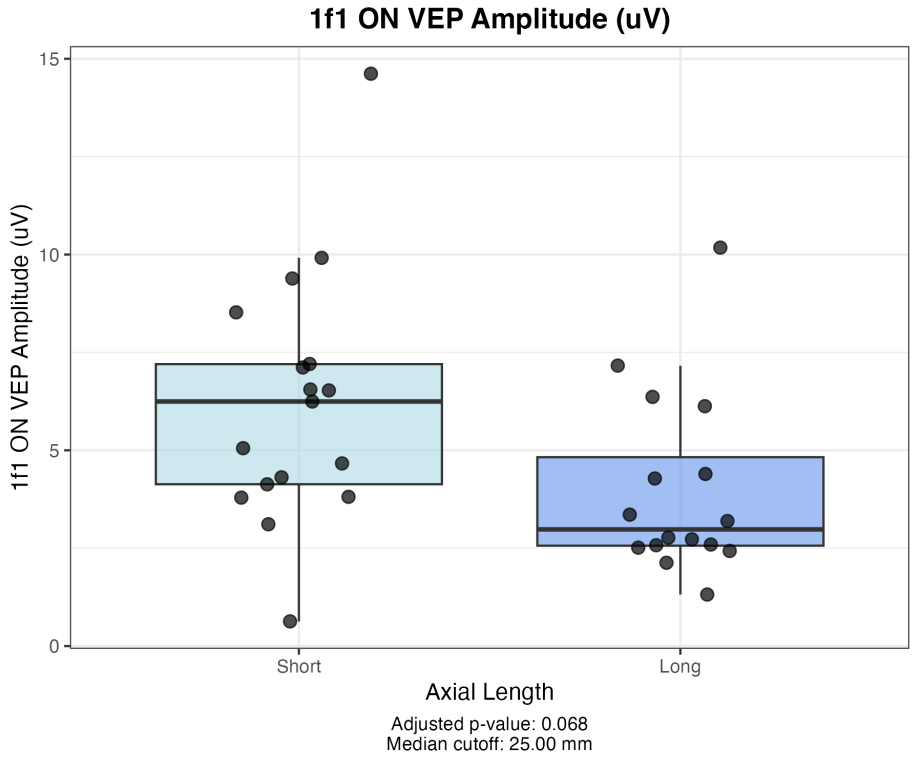

Figure 4.19 Median Split Analysis for 1f1 ON VEP Amplitude.
Box plots of 1f1 ON VEP amplitude (uV) for short and long AXL groups from the flicker VEP experiments with overlaid individual participant data points and horizontal lines indicating the median.

Latency Correlation with Axial Length

Latency was examined for relationship with AXL using Speraman correlation. No significant correlation was observed between latency and AXL for ON 1f1(r = -0.052, p = 0.775) or 2f1 VEP (r = 0.244, p = 0.186) and OFF 1f1 (r = -0.143, p = 0.426) or 2f1 VEP (r = -0.080, p = 0.685).

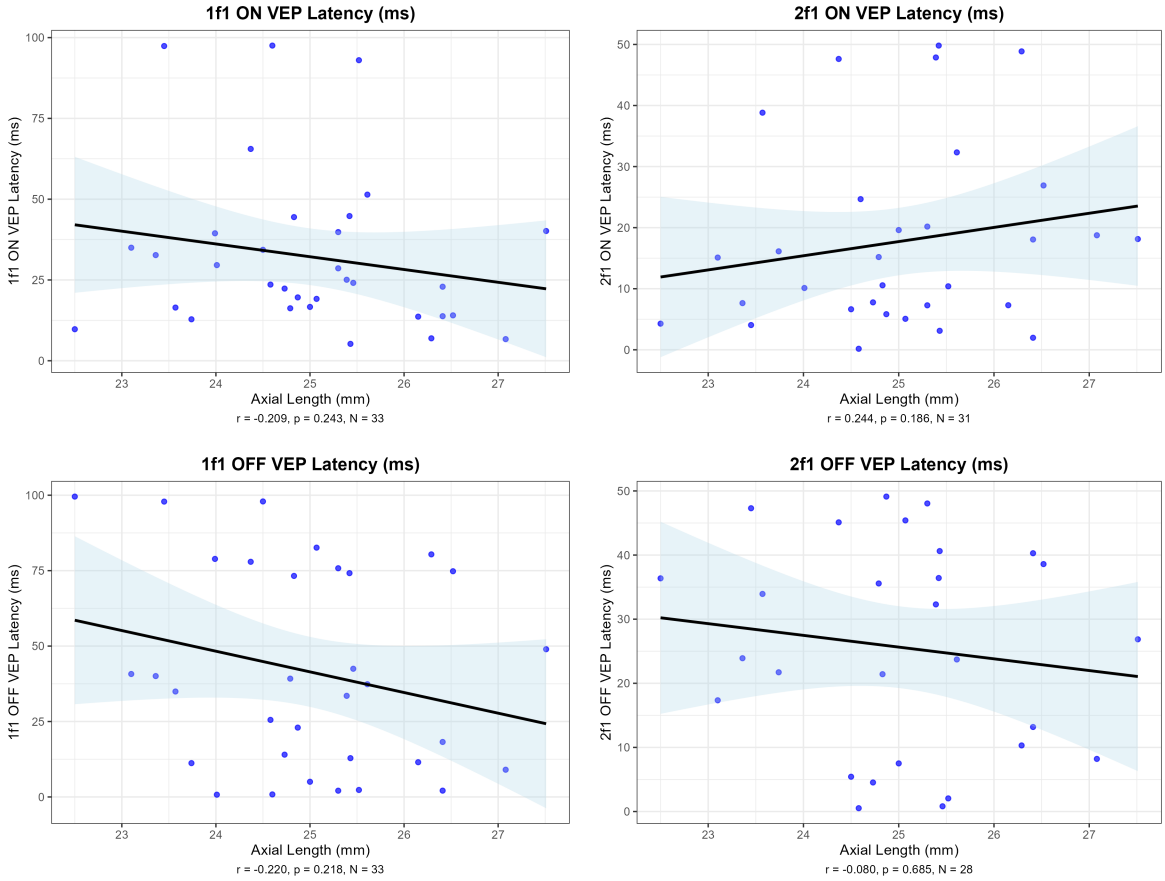

Figure 4.20 Correlation between Axial Length and latency for Flicker VEP. Scatter plots between AXL (mm) and 1f1 and 2f1 ON and OFF Flicker VEP latency (ms) from the flicker VEP experiments with linear regression lines of best fit and 95% confidence intervals (shaded regions).

ON/OFF pathway balance

ON/OFF VEP amplitude ratios were examined at both frequencies. Neither 1f1 ($p = 0.429$) nor 2f1 ($p = 0.769$) demonstrated significant correlation with AXL.

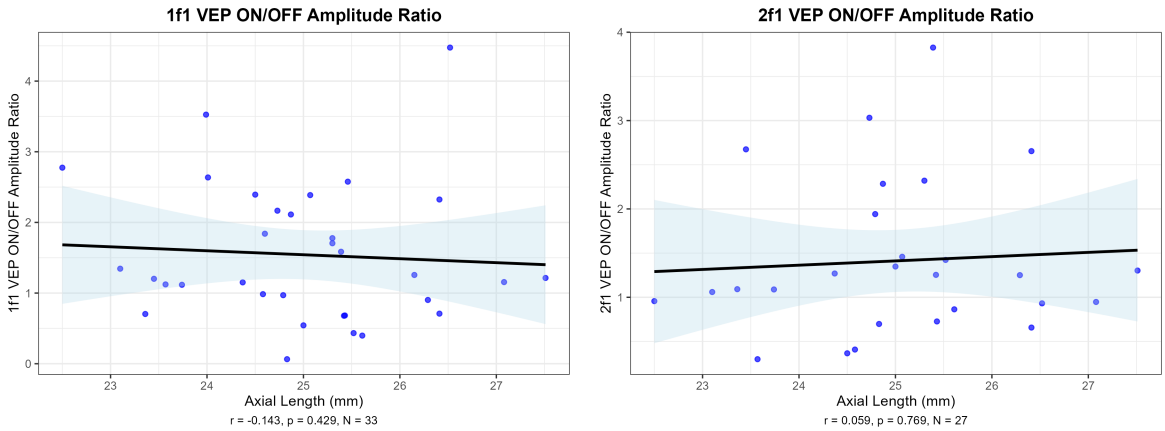

Figure 4.21 Correlation between Axial Length and ON/OFF VEP Amplitude Ratios. Scatter plots between AXL (mm) and 1f1 and 2f1 ON/OFF VEP amplitude ratios from the flicker VEP experiments with linear regression lines of best fit and 95% confidence intervals (shaded regions).

Neither 1f1 nor 2f1 ON/OFF amplitude ratio demonstrated significant correlations with AXL ON/OFF ratio 1.54 at 1f1 and 1.41 at 2f1, indicating ON pathway dominance in flicker response.

4.3 ON and OFF Psychophysical Contrast Sensitivity

To address Aim 3, contrast sensitivity for pathway-selective ON and OFF difference-of-Gaussians (DoG) stimuli was measured in 34 participants with lower radial spatial frequency (LSF, cpd 1.19) and higher radial spatial frequency (HSF, cpd 2.37). Spearman rank correlations served as the primary analytical approach, with median-split analysis applied to variables that demonstrated trend-level or significant associations with AXL ($p \leq 0.10$). The outcome variables were logarithmic contrast sensitivity (LogCS) for the ON and OFF pathways at each spatial frequency, with derived indices including the OFF/ON Index at each

spatial frequency and the Relative Sensitivity ratio for each pathway. Descriptive statistics for all psychophysical variables are summarized in Table 4.6

Table 4.6 Descriptive Summary Statistics for Psychophysical Contrast Sensitivity Measures. Summary of psychophysical contrast sensitivity measures (LogCS) and calculated indices including Mean, Median, Standard Deviation (SD), Minimum (Min), and Maximum (Max).

Variable	Mean	Median	SD	Min	Max	CV %
LSF ON Sensitivity (LogCS)	1.72	1.73	0.16	1.12	1.98	9.04
LSF OFF Sensitivity (LogCS)	1.70	1.72	0.16	1.30	1.97	9.14
LSF OFF/ON Relative Sensitivity	0.99	0.99	0.07	0.83	1.16	6.85
LSF OFF/ON Index	-0.00	-0.01	0.03	-0.09	0.07	NA
HSF ON Sensitivity (LogCS)	1.06	1.11	0.20	0.70	1.30	18.69
HSF OFF Sensitivity (LogCS)	1.04	1.05	0.20	0.70	1.30	19.22
HSF OFF/ON Relative Sensitivity	0.99	0.98	0.15	0.65	1.43	15.59
HSF OFF/ON Index	-0.01	-0.01	0.08	-0.21	0.18	NA
ON LSF/HSF Relative Sensitivity	1.67	1.61	0.31	1.23	2.51	18.79
OFF LSF/HSF Relative Sensitivity	1.68	1.61	0.31	1.15	2.33	18.38
Average LSF/HSF Relative Sensitivity	1.66	1.58	0.27	1.22	2.35	16.40

Abbreviations:
LSF: lower spatial frequency, HSF: higher spatial frequency

4.3.1 Lower Spatial Frequency

Contrast sensitivity measured at LSF showed no significant relationship with AXL in either pathway, shown in Figure 4.22. ON pathway Log CS ($r = -0.103$, $p = 0.561$) and OFF pathway LogCS ($r = -0.241$, $p = 0.170$) demonstrated minimal correlation with AXL. The OFF/ON Index at near similarly showed no significant association ($r = -0.235$, $p = 0.181$).

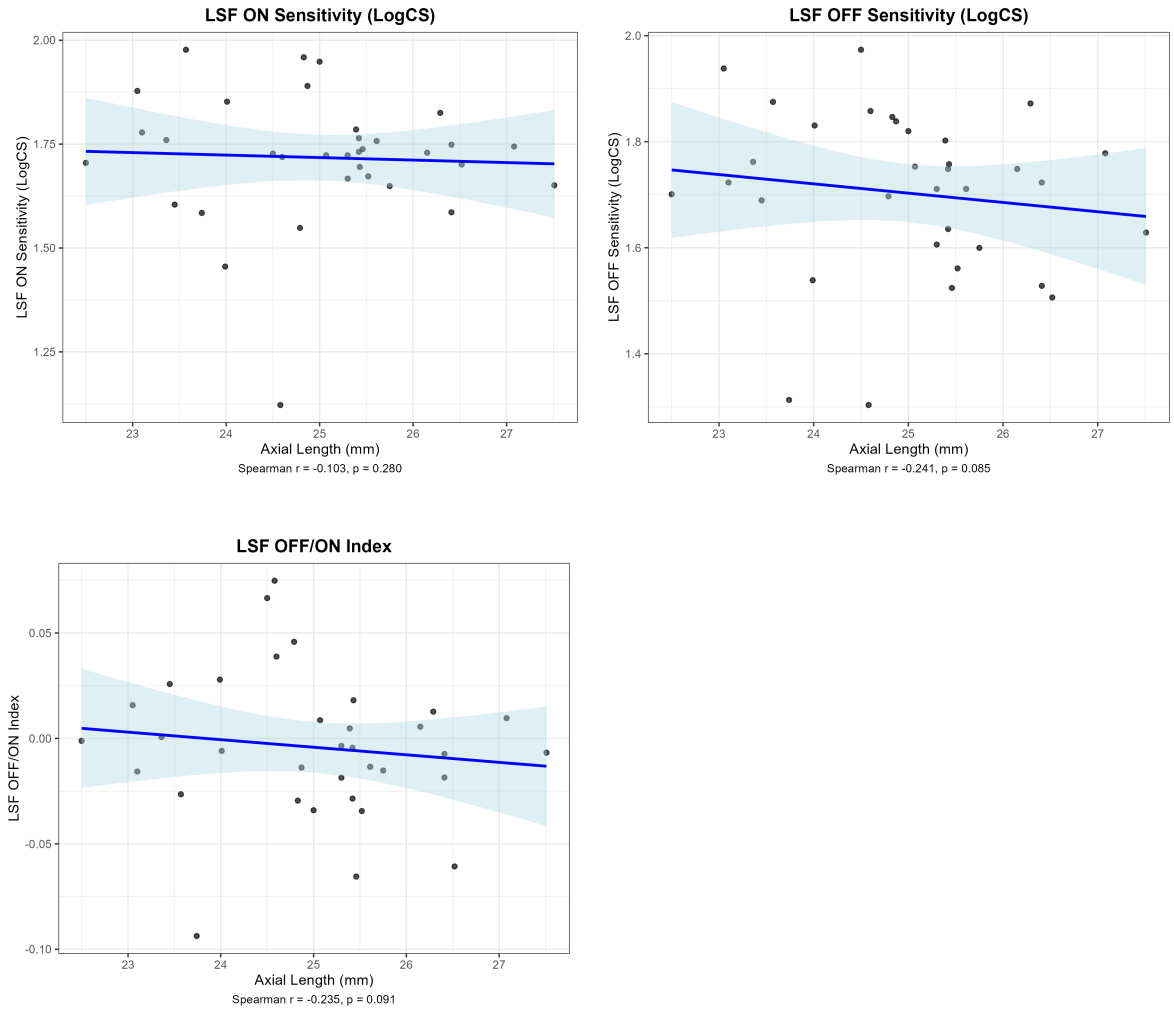

Figure 4.22 Correlation between Axial Length and LogCS at LSF
Scatter plots between AXL (mm) and ON pathway contrast sensitivity (LogCS), OFF pathway contrast sensitivity (LogCS), and the OFF/ON Index for the LSF psychophysical experiments with linear regression lines of best fit and 95% confidence intervals (shaded regions).

4.3.2 Higher Spatial Frequency

In contrast to the near viewing findings, contrast sensitivity measured at HSF demonstrated significant relationships with AXL for individual pathway measures. Spearman correlation

analysis between AXL and Log CS for each pathway and OFF/ON Index was performed, both shown in Figure 4.23. ON pathway contrast sensitivity exhibited a moderate negative correlation with AXL (r = -0.438, p = 0.010). OFF pathway contrast sensitivity showed a non-significant trend (r = -0.292, p = 0.094). Despite the significant individual pathway effects, the relative balance between pathways was preserved. The OFF/ON Index demonstrated no significant correlation with AXL (r = 0.072, p = 0.685).

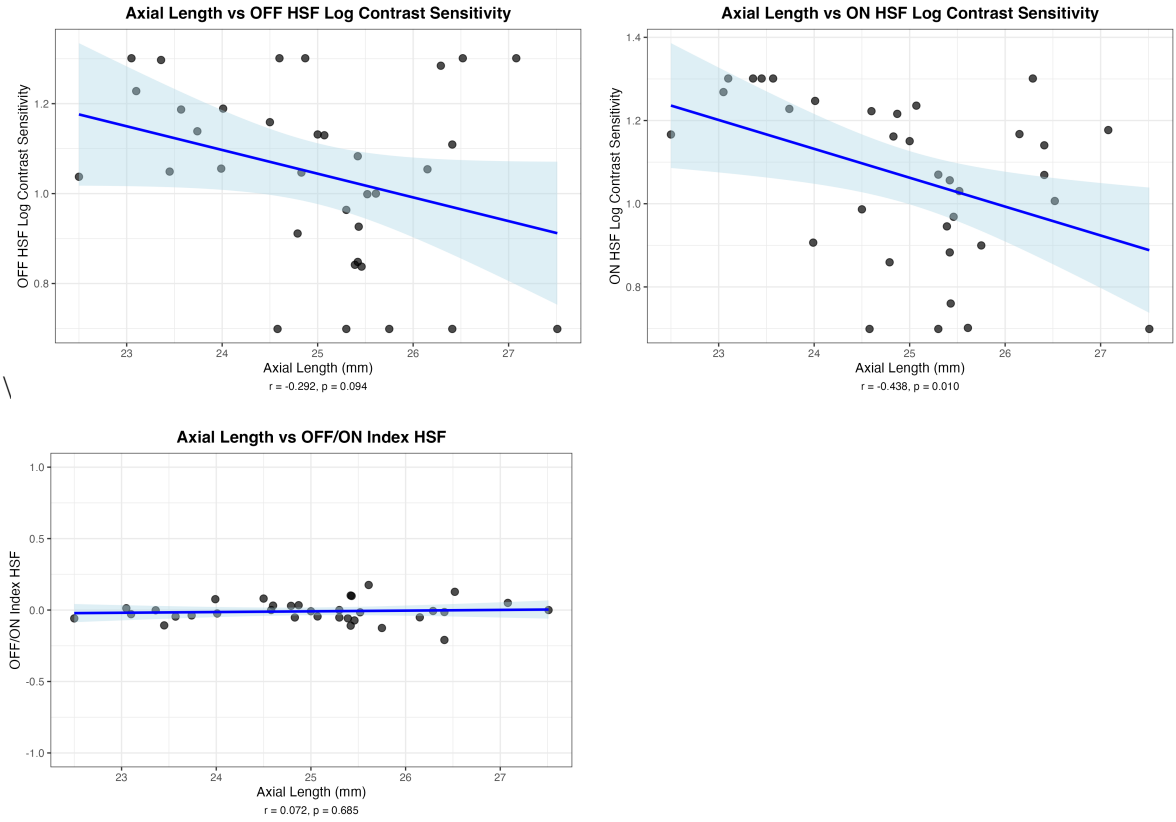

Figure 4.23 Correlation between Axial Length and LogCS at Higher Spatial Frequency. Scatter plots between AXL (mm) and ON pathway contrast sensitivity (LogCS), OFF pathway contrast sensitivity (LogCS), and the OFF/ON Index from the HSF psychophysical experiments with linear regression lines of best fit and 95% confidence intervals (shaded regions).

Median Split

Because ON HSF LogCS showed a significant negative association with AXL in the primary Spearman analysis ($r = -0.438$, $p = 0.010$), an exploratory median-split comparison was performed. Longer-AXL participants showed lower ON HSF LogCS than shorter-AXL participants (shorter AXL: 1.15 ± 0.18, $n = 17$; longer AXL: 0.97 ± 0.18, $n = 17$). This group-level pattern followed the same direction as the negative Spearman correlation and remained significant after correction for multiple comparisons ($p = 0.050$). OFF HSF LogCS showed a trend-level negative association with AXL in the primary Spearman analysis ($r = -0.292$, $p = 0.094$). Longer-AXL participants showed lower OFF HSF LogCS than shorter-AXL participants (shorter AXL: 1.13 ± 0.16, $n = 17$; longer AXL: 0.96 ± 0.21, $n = 17$). This group-level pattern followed the same direction as the trend-level negative Spearman association, but the exploratory comparison did not remain statistically significant after correction for multiple comparisons ($p = 0.082$).

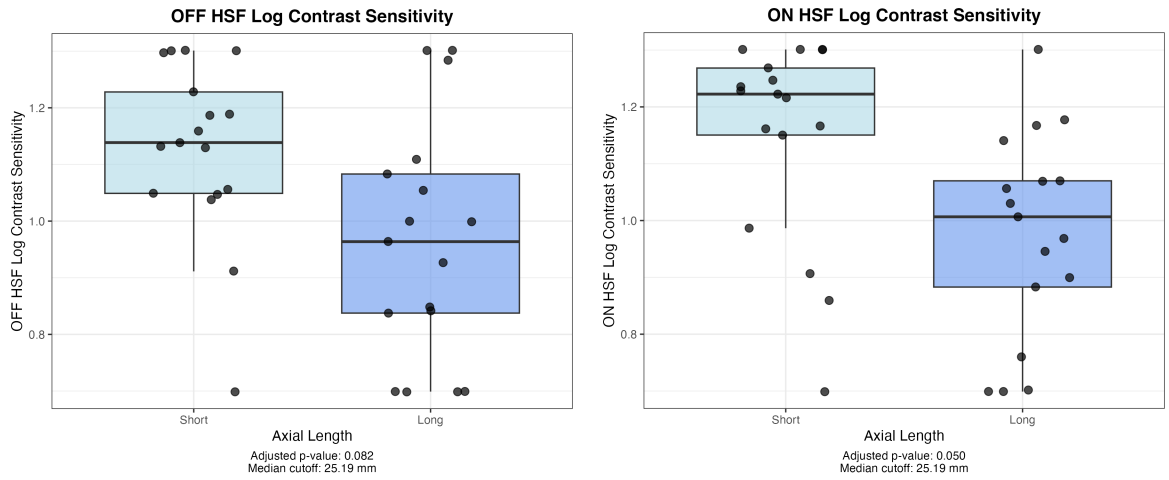

Figure 4.24 Median Split Analysis for ON and OFF HSF Contrast Sensitivity.
Box plots of ON and OFF pathway contrast sensitivity (LogCS) for short and long AXL groups from the HSF psychophysical experiments with overlaid individual participant data points and horizontal lines indicating the median.

4.3.3 Relative Sensitivity

Relative sensitivity ratios were used to assess whether contrast sensitivity loss differed across spatial frequency within each pathway. ON Relative Sensitivity showed a significant positive correlation with AXL ($r = 0.449$, $p = 0.008$), indicating that longer eyes had greater reduction in sensitivity at the relatively higher low-spatial-frequency condition compared with the lower spatial-frequency condition. Average Relative Sensitivity across both pathways also correlated significantly with AXL ($r = 0.387$, $p = 0.024$). OFF Relative Sensitivity showed a weaker trend in the same direction ($r = 0.289$, $p = 0.097$). Exploratory median-split comparisons followed the same direction and remained significant after Holm correction for multiple comparisons for ON Relative Sensitivity ($p = 0.034$) and Average

Relative Sensitivity (p = 0.043), but not for OFF Relative Sensitivity (p = 0.104). Results are shown in Figures 4.25 and 4.26.

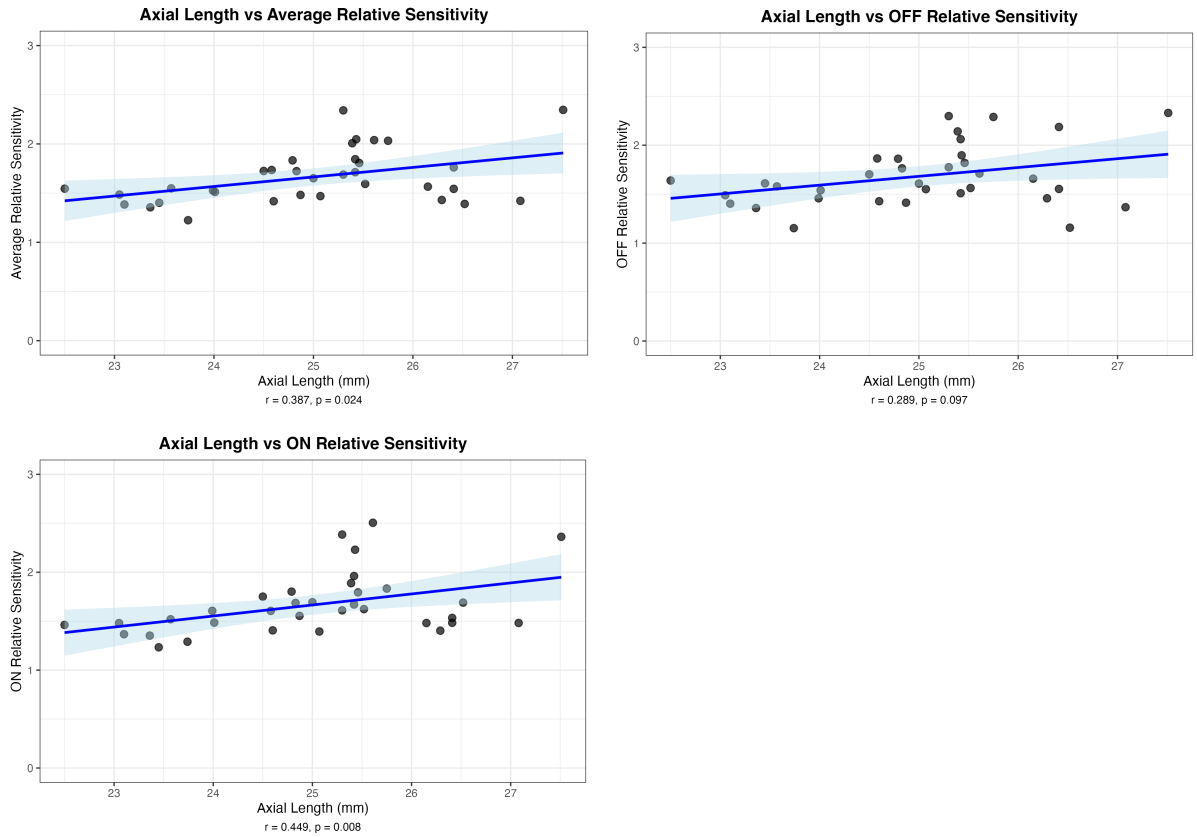

Figure 4.25 Correlation between Axial Length and Relative Contrast Sensitivity. Scatter plots between AXL (mm) and ON, OFF, and Average relative contrast sensitivity ratios from the psychophysical experiments with linear regression lines of best fit and 95% confidence intervals (shaded regions).

Median Split Analysis:

Because ON Relative Sensitivity showed a significant positive association with AXL in the primary Spearman analysis (r = 0.449, p = 0.008), an exploratory median-split comparison was performed. Longer-AXL participants had higher ON Relative

Sensitivity than shorter-AXL participants (shorter AXL: 1.51 ± 0.16, n = 17; longer AXL: 1.82 ± 0.35, n = 17). This group-level pattern followed the same direction as the positive Spearman correlation and remained significant after correction for multiple comparisons ($p = 0.034$). OFF Relative Sensitivity showed a trend-level positive association with AXL in the primary Spearman analysis ($r = 0.289$, $p = 0.097$). Longer-AXL participants had numerically higher OFF Relative Sensitivity than shorter-AXL participants (shorter AXL: 1.55 ± 0.18, n = 17; longer AXL: 1.81 ± 0.36, n = 17). This group-level pattern followed the same direction as the trend-level positive Spearman association, but the exploratory comparison did not remain statistically significant after correction for multiple comparisons ($p = 0.104$). Average Relative Sensitivity showed a significant positive association with AXL in the primary Spearman analysis ($r = 0.387$, $p = 0.024$). Longer-AXL participants had higher Average Relative Sensitivity than shorter-AXL participants (shorter AXL: 1.53 ± 0.16, n = 17; longer AXL: 1.80 ± 0.30, n = 17). This group-level pattern followed the same direction as the positive Spearman correlation and remained significant after correction for multiple comparisons ($p = 0.043$).

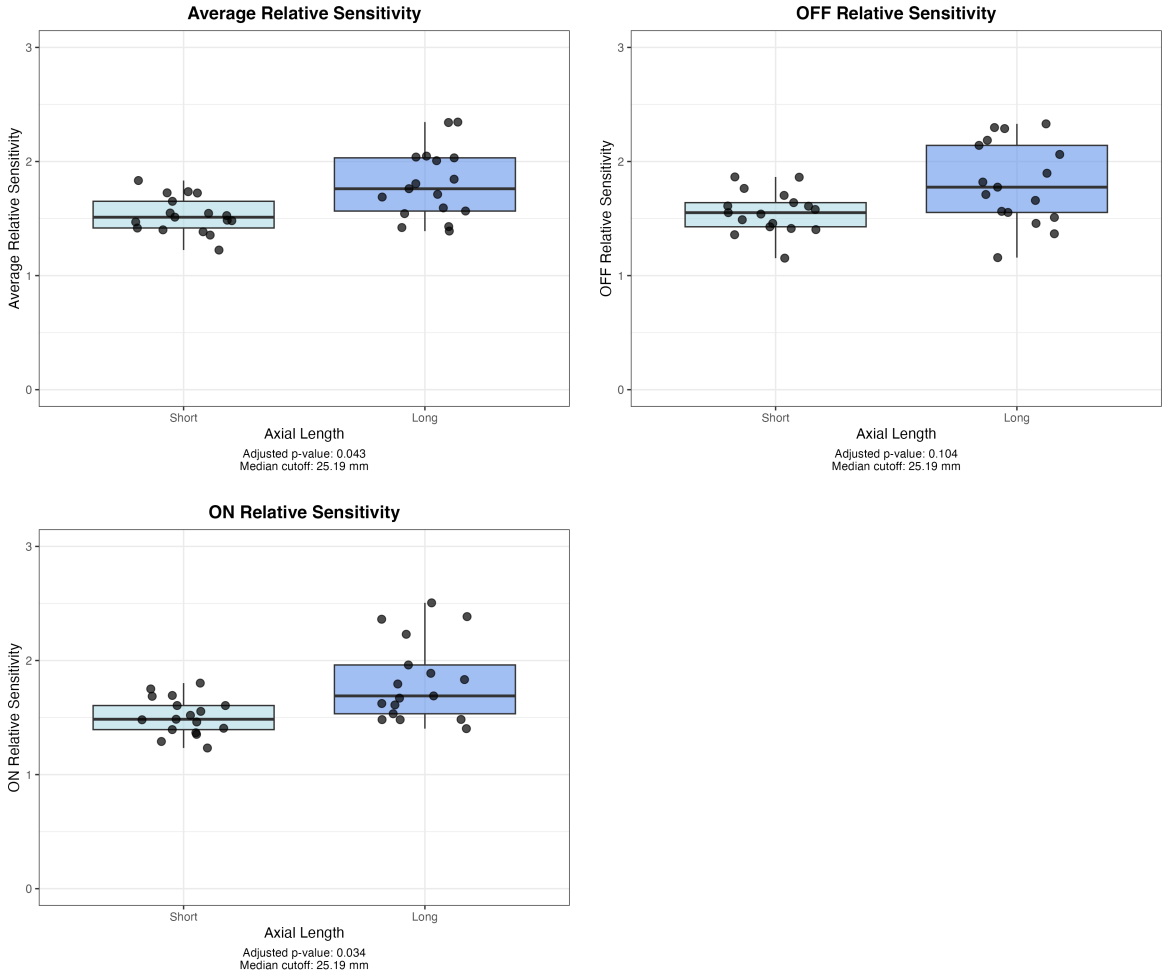

Figure 4.26 Median Split Analysis for Relative Contrast Sensitivity.
Box plots of ON, OFF, and Average relative contrast sensitivity ratios for short and long AXL groups from the psychophysical experiments, with overlaid individual participant data points and horizontal lines indicating the median.

5. Discussion

5.1 Summary

The purpose of this study was to determine whether AXL is associated with ON and OFF pathway function across retinal, cortical, and perceptual levels of visual processing. The primary analyses were Spearman correlations between AXL and each outcome measure. Overall, the results suggest that AXL-related functional differences were not global across all ON/OFF measures, but were instead dependent on stimulus paradigm, temporal demand, spatial frequency, and outcome measure.

Flash ERG and flash VEP measures did not show significant associations with AXL. This suggests that the transient photopic flash paradigms used in this study did not reveal measurable AXL-related changes in ON- or OFF-driven responses within the axial-length range tested. In contrast, flicker electrophysiology showed more selective ON-related associations. At the retinal level, 2f1 ON ERG amplitude showed a trend-level negative association with AXL, and 2f1 ON ERG latency showed a borderline positive association. At the cortical level, 1f1 ON VEP amplitude showed a significant negative association with AXL. The exploratory median-split comparisons for these electrophysiological variables followed the same direction as the Spearman correlations, but none remained statistically significant after correction for multiple comparisons. Therefore, the electrophysiological findings suggest that flicker stimulation may be more sensitive than flash stimulation for detecting subtle ON-related associations with AXL, while also requiring cautious interpretation.

The strongest evidence for an AXL-related functional change was observed in the psychophysical measures. ON HSF LogCS showed a significant negative association with AXL, indicating lower ON contrast sensitivity in longer eyes. ON Relative Sensitivity and Average Relative Sensitivity also showed significant positive associations with AXL, indicating that longer eyes showed greater reduction in HSF sensitivity relative to LSF sensitivity. The exploratory median-split comparisons for ON HSF LogCS, ON Relative Sensitivity, and Average Relative Sensitivity followed the same direction as the Spearman correlations and remained statistically significant after correction for multiple comparisons. OFF HSF LogCS and OFF Relative Sensitivity showed similar directional patterns but were trend-level in the Spearman analyses and did not remain significant after correction for multiple comparisons.

Across electrophysiological and psychophysical ratio measures, there was no significant evidence that AXL was associated with altered relative ON/OFF balance. This should be interpreted as a null finding for the specific ratio measures and stimulus conditions tested, rather than as proof that ON/OFF balance is biologically preserved or actively compensated. Taken together, the results support a condition-dependent relationship between AXL and selected ON-related or spatial-frequency-dependent measures, rather than a uniform ON/OFF pathway deficit across the visual hierarchy.

5.2 Flash Electrophysiology

Flash ERG and flash VEP measures did not show significant associations with AXL for either ON- or OFF-biased stimulation. In the ERG, neither ON flash components, OFF flash components, nor the b-wave/d-wave amplitude ratio were significantly associated with

AXL. Similarly, flash VEP measures did not show significant AXL-related changes in N2-P2 amplitude or peak timing, although OFF N2 time to peak showed a trend-level positive association with AXL. This trend followed the same direction in the exploratory median-split comparison, with longer-AXL participants showing increased delayed OFF N2 time to peak, but the comparison was not statistically significant after correction for multiple comparisons. Together, these results indicate that the transient photopic flash paradigms used in this study did not reveal measurable AXL-related alterations in ON- or OFF-biased retinal or cortical responses within the axial-length range examined.

These findings should be interpreted in relation to the broader ERG literature in myopia, where results vary by adaptation state, stimulus type, retinal region, and severity of myopia. Several studies have reported reduced ERG amplitudes or delayed timing in myopic eyes, particularly when using scotopic, focal, or multifocal paradigms, or when studying participants with higher myopia or longer AXL. For example, Ismael et al. (2017) reported reduced multifocal ERG amplitude and prolonged implicit time with increasing myopia, findings that were most pronounced in higher myopia and reflected regional retinal variation rather than a single global full-field response. This distinction is relevant because full-field flash ERG sums activity over a broad retinal area and may be less sensitive to localized retinal changes associated with axial elongation. Structural work also suggests that myopia-related retinal and RPE changes may vary by retinal region, including midperipheral involvement, which may not be well captured by a global photopic flash response (Jonas et al. 2023). Therefore, the absence of significant flash ERG correlations in the present study

does not rule out localized retinal dysfunction but suggests that this full-field photopic flash protocol did not detect AXL-related differences in transient ON/OFF responses.

The present null flash ERG findings should also be separated from rod-driven or dark-adapted ERG findings. Stapley et al. (2025) for example, reported delayed dark-adapted implicit times in myopes that correlated positively with AXL, while light-adapted amplitudes and implicit times did not show comparable refractive group differences. Similarly, Srirangam (2025), in a related NECO thesis from the same larger Retinal Layers Study, found that rod-isolating ERG Rmax was significantly associated with AXL, whereas cone ERG Rmax was not. This distinction is consistent with the broader principle described by Curcio et al. (2000) who emphasized in aging and age-related maculopathy that rod dysfunction can appear before comparable cone abnormalities. Although Curcio et al. studied aging and maculopathy rather than myopia, their work supports the general point that retinal dysfunction can be cell-type and adaptation-state specific. Thus, the present photopic flash findings should not be interpreted as evidence that all retinal electrophysiological function is unaffected by AXL.

The lack of significant flash ERG associations also differs from pathway-selective work by Poudel et al. (2024), who reported reduced ON-pathway ERG amplitude and increased ON-pathway latency with increasing AXL using light and dark flash stimuli across multiple contrast levels. This difference may reflect both stimulus design and sample characteristics. Poudel et al. measured contrast-response functions across multiple contrast levels, allowing estimation of response scaling, gain, and saturation properties. In contrast, the present study used a single-contrast flash protocol measuring a-wave, b-wave, d-wave,

and PhNR components. A fixed high-contrast transient response may be less sensitive to changes in contrast gain or response compression than a full contrast-response paradigm. Poudel et al. also included participants with longer AXL and higher refractive errors than the present cohort, which may have increased sensitivity to detecting pathway-specific effects.

The b-wave/d-wave ratio finding should also be interpreted cautiously. Because the photopic b-wave and d-wave are commonly associated with ON- and OFF-bipolar pathway activity, the absence of a significant relationship between the b-wave/d-wave amplitude ratio and AXL suggests that this flash paradigm did not detect an AXL-related shift in relative transient ON/OFF response amplitude. This is compatible with the idea that ON and OFF bipolar responses can show broadly similar contrast-processing ranges under some light-adapted conditions, as described by Burkhardt's (2011) However, the present result only shows that this specific ratio measure was not significantly associated with AXL in this sample; it does not prove that ON and OFF bipolar-cell mechanisms are unchanged.

Flash VEP findings should be interpreted with the same caution. Although the rapid-on and rapid-off sawtooth stimuli biased the initial luminance transition toward ON- or OFF-dominated input, the extracted N2 and P2 components reflect broad transient cortical responses rather than pure pathway isolation. Prior human VEP studies comparing increment- and decrement-biased stimulation have also reported mixed findings. Zemon et al. (1988) reported evidence of ON/OFF asymmetry, with OFF-biased responses showing finer spatial tuning and greater contrast gain, whereas Mutlukan et al. (1992) reported larger increment responses in a small transient-onset/offset VEP paradigm. These differences

suggest that cortical polarity effects depend strongly on stimulus design, contrast definition, luminance conditions, and sample characteristics.

Overall, the flash findings support a paradigm-specific interpretation of the study. Transient photopic flash ERG and VEP did not reveal measurable AXL-related changes in ON- or OFF-biased responses, despite prior literature showing ERG abnormalities in myopia under other testing conditions. The most likely explanation is not that retinal and cortical ON/OFF physiology is necessarily normal in longer eyes, but that full-field single-contrast photopic flash responses were not sensitive to the types of subtle, regional, contrast-dependent, or rod-driven changes that may occur with axial elongation. This distinction provides the rationale for interpreting the flicker findings separately, because flicker stimulation may reveal temporal-processing differences that are not apparent in transient flash responses.

5.3 Flicker Electrophysiology

The flicker recordings provided a different pattern from the flash ERG and VEP results. Whereas transient flash responses did not reveal measurable AXL-related changes, flicker stimulation showed selected ON-related associations, particularly under sustained temporal stimulation. This suggests that flicker paradigms may be more sensitive than single-flash responses for detecting subtle pathway-related effects in young adults with a physiologic-to-moderately myopic AXL range. However, these findings should be interpreted cautiously as evidence of condition-dependent ON-related sensitivity to AXL, rather than as definitive evidence of a broad ON-pathway vulnerability.

This distinction is physiologically plausible because flash and flicker paradigms emphasize different aspects of visual processing. Flash ERG and VEP responses capture transient responses to a single polarity-biased luminance transition, whereas sawtooth flicker stimulation places repeated temporal demand on ON- and OFF-biased response streams (Sustar et al. 2018; Pangeni et al. 2012). Prior work has shown that sawtooth ERG responses can vary with temporal frequency and contrast, supporting their use for probing pathway dynamics that may not be fully captured by transient flash responses (Kremers et al. 2014). AAt the cortical level, steady-state VEPs allow response amplitude, phase, and harmonic content to be quantified at the stimulus frequency and its harmonics (Norcia et al. 2015). Increment- and decrement-biased VEP responses also differ in amplitude and latency, supporting flicker VEP as a useful approach for assessing ON/OFF-biased cortical processing (Norcia et al. 2020). Therefore, the absence of significant flash findings in the present study should not be taken as evidence that ON and OFF function are unaffected by AXL, but rather that AXL-related effects may be more detectable under temporally demanding, frequency-domain conditions. This interpretation is consistent with recent reviews emphasizing that electrophysiological findings in myopia vary substantially by stimulus type, retinal region, adaptation condition, and analysis method (Ribeiro et al. 2025).

At the retinal level, the primary Spearman analysis showed a trend-level negative association between AXL and ON flicker ERG amplitude at the second harmonic response component, 2f1, corresponding to 20 Hz for the 10-Hz stimulus ($r = -0.32$, $p = 0.070$). In contrast, ON flicker ERG amplitude at the fundamental response component, 1f1, was not significantly associated with AXL, and OFF flicker ERG amplitudes were not significantly

associated with AXL at either 1f1 or 2f1. The exploratory median-split comparison for ON 2f1 amplitude followed the same direction as the Spearman correlation, but was not statistically significant after correction for multiple comparisons ($p = 0.137$). Together, this pattern suggests a possible ON-related retinal effect at 2f1, but not a generalized reduction in flicker ERG amplitude across pathways or frequencies.

The harmonic-specific nature of this finding is relevant. The fundamental response component reflects activity phase-locked to the stimulus repetition rate, whereas the second harmonic can contain additional information about waveform shape, temporal asymmetry, and nonlinear post-receptoral processing. Prior flicker ERG work has shown that first- and second-harmonic components can reflect different physiological sources, with the second harmonic containing stronger post-receptoral contributions than the fundamental response (Porciatti et al. 1993). Therefore, the trend-level reduction in ON 2f1 amplitude with increasing AXL may reflect altered ON-biased temporal processing or nonlinear post-receptoral response properties in longer eyes. Because this association did not reach conventional significance and the corrected median-split comparison was not significant, it should be described as a suggestive frequency-domain finding rather than as definitive evidence of retinal ON-pathway loss.

A similar cautious interpretation applies to ON flicker ERG latency. The primary Spearman analysis showed a borderline positive association between AXL and ON 2f1 latency, suggesting a possible delay in the ON second-harmonic response in longer eyes. The exploratory median-split comparison followed the same direction, but was not statistically significant after correction for multiple comparisons ($p = 0.104$). OFF pathway latency at

either 1f1 or 2f1 did not show a comparable relationship with AXL. This ON/OFF temporal pattern is physiologically plausible given known pathway differences in retinal signaling. OFF bipolar cells use ionotropic receptor-mediated transmission, whereas ON bipolar cells depend on the slower metabotropic cascade (Ichinose and Habib 2022; Wolffsohn and Gifford 2025). These timing findings also align broadly with population-based observations that AXL can predict ERG implicit time in human subjects (Kato et al. 2017; Inooka et al. 2023). However, because the continuous association was borderline and the corrected median-split comparison was not significant, these results should be interpreted as suggestive evidence that ON-biased retinal timing may be sensitive to AXL under flicker conditions, rather than as definitive evidence of selective ON-pathway delay.

At the cortical level, the strongest electrophysiological finding was the significant negative Spearman association between AXL and ON flicker VEP amplitude at 1f1 ($r = -0.39$, $p = 0.026$). Longer eyes showed lower mean ON VEP amplitude than shorter eyes in the exploratory median-split comparison (shorter AXL: 6.21 ± 3.22 uV; longer AXL: 4.01 ± 2.34 uV), but this group-level comparison did not remain significant after correction for multiple comparisons ($p = 0.082$). This cortical effect occurred at the fundamental response component, whereas the retinal ERG findings were most apparent at 2f1, suggesting that retinal and cortical flicker responses may not map onto AXL in a simple one-to-one feed-forward manner. Instead, the pattern may reflect frequency-specific differences in how temporal information is encoded at the retina and then integrated cortically. The 1f1 cortical effect is notable because human temporal contrast sensitivity is strongly tuned to flicker frequencies in this range (Tsoneva et al. 2023), and because prior work has reported ON-

biased electrophysiological changes with increasing AXL (Poudel et al. 2024). In the present study, however, ON VEP amplitude at 2f1 was not significantly associated with AXL, and OFF VEP amplitudes were not significantly associated with AXL at either 1f1 or 2f1. Therefore, these findings support a selective ON-related cortical amplitude association under flicker stimulation, but not a generalized cortical flicker deficit across pathways or harmonics.

VEP latency did not show a significant relationship with AXL for either the ON or OFF pathway at either 1f1 or 2f1. This suggests that the cortical amplitude association was not accompanied by a measurable change in phase-derived cortical timing. However, this null latency finding should be interpreted cautiously because VEP recordings can show substantial intersubject and intersession variability, partly related to background EEG activity and recording factors, which may reduce sensitivity for detecting subtle cortical timing effects (Klistorner and Graham 2001). This is especially relevant when interpreting small timing effects from frequency-domain VEP recordings.

Overall, the flicker findings suggest that temporally demanding stimulation may reveal AXL-related ON-biased associations that were not detectable with flash ERG or VEP. The strongest electrophysiological evidence was the negative association between AXL and ON flicker VEP amplitude at 1f1, with additional suggestive ON ERG findings at 2f1 for amplitude and latency. Because the electrophysiology median-split comparisons did not remain significant after correction for multiple comparisons, the primary interpretation should rest on the continuous Spearman analyses. Taken together, the flicker data support a

condition-dependent relationship between AXL and selected ON-related temporal responses, rather than a definitive retinal-to-cortical ON-pathway vulnerability signature.

5.4 Psychophysical Contrast Sensitivity

The psychophysical findings showed the strongest relationship with AXL in the present study, particularly for contrast sensitivity measured at HSF. Unlike the flash ERG and VEP measures, which did not reveal measurable AXL-related changes, and unlike the flicker electrophysiology measures, which showed selected ON-related associations, the psychophysical results demonstrated a clearer spatial-frequency-dependent pattern. Specifically, longer eyes showed reduced sensitivity at HSF, while LSF sensitivity was not significantly associated with AXL. This pattern suggests that perceptual sensitivity in longer eyes may be more affected when the task places greater demand on fine spatial resolution. At HSF, the primary Spearman analysis showed that ON HSF LogCS decreased significantly with AXL ($r = -0.438$, $p = 0.010$), representing one of the strongest associations observed across the study. OFF HSF LogCS showed a weaker trend in the same direction ($r = -0.292$, $p = 0.094$). In contrast, neither ON LSF LogCS nor OFF LSF LogCS showed a significant relationship with AXL. The exploratory median-split comparisons followed the same general pattern. ON HSF LogCS remained significant after correction for multiple comparisons ($p = 0.050$), while OFF HSF LogCS followed the same direction but did not remain significant after correction for multiple comparisons ($p = 0.082$). Therefore, the strongest psychophysical evidence was for reduced ON HSF LogCS in longer eyes, with weaker evidence for a similar OFF HSF effect.

The spatial-frequency dependence of this finding is consistent with prior work showing that contrast sensitivity deficits in myopia are more likely to emerge at higher spatial frequencies than at lower spatial frequencies. Several studies have reported mixed contrast sensitivity findings in myopia, but higher spatial frequency tasks appear more vulnerable, particularly in higher myopia or under testing conditions that increase optical and spatial-resolution demands (Collins et al. 1990; Liou and Chiu 2001; Jaworski et al. 2006). This interpretation also aligns with evidence that axial elongation may reduce effective retinal sampling density through retinal stretching, which would be expected to disproportionately affect fine spatial resolution rather than coarser low-spatial-frequency processing (Chui et al. 2005; Coletta and Watson 2006). However, these results should not be interpreted as proving that optical factors alone explain the psychophysical findings. Rather, the spatial-frequency dependence suggests that optical factors, retinal sampling, and spatial-frequency-dependent neural mechanisms may all contribute to reduced HSF sensitivity in longer eyes.

The relative sensitivity analyses further supported the spatial-frequency interpretation. ON Relative Sensitivity increased significantly with AXL, and Average Relative Sensitivity across pathways also increased significantly with AXL. These effects indicate that longer eyes showed a greater reduction in HSF sensitivity relative to LSF sensitivity. The exploratory median-split comparisons followed the same direction and remained significant for ON Relative Sensitivity ($p = 0.034$) and Average Relative Sensitivity ($p = 0.043$). OFF Relative Sensitivity showed a weaker trend-level relationship with AXL, but the exploratory median-split comparison did not remain significant after

correction for multiple comparisons ($p = 0.104$). Taken together, these findings suggest that the psychophysical effect was not simply a uniform decrease in contrast sensitivity, but instead reflected a spatial-frequency-dependent reduction, with HSF sensitivity more affected than LSF sensitivity in longer eyes.

These findings are relevant when compared with prior ON/OFF psychophysical work from Hogue and Taylor. Hogue and Taylor reported that the OFF/ON threshold index increased with AXL for DoG targets, suggesting that axial elongation may alter the perceptual balance between OFF and ON contrast processing. The present study did not replicate that OFF/ON ratio finding. Instead, the strongest effects were seen in individual HSF LogCS and relative sensitivity measures, while the OFF/ON Index was not significantly associated with AXL at either LSF or HSF. Several methodological differences may help explain this discrepancy. Hogue and Taylor studied a broader cohort with a wider age and refractive error range, whereas the present study examined a younger cohort with a narrower AXL range. In addition, even subtle differences in spatial frequency, stimulus size, viewing distance, and subject population may affect ON/OFF psychophysical outcomes. Therefore, the non-replication of the OFF/ON ratio effect should not be interpreted as disproving the earlier finding, but rather as suggesting that ON/OFF perceptual balance effects may depend on stimulus parameters, cohort characteristics, and the range of axial elongation tested.

The present results also partially align with Poudel et al. (2024), who reported that ON-pathway responses became less responsive, slower, and less sensitive with increasing AXL, particularly under specific contrast conditions. In the current study, ON HSF LogCS showed the clearest psychophysical association with AXL, while OFF HSF LogCS showed a

weaker trend. However, the absence of significant OFF/ON Index correlations argues against a simple pathway-specific imbalance in this cohort. This distinction is important because the present task measured absolute detection thresholds for ON and OFF DoG stimuli against a gray background. It did not directly measure contrast gain or response compression. Pedestal-based threshold-versus-contrast paradigms can reveal gain-control effects that may not be visible in absolute detection tasks, because contrast discrimination depends on how the visual system responds to changes around an existing contrast pedestal (Legge and Foley 1980; Legge and Kersten 1987). Therefore, the present findings do not rule out pathway-specific contrast gain changes; they show that, under the current DoG detection conditions, AXL was most strongly associated with HSF detection sensitivity rather than with a significant OFF/ON ratio change.

The spatial-frequency-dependent pattern may also be influenced by retinal eccentricity and stimulus design. The current psychophysical task used central ON and OFF DoG detection, whereas axial elongation may produce larger structural and sampling changes outside the fovea. Peripheral ON and OFF responses can vary by visual field location, contrast level, and stimulus conditions, and peripheral testing may be more sensitive to effects related to retinal stretching or reduced ganglion cell sampling density (Chui et al. 2005; Scott et al. 2024). Related work by Taylor et al. (2018), using cone-isolating silent substitution, also suggests that chromatic and low-spatial-frequency mechanisms may show refractive-error-dependent changes under different stimulus conditions. Because the present study used achromatic ON- and OFF-selective DoG targets rather than cone-isolating stimuli, future studies combining ON/OFF polarity, spatial frequency, retinal eccentricity, and

chromatic pathway isolation may help determine whether longer eyes show a generalized reduction in fine spatial contrast sensitivity, a chromatic sensitivity deficit, or a pathway-specific ON/OFF effect that emerges only under particular stimulus conditions.

Overall, the psychophysical results provide the clearest evidence for an AXL-related functional change in the present study. ON HSF LogCS decreased significantly with AXL, OFF HSF LogCS showed a weaker trend in the same direction, and ON and Average Relative Sensitivity indicated greater HSF loss relative to LSF in longer eyes. However, OFF/ON Index measures were not significantly associated with AXL, meaning that the present study did not detect significant evidence of altered ON/OFF relative balance under these psychophysical conditions. The most cautious interpretation is that longer eyes showed spatial-frequency-dependent reductions in contrast sensitivity, especially for ON HSF LogCS, rather than a uniform or definitive ON/OFF pathway imbalance.

5.5 ON/OFF Pathway Balance

Across electrophysiological and psychophysical ratio measures, the present study did not detect significant evidence of altered ON/OFF relative balance with AXL. This was observed across flash ERG, flash VEP, flicker ERG, flicker VEP, and psychophysical OFF/ON Index measures. Flash ERG b-wave/d-wave amplitude ratio showed no significant relationship with AXL ($p = 0.953$), and flash VEP ON/OFF N2-P2 peak-to-peak amplitude ratio was similarly not associated with AXL ($p = 0.438$). Flicker ERG ON/OFF amplitude ratios were not significantly associated with AXL at either 1f1 ($p = 0.558$) or 2f1 ($p = 0.916$), and flicker VEP ON/OFF amplitude ratios were also not significantly associated with AXL at

1f1 ($p = 0.429$) or 2f1 ($p = 0.769$). Psychophysical OFF/ON Index measures showed no significant association with AXL at either HSF ($p = 0.685$) or LSF ($p = 0.181$).

These findings suggest that, under the stimulus conditions tested, AXL was not associated with a measurable shift in relative ON/OFF balance. This interpretation should be separated from the individual pathway findings discussed in Sections 5.3 and 5.4. Selected ON-related measures showed AXL associations, including ON flicker VEP amplitude at 1f1 and ON HSF LogCS. However, the ratio measures did not show significant AXL-related changes. Therefore, the present data support a more specific conclusion: longer eyes showed selected ON-related and spatial-frequency-dependent effects, but these effects did not translate into a detectable change in relative ON/OFF ratio measures.

This distinction is especially relevant when comparing the present findings with prior psychophysical work. Hogue and Taylor reported that OFF/ON sensitivity ratios for DoG stimuli increased with AXL, suggesting that axial elongation may alter perceptual ON/OFF balance under some stimulus conditions. The present study did not replicate that ratio effect. Instead, the strongest psychophysical findings were reduced ON HSF LogCS and increased ON and Average Relative Sensitivity with AXL, while OFF/ON Index measures were not significantly associated with AXL. This difference may reflect variation in cohort characteristics, AXL range, stimulus geometry, viewing distance, or threshold estimation procedures. Therefore, the current findings should not be interpreted as contradicting Hogue and Taylor, but as suggesting that OFF/ON balance effects may depend on the specific psychophysical paradigm and participant sample.

The present findings also partly align with Poudel et al. (2024), who reported ON-biased electrophysiological and psychophysical effects with increasing AXL. In the current study, selected ON-related effects were observed, particularly ON flicker VEP amplitude at 1f1 and ON HSF LogCS. However, the absence of significant ON/OFF ratio associations suggests that these individual ON-related findings did not produce a measurable relative pathway imbalance under the present testing conditions. This distinction is important because an individual ON measure can change with AXL without necessarily producing a significant ON/OFF ratio change, especially if the corresponding OFF measure shows a weaker change in the same direction or if ratio measures have lower statistical sensitivity.

The lack of significant ratio findings should also be interpreted within the limits of the methods used. The electrophysiological ratio measures were derived from full-field sawtooth ERG and VEP responses, while the psychophysical ratios were derived from central DoG detection thresholds. These measures assess relative ON/OFF responses under specific stimulus conditions, but they do not directly measure contrast gain, response saturation, adaptation, or cortical normalization. Prior work has shown that ON/OFF dominance can vary with contrast level, stimulus conditions, and visual field location (Rahimi-Nasrabadi et al. 2023; Scott et al. 2024). Therefore, the absence of a significant OFF/ON Index relationship in this study does not rule out ON/OFF gain changes under other paradigms, such as pedestal-based threshold-versus-contrast tasks or peripheral ON/OFF testing.

Clinical and developmental studies also show that ON/OFF balance can be disrupted under other conditions. Pons et al. (2019) reported ON-biased abnormalities in amblyopia,

and Hathibelagal et al. (2022) described age-related differences in ON and OFF pathway function. More recent work suggests that ON/OFF asymmetries can vary across ganglion cell types, indicating that ON/OFF pathway organization is not uniform across all retinal circuits (Ravi et al. 2018). These findings provide useful context, but they should not be taken as direct evidence that the present cohort underwent compensatory pathway rebalancing. Rather, they show that ON/OFF balance is biologically flexible and may vary by disease state, age, retinal circuit, and testing condition.

A cautious interpretation is that relative ON/OFF balance may remain stable within the AXL range and stimulus conditions tested in this study. However, this remains a hypothesis that would require direct testing in larger samples, broader AXL ranges, and paradigms designed to assess gain control, adaptation, and peripheral pathway function. In the present study, the safest conclusion is that no significant evidence of altered ON/OFF relative balance was detected, despite selected ON-related and HSF-dependent associations with AXL.

Taken together, the ON/OFF ratio findings refine the interpretation of the individual pathway results. The data do not support a generalized ON/OFF imbalance across the visual hierarchy. Instead, they suggest that AXL-related effects in this cohort were condition-dependent: flicker electrophysiology revealed selected ON-related associations, psychophysics showed the strongest effects at HSF, and ratio measures did not detect significant shifts in relative ON/OFF balance. This supports a model in which AXL is associated with specific functional changes under particular stimulus demands, rather than a uniform disruption of ON/OFF pathway balance.

5.6 Limitations

Several limitations should be considered when interpreting these findings. First, the sample size was modest, with 34 participants contributing psychophysics data and 33 contributing electrophysiological data. This limits the precision of correlation estimates and reduces sensitivity for detecting small-to-moderate effects. Therefore, trend-level or borderline findings, including ON ERG amplitude at 2f1, ON ERG latency at 2f1, OFF HSF LogCS, and OFF flash VEP N2 time to peak, should be interpreted cautiously. These effects may represent true AXL-related associations, but they may also reflect sampling variability. Future studies should use pre-study power calculations based on prespecified primary outcomes.

A second limitation is that several interpretations rely partly on exploratory median-split analyses. Spearman correlations with AXL were treated as the primary analyses because AXL is a continuous variable. Median-split analyses were included only as secondary visualizations of shorter- versus longer-AXL groups. Because dichotomizing a continuous variable reduces statistical information, these comparisons should not be used to confirm or override the continuous analyses. This is especially relevant for the electrophysiological findings, where the median-split comparisons followed the same direction as the Spearman correlations but did not remain significant after correction for multiple comparisons.

A third limitation is that the ON and OFF stimuli were pathway-biased rather than pathway-pure. Rapid-on and rapid-off sawtooth stimuli preferentially emphasize luminance increments and decrements, and ON/OFF DoG stimuli preferentially probe positive and

negative contrast detection. However, both pathways may contribute to the measured responses depending on contrast, temporal frequency, spatial frequency, adaptation state, and retinal location. For this reason, the results should be interpreted as ON- and OFF-biased responses rather than isolated ON- or OFF-pathway measurements.

A fourth limitation is that the ERG, VEP, and psychophysical stimuli were not directly equivalent. The electrophysiology experiments used full-field sawtooth stimulation, whereas the psychophysical experiment used central DoG detection. These methods probe different stimulus dimensions and different levels of visual processing. Therefore, the multimodal findings should be interpreted as complementary measures of ON/OFF-biased function, not as direct one-to-one measurements of the same neural response.

The psychophysical task also measured absolute detection threshold rather than contrast gain, response saturation, or adaptation. Therefore, the absence of significant OFF/ON Index associations with AXL does not rule out ON/OFF gain-control differences under other testing conditions. Pedestal-based threshold-versus-contrast paradigms or adaptation paradigms would be better suited to test whether longer eyes show altered contrast gain, response compression, or pathway plasticity. Similarly, because the psychophysical testing was central/foveal, the present study may not capture peripheral ON/OFF effects that could be more relevant to axial elongation and visually guided eye growth.

The cross-sectional design is another major limitation. Because AXL and visual function were measured at one time point, this study cannot determine whether the observed associations reflect changes that contributed to axial elongation, consequences of axial elongation, or both. Li et al. (2017) demonstrated that subclinical reductions in central inner

retinal activity measured with mfERG preceded and predicted later axial elongation in children, but that study did not use pathway-selective ON/OFF stimuli. Future longitudinal studies using sawtooth ERG/VEP and ON/OFF psychophysics during active myopia progression would be needed to determine whether ON/OFF-biased functional changes precede or follow ocular growth.

The cohort also limits generalizability. Participants were healthy young adults with an AXL range of 22.50 to 27.51 mm. This range is appropriate for studying physiologic-to-moderate axial elongation without ocular pathology, but it does not address children undergoing active myopia progression or individuals with high/pathologic myopia. Effects may differ in eyes with AXL beyond 28 mm, in eyes with myopic retinal pathology, or during childhood when emmetropization and axial growth are still active.

Finally, the present study did not include direct optical quality measurements such as higher-order aberrations or wavefront error during psychophysical testing. This limits interpretation of the HSF contrast sensitivity findings, which may reflect optical factors, retinal sampling, neural mechanisms, or a combination of these. Future studies combining ON/OFF psychophysics with wavefront aberrometry and OCT-based retinal layer measurements would help separate optical, structural, and neural contributions. OCT measures may be especially useful given prior evidence linking axial elongation with ganglion cell complex thinning (Hirasawa and Shoji 2013).

Overall, these limitations mean that the present findings should be interpreted as condition-dependent associations between AXL and selected ON-related or spatial-frequency-dependent measures, rather than as definitive evidence of pathway dysfunction,

preserved biological balance, or compensatory rebalancing. Future work with larger samples, longitudinal designs, peripheral testing, contrast-gain paradigms, optical measurements, and structural imaging will be needed to determine whether these associations represent early functional markers of axial elongation or secondary changes in the myopic visual system.

5.7 Conclusions

This study examined the relationship between AXL and ON/OFF-biased visual pathway function across retinal, cortical, and perceptual levels. Overall, AXL-related associations were condition-dependent rather than uniform across the visual hierarchy. Flash ERG and VEP responses did not reveal measurable AXL-related changes in ON- or OFF-biased transient responses, whereas flicker electrophysiology showed selected ON-related associations under temporal demand. The strongest electrophysiological finding was the negative association between AXL and ON flicker VEP amplitude at 1f1, with additional suggestive ON ERG findings at 2f1 for amplitude and latency. Because the electrophysiology median-split comparisons did not remain significant after correction for multiple comparisons, these findings should be interpreted primarily through the continuous Spearman analyses and not as evidence of global ON-pathway differences

The clearest AXL-related effects were observed psychophysically. ON contrast sensitivity at the relatively higher low-spatial-frequency condition decreased significantly with increasing AXL, while OFF contrast sensitivity showed a weaker trend in the same direction. Relative sensitivity measures also indicated greater reduction at the higher

compared with the lower spatial-frequency condition in longer eyes. Across electrophysiological and psychophysical ratio measures, no significant AXL-related change in ON/OFF relative balance was detected. Taken together, these findings suggest that longer eyes showed selected ON-related and spatial-frequency-dependent functional associations, rather than a broad ON/OFF pathway deficit or measurable shift in ON/OFF balance within this sample.

Reference List

Agrawal, A., Puthalath, A. S., Mittal, S. K., Mittal, S., Singh, Y., & Singh, A. (2022). Alteration in pattern reversal visual evoked potential in pediatric population with amblyopia and spherical refractive errors. Indian Journal of Ophthalmology, 70(5): 1727–1731. https://doi.org/10.4103/ijo.IJO_2692_21.

American Clinical Neurophysiology Society (2006). Guideline 5: Guidelines for standard electrode position nomenclature. Journal of Clinical Neurophysiology: Official Publication of the American Electroencephalographic Society, 23(2): 107–110. https://doi.org/10.1097/00004691-200604000-00006.

Barboni, M. T. S., Nagy, B. V., de Araújo Moura, A. L., Damico, F. M., da Costa, M. F., Kremers, J., & Ventura, D. F. (2013). ON and OFF Electroretinography and Contrast Sensitivity in Duchenne Muscular Dystrophy. Investigative Ophthalmology & Visual Science, 54(5): 3195–3204. https://doi.org/10.1167/iovs.13-11700.

Bergen, M. A., Park, H. N., Chakraborty, R., Landis, E. G., Sidhu, C., He, L., Iuvone, P. M., & Pardue, M. T. (2016). Altered Refractive Development in Mice With Reduced Levels of Retinal Dopamine. Investigative Ophthalmology & Visual Science, 57(10): 4412–4419. https://doi.org/10.1167/iovs.15-17784.

Brainard, D. H. (1997). The Psychophysics Toolbox. Spatial Vision, 10(4): 433–436.

Bullimore, M. A., Saunders, K. J., Baraas, R. C., Berntsen, D. A., Chen, Z., Chia, A. W. L., Goto, S., Jiang, J., Lan, W., Logan, N. S., Najjar, R. P., Polling, J. R., Read, S. A., Woodman-Pieterse, E. C., Széll, N., Verkicharla, P. K., Wu, P.-C., Zhu, X.,

Loughman, J., Nagra, M., Phillips, J. R., Tran, H. D. M., Vera-Diaz, F. A., Yam, J., Liu, Y. M., Singh, S. E., & Wildsoet, C. F. (2025). IMI—Interventions for Controlling Myopia Onset and Progression 2025. Investigative Ophthalmology & Visual Science, 66(12): 39. https://doi.org/10.1167/iovs.66.12.39.

Burkhardt, D. A. (2011). Contrast processing by ON and OFF bipolar cells. Visual Neuroscience, 28(1): 69–75. https://doi.org/10.1017/S0952523810000313.

Chakraborty, R., Park, H. N., Hanif, A. M., Sidhu, C., Iuvone, P. M., & Pardue, M. T. (2015). ON pathway mutations increase susceptibility to form-deprivation myopia. Experimental eye research, 137: 79–83. https://doi.org/10.1016/j.exer.2015.06.009.

Chen, J. C., Brown, B., & Schmid, K. L. (2006). Delayed mfERG responses in myopia. Vision Research, 46(8-9): 1221–1229. https://doi.org/10.1016/j.visres.2005.06.030.

Chichilnisky, E. J., & Kalmar, R. S. (2002). Functional asymmetries in ON and OFF ganglion cells of primate retina. The Journal of Neuroscience: The Official Journal of the Society for Neuroscience, 22(7): 2737–2747. https://doi.org/10.1523/JNEUROSCI.22-07-02737.2002.

Chui, T. Y. P., Yap, M. K. H., Chan, H. H. L., & Thibos, L. N. (2005). Retinal stretching limits peripheral visual acuity in myopia. Vision Research, 45(5): 593–605. https://doi.org/10.1016/j.visres.2004.09.016.

Coletta, N. J., & Watson, T. (2006). Effect of myopia on visual acuity measured with laser interference fringes. Vision Research, 46(5): 636–651. https://doi.org/10.1016/j.visres.2005.05.025.

Collins, J. W., & Carney, L. G. (1990). Visual performance in high myopia. Current Eye Research, 9(3): 217–224. https://doi.org/10.3109/02713689009044516.

Cooper, E. A., & Norcia, A. M. (2015). Predicting Cortical Dark/Bright Asymmetries from Natural Image Statistics and Early Visual Transforms. PLoS Computational Biology, 11(5): e1004268. https://doi.org/10.1371/journal.pcbi.1004268.

Crewther, S. G., & Crewther, D. P. (2003). Inhibition of retinal ON/OFF systems differentially affects refractive compensation to defocus. NeuroReport, 14(9): 1233–1237. https://doi.org/10.1097/00001756-200307010-00009.

Curcio, C. A., Owsley, C., & Jackson, G. R. (2000). Spare the Rods, Save the Cones in Aging and Age-related Maculopathy. Investigative Ophthalmology & Visual Science, 41(8): 2015–2018.

Dacey, D. M., & Petersen, M. R. (1992). Dendritic field size and morphology of midget and parasol ganglion cells of the human retina. Proceedings of the National Academy of Sciences of the United States of America, 89(20): 9666–9670. https://doi.org/10.1073/pnas.89.20.9666.

Ehsaei, A., Chisholm, C. M., MacIsaac, J. C., Mallen, E. A. H., & Pacey, I. E. (2011). Central and peripheral visual performance in myopes: contact lenses versus spectacles. Contact Lens & Anterior Eye: The Journal of the British Contact Lens Association, 34(3): 128–132. https://doi.org/10.1016/j.clae.2011.02.011.

Falsini, B., Iarossi, G., Porciatti, V., Merendino, E., Fadda, A., Cermola, S., & Buzzonetti, L. (1994). Postreceptoral contribution to macular dysfunction in retinitis pigmentosa. Investigative Ophthalmology & Visual Science, 35(13): 4282–4290.

Farshi, P., Fyk-Kolodziej, B., Krolewski, D. M., Walker, P. D., & Ichinose, T. (2016). Dopamine D1 receptor expression is bipolar cell type-specific in the mouse retina. Journal of Comparative Neurology, 524(10): 2059–2079. https://doi.org/10.1002/cne.23932.

Feldkaemper, M., & Schaeffel, F. (2013). An updated view on the role of dopamine in myopia. Experimental Eye Research, 114: 106–119. https://doi.org/10.1016/j.exer.2013.02.007.

Frishman, L., Sustar, M., Kremers, J., McAnany, J. J., Sarossy, M., Tzekov, R., & Viswanathan, S. (2018). ISCEV extended protocol for the photopic negative response (PhNR) of the full-field electroretinogram. Documenta Ophthalmologica, 136(3): 207–211. https://doi.org/10.1007/s10633-018-9638-x.

García-Pérez, M. A., & Alcalá-Quintana, R. (2011). Interval bias in 2AFC detection tasks: sorting out the artifacts. Attention, Perception & Psychophysics, 73(7): 2332–2352. https://doi.org/10.3758/s13414-011-0167-x.

Gupta, S. K., Chakraborty, R., & Verkicharla, P. K. (2021). Electroretinogram responses in myopia: a review. Documenta Ophthalmologica. Advances in Ophthalmology. https://doi.org/10.1007/s10633-021-09857-5.

Hathibelagal, A. R., Prajapati, V., Jayagopi, I., Jalali, S., & Ganeshrao, S. B. (2022). Age-related decline in function of ON and OFF visual pathways. PloS One, 17(3): e0261489. https://doi.org/10.1371/journal.pone.0261489.

Hirasawa, H., Miwa, N., & Watanabe, S.-I. (2021). GABAergic and glycinergic systems regulate ON-OFF electroretinogram by cooperatively modulating cone pathways in

the amphibian retina. The European Journal of Neuroscience, 53(5): 1428–1440. https://doi.org/10.1111/ejn.15054.

Hirasawa, K., & Shoji, N. (2013). Association between ganglion cell complex and axial length. Japanese Journal of Ophthalmology, 57(5): 429–434. https://doi.org/10.1007/s10384-013-0241-0.

Ho, W.-C., Kee, C.-S., & Chan, H. H.-L. (2012). Myopic children have central reduction in high contrast multifocal ERG response, while adults have paracentral reduction in low contrast response. Investigative Ophthalmology & Visual Science, 53(7): 3695–3702. https://doi.org/10.1167/iovs.11-9379.

Hogue, W., & Taylor, C. P. (2021). Axial length is associated with individual differences in ON- and OFF- pattern detection. Investigative Ophthalmology & Visual Science, 62(8): 2894.

Hogue, W., & Taylor, C. P. (2022). Individual differences in ON- versus OFF-contrast pattern detection and identification in axial myopia. Preprint manuscript, New England College of Optometry, July 19, 2022.

Holden, B. A., Fricke, T. R., Wilson, D. A., Jong, M., Naidoo, K. S., Sankaridurg, P., Wong, T. Y., Naduvilath, T. J., & Resnikoff, S. (2016). Global Prevalence of Myopia and High Myopia and Temporal Trends from 2000 through 2050. Ophthalmology, 123(5): 1036–1042. https://doi.org/10.1016/j.ophtha.2016.01.006.

Holm, S. (1979). A Simple Sequentially Rejective Multiple Test Procedure. Scandinavian Journal of Statistics, 6(2): 65–70.

Ichinose, T., & Habib, S. (2022). On and off signaling pathways in the retina and the visual system. Frontiers in Ophthalmology, 2: 989002. https://doi.org/10.3389/fopht.2022.989002.

Inooka, T., Kominami, T., Yasuda, S., Koyanagi, Y., Ota, J., Okado, S., Tomita, R., Ito, Y., Iwase, T., Terasaki, H., Nishiguchi, K. M., & Ueno, S. (2023). Assessment of factors affecting flicker ERGs recorded with RETeval from data obtained from health checkup screening. PloS One, 18(4): e0284686. https://doi.org/10.1371/journal.pone.0284686.

Ismael, Z. F., El-Shazly, A. A. E.-F., Farweez, Y. A., & Osman, M. M. M. (2017). Relationship between functional and structural retinal changes in myopic eyes. Clinical & Experimental Optometry, 100(6): 695–703. https://doi.org/10.1111/cxo.12527.

Jaworski, A., Gentle, A., Zele, A. J., Vingrys, A. J., & McBrien, N. A. (2006). Altered Visual Sensitivity in Axial High Myopia: A Local Postreceptoral Phenomenon?. Investigative Ophthalmology & Visual Science, 47(8): 3695–3702. https://doi.org/10.1167/iovs.05-1569.

Jin, J., Wang, Y., Lashgari, R., Swadlow, H. A., & Alonso, J.-M. (2011). Faster Thalamocortical Processing for Dark than Light Visual Targets. The Journal of Neuroscience, 31(48): 17471–17479. https://doi.org/10.1523/JNEUROSCI.2456-11.2011.

Jin, J. Z., Weng, C., Yeh, C.-I., Gordon, J. A., Ruthazer, E. S., Stryker, M. P., Swadlow, H. A., & Alonso, J.-M. (2008). On and off domains of geniculate afferents in cat primary visual cortex. Nature Neuroscience, 11(1): 88–94. https://doi.org/10.1038/nn2029.

Jonas, J. B., Spaide, R. F., Ostrin, L. A., Logan, N. S., Flitcroft, I., & Panda-Jonas, S. (2023). IMI-Nonpathological Human Ocular Tissue Changes With Axial Myopia. Investigative Ophthalmology & Visual Science, 64(6): 5. https://doi.org/10.1167/iovs.64.6.5.

Kato, K., Kondo, M., Nagashima, R., Sugawara, A., Sugimoto, M., Matsubara, H., McCulloch, D. L., & Ikesugi, K. (2017). Factors Affecting Mydriasis-Free Flicker ERGs Recorded With Real-Time Correction for Retinal Illuminance: Study of 150 Young Healthy Subjects. Investigative Ophthalmology & Visual Science, 58(12): 5280–5286. https://doi.org/10.1167/iovs.17-22587.

Klistorner, A. I., & Graham, S. L. (2001). Electroencephalogram-Based Scaling of Multifocal Visual Evoked Potentials: Effect on Intersubject Amplitude Variability. Investigative Ophthalmology & Visual Science, 42(9): 2145–2152.

Koike, C., Obara, T., Uriu, Y., Numata, T., Sanuki, R., Miyata, K., Koyasu, T., Ueno, S., Funabiki, K., Tani, A., Ueda, H., Kondo, M., Mori, Y., Tachibana, M., & Furukawa, T. (2010). TRPM1 is a component of the retinal ON bipolar cell transduction channel in the mGluR6 cascade. Proceedings of the National Academy of Sciences of the United States of America, 107(1): 332–337. https://doi.org/10.1073/pnas.0912730107.

Komban, S. J., Kremkow, J., Jin, J., Wang, Y., Lashgari, R., Li, X., Zaidi, Q., & Alonso, J.-M. (2014). Neuronal and perceptual differences in the temporal processing of darks and lights. Neuron, 82(1): 224–234. https://doi.org/10.1016/j.neuron.2014.02.020.

Kremers, J., Pangeni, G., Tsaousis, K. T., McKeefry, D., Murray, I. J., & Parry, N. R. A. (2014). Incremental and decremental L- and M-cone driven ERG responses: II. Sawtooth stimulation. Journal of the Optical Society of America. A, Optics, Image Science, and Vision, 31(4): A170–178. https://doi.org/10.1364/JOSAA.31.00A170.

Legge, G. E., & Foley, J. M. (1980). Contrast masking in human vision. Journal of the Optical Society of America, 70(12): 1458–1471. https://doi.org/10.1364/josa.70.001458.

Legge, G. E., & Kersten, D. (1987). Contrast discrimination in peripheral vision. Journal of the Optical Society of America. A, Optics and Image Science, 4(8): 1594–1598. https://doi.org/10.1364/josaa.4.001594.

Li, S. Z.-C., Yu, W.-Y., Choi, K.-Y., Lam, C. H.-I., Lakshmanan, Y., Wong, F. S.-Y., & Chan, H. H.-L. (2017). Subclinical Decrease in Central Inner Retinal Activity Is Associated With Myopia Development in Children. Investigative Ophthalmology & Visual Science, 58(10): 4399–4406. https://doi.org/10.1167/iovs.16-21279.

Liou, S. W., & Chiu, C. J. (2001). Myopia and contrast sensitivity function. Current Eye Research, 22(2): 81–84. https://doi.org/10.1076/ceyr.22.2.81.5530.

Luu, C. D., Lau, A. M. I., & Lee, S.-Y. (2006). Multifocal Electroretinogram in Adults and Children With Myopia. Archives of Ophthalmology, 124(3): 328–334. https://doi.org/10.1001/archopht.124.3.328.

Masland, R. H. (2012). The Neuronal Organization of the Retina. Neuron, 76(2): 266–280. https://doi.org/10.1016/j.neuron.2012.10.002.

Mazade, R., Jin, J., Pons, C., & Alonso, J.-M. (2019). Functional Specialization of ON and OFF Cortical Pathways for Global-Slow and Local-Fast Vision. Cell Reports, 27(10): 2881–2894.e5. https://doi.org/10.1016/j.celrep.2019.05.007.

Morgans, C. W., Zhang, J., Jeffrey, B. G., Nelson, S. M., Burke, N. S., Duvoisin, R. M., & Brown, R. L. (2009). TRPM1 is required for the depolarizing light response in retinal ON-bipolar cells. Proceedings of the National Academy of Sciences of the United States of America, 106(45): 19174–19178. https://doi.org/10.1073/pnas.0908711106.

Munteanu, T., Noronha, K. J., Leung, A. C., Pan, S., Lucas, J. A., & Schmidt, T. M. (2018). Light-dependent pathways for dopaminergic amacrine cell development and function. eLife, 7: e39866. https://doi.org/10.7554/eLife.39866.

Mutlukan, E., Bradnam, M., Keating, D., & Damato, B. E. (1992). Visual evoked cortical potentials from transient dark and bright stimuli. Selective 'on' and 'off-pathway' testing?. Documenta Ophthalmologica. Advances in Ophthalmology, 80(2): 171–181. https://doi.org/10.1007/BF00161243.

Nomura, A., Shigemoto, R., Nakamura, Y., Okamoto, N., Mizuno, N., & Nakanishi, S. (1994). Developmentally regulated postsynaptic localization of a metabotropic glutamate receptor in rat rod bipolar cells. Cell, 77(3): 361–369. https://doi.org/10.1016/0092-8674(94)90151-1.

Norcia, A. M., Appelbaum, L. G., Ales, J. M., Cottereau, B. R., & Rossion, B. (2015). The steady-state visual evoked potential in vision research: A review. Journal of Vision, 15(6): 4. https://doi.org/10.1167/15.6.4.

Norcia, A. M., Yakovleva, A., Hung, B., & Goldberg, J. L. (2020). Dynamics of Contrast Decrement and Increment Responses in Human Visual Cortex. Translational Vision Science & Technology, 9(10): 6. https://doi.org/10.1167/tvst.9.10.6.

Pangeni, G., & Kremers, J. (2013). Human photopic ON- and OFF-ERG responses elicited by square wave and sawtooth stimuli. Psychology & Neuroscience, 6(2): 165–178. https://doi.org/10.3922/j.psns.2013.2.05.

Pangeni, G., Lämmer, R., Tornow, R. P., Horn, F. K., & Kremers, J. (2012). On- and off-response ERGs elicited by sawtooth stimuli in normal subjects and glaucoma patients. Documenta Ophthalmologica. Advances in Ophthalmology, 124(3): 237–248. https://doi.org/10.1007/s10633-012-9323-4.

Pardue, M. T., Faulkner, A. E., Fernandes, A., Yin, H. Y., Schaeffel, F., Williams, R. W., & Iuvone, P. M. (2008). High susceptibility to experimental myopia in a mouse model with a retinal ON pathway defect. Investigative Ophthalmology & Visual Science, 49(2): 706–712. https://doi.org/10.1167/iovs.07-0643.

Pons, C., Jin, J., Mazade, R., Dul, M., Zaidi, Q., & Alonso, J.-M. (2019). Amblyopia Affects the ON Visual Pathway More than the OFF. The Journal of Neuroscience: The Official Journal of the Society for Neuroscience, 39(32): 6276–6290. https://doi.org/10.1523/JNEUROSCI.3215-18.2019.

Porciatti, V., Moretti, G., Ciavarella, P., & Falsini, B. (1993). The second harmonic of the electroretinogram to sinusoidal flicker: spatiotemporal properties and clinical application. Documenta Ophthalmologica. Advances in Ophthalmology, 84(1): 39–46. https://doi.org/10.1007/BF01203281.

Poudel, S., Jin, J., Rahimi-Nasrabadi, H., Dellostritto, S., Dul, M. W., Viswanathan, S., & Alonso, J.-M. (2024). Contrast Sensitivity of ON and OFF Human Retinal Pathways in Myopia. The Journal of Neuroscience: The Official Journal of the Society for Neuroscience, 44(3): e1487232023. https://doi.org/10.1523/JNEUROSCI.1487-23.2023.

Puopolo, M., Hochstetler, S. E., Gustincich, S., Wightman, R. M., & Raviola, E. (2005). Extrasynaptic Release of Dopamine and Volume Transmission in the Retina, in: Ludwig, M. (Ed.), Dendritic Neurotransmitter Release. Springer US, Boston, MA, pp. 175–189. https://doi.org/10.1007/0-387-23696-1_12.

Rahimi-Nasrabadi, H., Moore-Stoll, V., Tan, J., Dellostritto, S., Jin, J., Dul, M. W., & Alonso, J.-M. (2023). Luminance Contrast Shifts Dominance Balance between ON and OFF Pathways in Human Vision. The Journal of Neuroscience, 43(6): 993–1007. https://doi.org/10.1523/JNEUROSCI.1672-22.2022.

Ravi, S., Ahn, D., Greschner, M., Chichilnisky, E. J., & Field, G. D. (2018a). Pathway-Specific Asymmetries between ON and OFF Visual Signals. The Journal of Neuroscience: The Official Journal of the Society for Neuroscience, 38(45): 9728–9740. https://doi.org/10.1523/JNEUROSCI.2008-18.2018.

Ribeiro, B., Fernandes, A., Brardo, F. M., Vaz Pato, M., & Pinto, N. (2025). Electrophysiological Insights into Neurovisual Dysfunctions in Myopia: A Systematic Review. Seminars in Ophthalmology: 1–10. https://doi.org/10.1080/08820538.2025.2546535.

Robson, A. G., Frishman, L. J., Grigg, J., Hamilton, R., Jeffrey, B. G., Kondo, M., Li, S., & McCulloch, D. L. (2022). ISCEV Standard for full-field clinical electroretinography (2022 update). Documenta Ophthalmologica. Advances in Ophthalmology, 144(3): 165–177. https://doi.org/10.1007/s10633-022-09872-0.

Roy, S., & Field, G. D. (2019). Dopaminergic modulation of retinal processing from starlight to sunlight. Journal of Pharmacological Sciences, 140(1): 86–93. https://doi.org/10.1016/j.jphs.2019.03.006.

Schaeffel, F., & Swiatczak, B. (2024). Mechanisms of emmetropization and what might go wrong in myopia. Vision Research, 220: 108402. https://doi.org/10.1016/j.visres.2024.108402.

Schaeffel, F., Wildsoet, C., & Chakraborty, R. (2025). Is central vision (and a fovea) needed for emmetropisation?. Ophthalmic and Physiological Optics, 45(4): 941–946. https://doi.org/10.1111/opo.13494.

Schiller, P. H. (1992). The ON and OFF channels of the visual system. Trends in Neurosciences, 15(3): 86–92. https://doi.org/10.1016/0166-2236(92)90017-3.

Schiller, P. H., Sandell, J. H., & Maunsell, J. H. (1986). Functions of the ON and OFF channels of the visual system. Nature, 322(6082): 824–825. https://doi.org/10.1038/322824a0.

Scott, M. T. W., Yakovleva, A., & Norcia, A. M. (2024). Visual Field Asymmetries in Responses to ON and OFF Pathway Biasing Stimuli. Visual Neuroscience, 41: E007. https://doi.org/10.1017/S095252382400004X.

Slaughter, M. M., & Miller, R. F. (1981). 2-amino-4-phosphonobutyric acid: a new pharmacological tool for retina research. Science (New York, N.Y.), 211(4478): 182–185. https://doi.org/10.1126/science.6255566.

Srirangam, S. R. (2025). The effect of ocular axial length on photoreceptors. Master's thesis, New England College of Optometry.

Stapley, V., Anderson, R. S., Saunders, K., & Mulholland, P. J. (2025). Measuring differences in the ERG in myopia using the RETeval device with skin electrodes. Ophthalmic & Physiological Optics, 45(3): 666–680. https://doi.org/10.1111/opo.13460.

Stockton, R. A., & Slaughter, M. M. (1989). B-wave of the electroretinogram. A reflection of ON bipolar cell activity. The Journal of General Physiology, 93(1): 101–122. https://doi.org/10.1085/jgp.93.1.101.

Sustar, M., Holder, G. E., Kremers, J., Barnes, C. S., Lei, B., Khan, N. W., & Robson, A. G. (2018). ISCEV extended protocol for the photopic On-Off ERG. Documenta Ophthalmologica. Advances in Ophthalmology, 136(3): 199–206. https://doi.org/10.1007/s10633-018-9645-y.

Šuštar Habjan, M., Bach, M., van Genderen, M. M., Li, S., Mizota, A., Nilsson, J., Thompson, D. A., & Robson, A. G. (2025). ISCEV standard for clinical visual

evoked potentials (2025 update). Documenta Ophthalmologica. Advances in Ophthalmology, 151(2): 97–112. https://doi.org/10.1007/s10633-025-10042-1.

Taylor, C. P., Shepard, T. G., Rucker, F. J., & Eskew, R. T. J. (2018). Sensitivity to S-Cone Stimuli and the Development of Myopia. Investigative Ophthalmology & Visual Science, 59(11): 4622–4630. https://doi.org/10.1167/iovs.18-24113.

Thibos, L. N., Wheeler, W., & Horner, D. (1997). Power vectors: An application of Fourier analysis to the description and statistical analysis of refractive error. Optometry and Vision Science, 74(6): 367–375. https://doi.org/10.1097/00006324-199706000-00019.

Thomson, K., Karouta, C., & Ashby, R. (2020a). Form-deprivation and lens-induced myopia are similarly affected by pharmacological manipulation of the dopaminergic system in chicks. Investigative Ophthalmology & Visual Science, 61(12): 4. https://doi.org/10.1167/iovs.61.12.4.

Thomson, K., Morgan, I. G., Karouta, C., & Ashby, R. (2020b). Levodopa inhibits the development of lens-induced myopia in chicks. Scientific Reports, 10: 13242. https://doi.org/10.1038/s41598-020-70271-z.

Tsoneva, T., Garcia-Molina, G., & Desain, P. (2023). Electrophysiological model of human temporal contrast sensitivity based on SSVEP. Frontiers in Neuroscience, 17: 1180829. https://doi.org/10.3389/fnins.2023.1180829.

Wallman, J., & Winawer, J. (2004). Homeostasis of eye growth and the question of myopia. Neuron, 43(4): 447–468. https://doi.org/10.1016/j.neuron.2004.08.008.

Wässle, H. (2004). Parallel processing in the mammalian retina. Nature Reviews. Neuroscience, 5(10): 747–757. https://doi.org/10.1038/nrn1497.

Werblin, F. S., & Dowling, J. E. (1969). Organization of the retina of the mudpuppy, Necturus maculosus. II. Intracellular recording. Journal of Neurophysiology, 32(3): 339–355. https://doi.org/10.1152/jn.1969.32.3.339.

Williams, K., & Hammond, C. (2019). High myopia and its risks. Community Eye Health, 32(105): 5–6.

Wolffsohn, J. S., & Gifford, K. L. (2025). Optical Strategy Utilizing Contrast Modulation to Slow Myopia. Ophthalmology Science, 5(4). https://doi.org/10.1016/j.xops.2024.100672.

Yamamoto, S., Nitta, K., & Kamiyama, M. (1997). Cone electroretinogram to chromatic stimuli in myopic eyes. Vision Research, 37(15): 2157–2159. https://doi.org/10.1016/s0042-6989(96)00303-3.

Zeitz, C., Roger, J. E., Audo, I., Michiels, C., Sánchez-Farías, N., Varin, J., Frederiksen, H., Wilmet, B., Callebert, J., Gimenez, M.-L., Bouzidi, N., Blond, F., Guilllonneau, X., Fouquet, S., Léveillard, T., Smirnov, V., Vincent, A., Héon, E., Sahel, J.-A., Kloeckener-Gruissem, B., Sennlaub, F., Morgans, C. W., Duvoisin, R. M., Tkatchenko, A. V., & Picaud, S. (2023). Shedding light on myopia by studying complete congenital stationary night blindness. Progress in Retinal and Eye Research, 93: 101155. https://doi.org/10.1016/j.preteyeres.2022.101155.

Zemon, V., Gordon, J., & Welch, J. (1988). Asymmetries in ON and OFF visual pathways of humans revealed using contrast-evoked cortical potentials. Visual Neuroscience, 1(1): 145–150. https://doi.org/10.1017/s0952523800001085.